AD-A121 461 A NEW ENGINEERING THEORY OF PLANAR BENDING AND 1/2
APPLICATIONS(U) GEORGIA INST OF TECH ATLANT SCHOOL OF
AEROSPACE ENGINEERING P L MURTHY ET AL. JAN 82
UNCLASSIFIED AFOSR-TR-82-0960 AFOSR-81-0056 F/G 12/1 NL

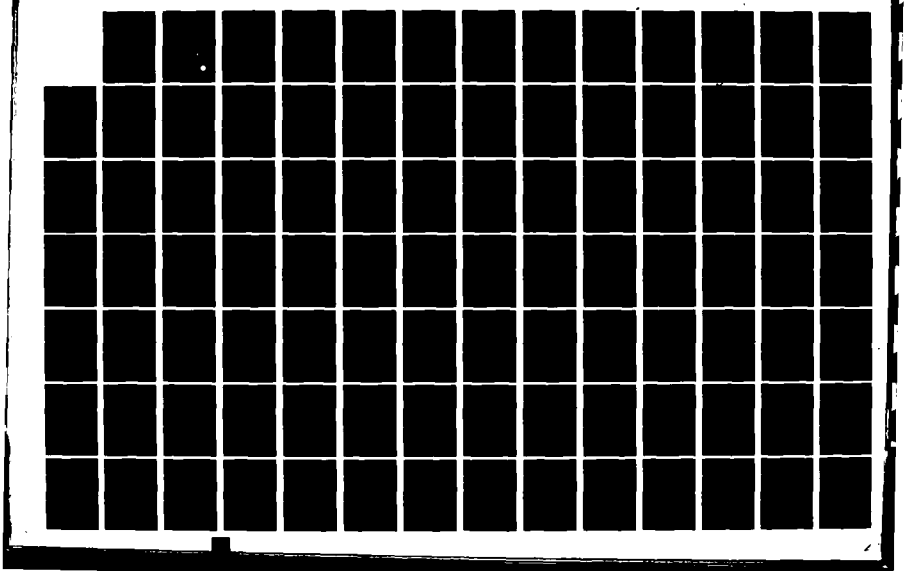

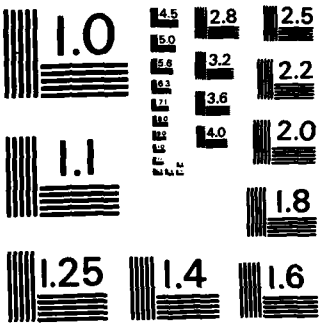

MICROCOPY RESOLUTION TEST CHART
NATIONAL BUREAU OF STANDARDS-1963-A

AFOSR-TR- 82-0960

(4)

AFOSR–TR–

Interim Scientific Report

[redacted]

AFOSR-81-0056

AD A121461

A NEW ENGINEERING THEORY OF PLANAR BENDING AND APPLICATIONS

By
Pappu L. N. Murthy and Lawrence W. Rehfield

January 1982

GEORGIA INSTITUTE OF TECHNOLOGY
A UNIT OF THE UNIVERSITY SYSTEM OF GEORGIA
SCHOOL OF AEROSPACE ENGINEERING
ATLANTA, GEORGIA 30332

UNCLASSIFIED

SECURITY CLASSIFICATION OF THIS PAGE *(When Data Entered)*

REPORT DOCUMENTATION PAGE		READ INSTRUCTIONS BEFORE COMPLETING FORM
1. REPORT NUMBER AFOSR-TR -82-0960	2. GOVT ACCESSION NO. AD-A121461	3. RECIPIENT'S CATALOG NUMBER
4. TITLE *(and Subtitle)* A New Engineering Theory of Planar Bending and Applications		5. TYPE OF REPORT & PERIOD COVERED Interim Scientific 6. PERFORMING ORG. REPORT NUMBER
7. AUTHOR(s) Pappu L.N. Murthy and Lawrence W. Rehfield		8. CONTRACT OR GRANT NUMBER(s) AFOSR-81-0056
9. PERFORMING ORGANIZATION NAME AND ADDRESS Georgia Institute of Technology School of Aerospace Engineering Atlanta, Georgia 30332		10. PROGRAM ELEMENT, PROJECT, TASK AREA & WORK UNIT NUMBERS 2307 B2 61102 F
11. CONTROLLING OFFICE NAME AND ADDRESS Air Force Office of Scientific Research (NA) Building 410 Bolling AFB, D.C. 20332		12. REPORT DATE January 1982 13. NUMBER OF PAGES 151
14. MONITORING AGENCY NAME & ADDRESS*(if different from Controlling Office)*		15. SECURITY CLASS. *(of this report)* Unclassified 15a. DECLASSIFICATION/DOWNGRADING SCHEDULE

16. DISTRIBUTION STATEMENT *(of this Report)*

Approved for public release. Distribution unlimited.

17. DISTRIBUTION STATEMENT *(of the abstract entered in Block 20, if different from Report)*

18. SUPPLEMENTARY NOTES

19. KEY WORDS *(Continue on reverse side if necessary and identify by block number)*

Bending Theory, Flexure, Beam Theory

20. ABSTRACT *(Continue on reverse side if necessary and identify by block number)*

(See Reverse Side)

DD FORM 1 JAN 73 1473 EDITION OF 1 NOV 65 IS OBSOLETE

UNCLASSIFIED

SECURITY CLASSIFICATION OF THIS PAGE *(When Data Entered)*

Abstract

The classical engineering theory of bending due to Bernoulli and Euler serves as a cornerstone for structural analysis and design. Limitations of this theory, however become apparent in flexural wave propagation studies; it predicts infinite phase velocity as the wavelength becomes shorter. This theoretical deficiency is corrected by Timoshenko theory which accounts for transverse shear deformation. A thorough study of several exact elasticity solutions reveals that there are two additional effects that are of the same order as transverse shear in bending behavior. These are due to (a) transverse normal strain and (b) an additional contribution to axial stress. A new engineering bending theory which accounts for these is presented. Predictions of static bending response using this theory agree exactly with elasticity solutions for several uniformly distributed loading cases. The contributions due to various physical effects are found to be more pronounced for orthotropic materials with low shear and transverse extensional moduli. Such properties are typical of advanced composite materials used in the aerospace industry. The theory is extended to study the dynamic behavior of beams and static buckling of columns.

Validation for the theory is provided by analysis of classic benchmark problems - - - a simply supported beam under sinusoidally distributed loading and flexural wave propagation in rectangular slabs. Numerous applications are presented. Effects of property degradation due to hygrothermal conditioning on the behavior of several elementary unidirectional composite structures are studied. The hygrothermal condition used to simulate long term aircraft service does not pose a serious problem. The loss of performance is approximately ten percent. However, complete moisture saturation produces significant effects. Reductions in the performance up to 35 percent can be expected, thus indicating that this condition should be avoided.

A NEW ENGINEERING THEORY OF PLANAR BENDING AND APPLICATIONS

Interim Scientific Report
AFOSR Contract 81-0056

Pappu L.N. Murthy[1] and Lawrence W. Rehfield[2]
School of Aerospace Engineering
Georgia Institute of Technology
Atlanta, Georgia 30332

Conditions of Reproduction

---

1. Post-Doctoral Fellow.
2. Professor.

TABLE OF CONTENTS

TABLE OF CONTENTS Cont.

TABLE OF CONTENTS Cont.

LIST OF TABLES

LIST OF FIGURES

LIST OF FIGURES CONTINUED

LIST OF FIGURES CONTINUED

NOMENCLATURE

A	Area of cross section
$A_1 - A_4$	Arbitrary constants
B	A constant
$C, \bar{C}$	Arbitrary constants
C1,C2,C3,C4	Models for clamped ends
c	Semi depth
c_s	Shear wave velocity
c_B	Bar velocity
c_p	Frequency parameter defined by Equation (A.9)
$\bar{c}$	Phase velocity
$D, \bar{D}$	Arbitrary Constants
E	Young's modulus for an isotropic material
E_{11}	Extensional modulus along the direction of fibers
E_{33}	Transverse extensional modulus
F	Axial force acting normal to deformed cross section
F_1, F_2	Parameters defined in Equations (A.18) and (A.20)
f_2	Arbitrary function
G	Shear modulus
G_{13}	Transverse shear modulus for an orthotropic material
H	Depth of the beam
I	Moment of inertia
i	A subscript ranging from 1 to 3

NOMENCLATURE CONTINUED

K	Correction factor defined by Equation (41)
$K_1 - K_3$	Correction factors defined by Equations (47)-(49)
k_b	A correction factor defined by Equation (142)
k_x	Orthotropicity parameter
L	Length of the beam
ℓ	Semi span of the beam
M	Bending moment
M_o	Bending moment at supports
m_1, m_2	Roots of the characteristic equation of Equation (67)
N	Axial force aiding along the tangent to neutral axis
n	Mode number
0	Order symbol
P	Applied compressive force
P_E	Euler buckling load
P_c	Buckling load
p_1, p_2	Roots of characteristic equation (C.8)
$\bar{P}$	A parameter introduced in Equation (C.6)
Q	Shear force
Q_o	Shear force at the supports
q	Uniformly distributed loading
q_o	Maximum intensity of the sinusoidal loading
s	Universal slenderness parameter defined by Equation 148

NOMENCLATURE CONTINUED

t	Time coordinate
U	Axial displacement of beam axis
U_1	Arbitrary constant
u	Axial displacement component
u_1	Clamped end axial displacement
$\bar{u}$	Applied boundary displacement
W	Beam axis transverse displacement
W_1	Arbitrary constant
w	Transverse displacement component
w_1	Clamped end transverse displacement
$\bar{w}$	Applied boundary displacement
$\tilde{W}$	Reissner variable for W
$\bar{W}$	Stephen and Levinson's variable for W
x,y,z	Coordinate axes
x	Mode shapes
$(,)$	A derivative with respect to space coordinate x
$(\dot{})$	A derivative with respect to t
$\alpha_a, \alpha_n, \alpha_s$	Tracer constants
β	Bending slope of cross section
γ	Shear angle, also modulus ratio $\bar{E}_{11}/G_{13}$
γ_{xz}	Shear strain
δ	Maximum deflection
ϵ_{xx}	Axial strain

NOMENCLATURE CONTINUED

ϵ_{zz}	Normal strain
$\bar{\xi}$	Dimensionless distance defined by Equation (76A)
ξ	Wave number parameter, also dimensionless length defined in Equation (A.12)
λ	Wave length
μ	Modulus ratio, E_{11}/E_{33}
ν, ν_{13}	Poisson's ratio for isotropic and orthotropic materials
ζ	Radius of gyration
$\bar{\zeta}$	Mass density
ϕ, $\bar{\phi}$	Reissner and Stephen and Levinson's rotation related variables
$\phi_1 - \phi_3$	Rotation-related variables
Ω	Frequency ratio
ω	First fundamental frequency
ω_1	First fundamental frequency for a simply supported beam
σ	Measure for bending stress
σ_{xx}	Axial stress
σ_{xz}	Transverse shear stress
σ_{zz}	Transverse normal stress
Φ	Total slope of the beam axis
τ	Dimensionless time

SUMMARY

The classical engineering theory of bending due to Bernoulli and Euler dates back to 1705 and precedes the theory of elasticity by over 100 years. It has long been recognized as a convenient approximation for slender beams and serves as a cornerstone for structural analysis and design.

Limitations of engineering bending theory become apparent in studying the propagation of elastic flexural waves of short wavelength. The Bernoulli-Euler theory predicts infinite phase velocity for harmonic waves as the wavelength becomes shorter. This result is of course, physically absurd. This theoretical deficiency is corrected by the theory proposed by Timoshenko. In Timoshenko theory, the influence of transverse shear deformations are accounted for, which results in a finite limit for phase velocity.

A thorough study of several exact elasticity solutions reveals that there are two additional effects that are of the same order as transverse shear in bending behavior. These are due to transverse normal strain and an additional term in the axial stress. A new engineering theory of planar bending which accounts for these is presented in this work. Predictions of static beam bending response using the new equations agree exactly with elasticity solutions for several uniformly distributed loading cases. The theory is validated by means of a thorough consistency analysis and by comparing with an exact solution to a nonuniform loading case.

The theory is extended to dynamics and validated through a consistency analysis. It is applied to study flexural wave propagation in slabs and vibration behavior of beams. The theory is validated quantitatively by comparing with the classic benchmark problem - - - flexural wave propagation in slabs. The results indicated superior range of applicability compared to Timoshenko or Bernoulli-Euler theories. The theory is further established by extracting Stephen and Levinson's theory specialized to thin rectangular beams from the new dynamic equations.

An elementary theory to static buckling analysis and preliminary estimates of buckling loads are provided for simply supported columns. Results are in general agreement with Timoshenko theoretical predictions.

Applications of practical interest are provided through the study of hygrothermal effects on the flexural behavior of composite beams of unidirectional layup. Hygrothermally degraded mechanical properties are used in computing the response under static and dynamic situations.

A summary of the conclusions based on the results and suggestions for future work are provided.

CHAPTER 1

INTRODUCTION

Use of fiber reinforced resin matrix composite materials in aerospace vehicles is increasing. This is primarily due to their superior mechanical properties and the ease with which they can be tailored to a specific application. The properties of composites depend on the individual properties of the constituents and the manner in which the fibers are utilized. The most structurally efficient type of laminated composite is composed of layers of unidirectional continuous fibers. In this case, mechanical properties depend also upon the fiber orientation, which may be chosen arbitrarily. This permits tailoring to specific design requirements.

The directional nature of the composite material's mechanical properties poses unique challenges for the analyst. Consider, for example, a single layer or lamina made of a composite material. The extensional modulus along the direction of fibers is usually very large relative to the extensional moduli in the lateral directions and the shear moduli. This is a marked departure from conventional isotropic materials. The result is that the relative importance of physical effects is influenced by the directional nature of properties and their relative magnitude. Transverse shear deformations, for example, are much more pronounced for composite structures.

Transverse shear deformation effects in connection with beam and

plate bending have been studied extensively. However, there still is no unique way of accounting for them. An engineering theory which includes them in a simple, rational way is desirable. This is a primary objective of the present work.

Currently, considerable research activity in the area of composite materials is directed towards the study of hygrothermal effects and three-dimensional effects such as delamination. Resin matrix materials absorb moisture, particularly in elevated temperature environments. As a result, the matrix softens and matrix controlled properties show significant degradation. This is due to a lowering of glass transition temperature of the resin matrix material. The resulting degradation of stiffness-related and strength-related properties is a serious problem for designers.

Other problems of considerable concern are attributed to three-dimensional effects. Two such problems are matrix micro-cracking and delamination. Analytical solutions are accomplished by using three-dimensional numerical techniques. These solutions are very expensive to construct and are often inaccurate in transition regions. Interlaminar shear stresses and transverse normal stresses are thought to be the primary causes of the aforementioned failures. Several theories have been proposed recently to determine these stresses more accurately. The resulting equations are cumbersome and the results are not fully satisfactory. For a preliminary design analysis, an engineering theory that is simple yet reliable would be a positive contribution.

An historical discussion of bending theory is presented to establish the basis for new developments and to permit the present work to be placed in proper perspective. Second, an analysis of bending behavior

is described which utilizes an exact solution from the theory of elasticity for isotropic materials. A unique feature is the use of tracer constants in order to track the contributions due to various physical effects throughout the course of the analysis. With the aid of insight from this analysis, a new engineering theory is proposed. The theory is applied to elementary static applications for beam-type structures which illustrate its use and permit comparisons with exact elasticity solutions to establish its validity. It is extended to study the dynamic behavior of beams and static buckling of columns.

The theory is applied to study the effects of the property degradation due to hygrothermal conditioning on composite structural behavior under static and dynamic loading situations.

The scope of this work is restricted to planar bending situations. In its present form, the theory applies to beams with thin rectangular cross sections which respond to planar bending in plane stress or to infinitely wide plates which respond in plane strain (cylindrical bending). Both isotropic and orthotropic materials are considered. Beams of orthotropic material are the simplest type of structures where composite material behavior can be studied.

CHAPTER II

HISTORICAL SKETCH

Introductory Remarks

A brief history of the development of bending theory is given below. Although the emphasis is on engineering-type bending theories, some studies involving three-dimensional exact elasticity equations and higher order beam and plate bending theories are included.

Classical Theories of Bending

The detailed historical development of the mathematical theory of elasticity is given in the books by Love[1], Todhunter and Pearson[2], and Sokolnikoff[3]. The classical theory of planar bending of beams is due to Bernoulli and Euler. James Bernoulli derived the relationship between bending moment and curvature in 1705. Euler assumed this relation in his analysis of the elastica and vibration of thin rods[2]. However, the full engineering bending theory in its present form is due to Coulomb[2]. Coulomb clarified the equilibrium equations and introduced the notion of neutral axis. The theory is based on the hypothesis that plane sections normal to the neutral axis remain plane and unextended after bending. It provides a convenient approximation for slender beams and serves as a cornerstone for structural analysis and design.

The classical engineering theory of plate bending had its origin in the pioneering work of Sophie Germain. She was awarded a prize in 1815 for her attempt to provide a theoretical basis for the modal figures obtained

in Chladni's vibration experiments[1]. Her work was finally published in 1821[4]. It contained an error in the expression for strain energy of bending, which was corrected by Lagrange[2]. The governing differential equation for flexural vibration of plates was independently established by Navier[5], Poisson[6], and Cauchy[7]. However, it was Kirchhoff[8] who resolved the famous controversy concerning the nature and number of proper boundary conditions. Love[1] provided an extension for the bending of shells.

The Kirchhoff-Love theory of plate and shell bending is based on the hypothesis that normals to the neutral surface remain normal and unstretched after bending. This permits only two boundary conditions per edge. Three boundary conditions per edge, however, provide a more realistic behavioral description of the plate and shell bending.

Limitations of elementary bending theory become apparent in studying the propagation of elastic waves of short wavelengths. It was pointed out by Lamb[9] that Bernoulli-Euler theory is inadequate for impact type loads. It leads to the physically absurd conclusion that disturbances are propagated instantaneously throughout the beam. This is because it predicts infinite phase velocity for harmonic waves as the wavelength becomes shorter. According to the exact solution of Rayleigh[10], this should approach a finite limit. Rayleigh attempted to improve the classical beam bending theory by accounting for rotatory inertia effects and obtained a finite limit.

Elasticity Solutions

The adequacy of a specific theory can best be decided by comparing

it with exact solutions. Solutions of the full three-dimensional elasticity equations are rare. Usually simple, closed form solutions do not exist. Some can be found, however, for a few sufficiently simple geometric configurations and for simple loadings. Normally, some numerical technique is required to solve a practical problem.

Reference 1 gives some of the earliest solutions for beams bent under arbitrarily continuous loading. Closed form solutions for beams of arbitrary cross-section bent by terminal couples and loads are provided by Saint Venant[2]. Pochhammer[11] and Chree[12] have studied independently wave propagation in an infinitely long beam of solid circular cross-section. A similar study for an infinitely wide rectangular plate was done by Lord Rayleigh[10]. His solution for the flexural wave velocity of propagation in an isotropic rectangular slab is a bench mark.

Von Karman[13] and Seewald[14] undertook studies of the flexure of rectangular beams. Their attempts to correlate elasticity solutions with the classical beam bending theory yield corrections to the moment-curvature relationship. It appears that Pearson[1] was first to report these corrections. Later, Grashof, Michell and Filon[1] also provided similar corrections for beams subjected to distributed loading independently. These are later attributed to shear deformation by several analysts. Goodier[15], however, in his three-dimensional order of magnitude analysis of beam bending, showed that the correction term is not necessarily due only to transverse shear stress effects. His analysis indicates that the transverse normal stresses and an additional term in the expression for axial stress may also contribute to beam bending response. No means of

accounting for these effects is offered, however. It is rather perplexing that later researchers have not followed up on Goodier's work or made an effort account for the aforementioned effects. A recent exception is Reference 36.

Using a different approach, Donnell[16,17] obtained solutions like those of References 13 and 14. Hashin[18] proposed a simple direct method to obtain compatible stress field in beams subjected to polynomial loading. Later, he extended it to obtain exact stresses in plane orthotropic beams[19]. Hashin's approach differs from earlier work in that there is no guess work involved in obtaining solutions. In the earlier work, the solutions are guessed or found by combining known solutions so as to satisfy boundary conditions. Though a direct method was first proposed by Neou[20], the choice of the degree of polynomial remained arbitrary in his study.

Recently Cheng[21] has provided a plate theory based upon the three-dimensional equations of elasticity. He did not consider any transverse loading in the development.

Shear Deformation Theories

Attempts to remove the theoretical shortcomings in classical bending theories gave rise to theories incorporating certain refinements. During vibration, beam cross sections experience rotatory motions as well as translations. Also, the transverse deflection of a beam has contributions due to the transverse shearing forces as well as the bending moment. Correction for the influence of rotatory inertia was provided by Rayleigh[10] as mentioned earlier. Grashof[22] (1878) and Rankine[22] (1895) included the effects of transverse shear deformation in analyzing some static beam bending problems.

A more refined theory that accounts for rotatory inertia and transverse shear deformation was proposed by Timoshenko in his famous paper[23] in 1921. Timoshenko's theory is widely recognized and used wherever improvement on classical theory is sought. It is of some historical interest that both the rotatory inertia correction and transverse shear correction were given first by the French analyst M. Bresse in 1859 in his Cours de Mecanique Appliquee. This work has been overlooked in the later development of the subject.

In Timoshenko's theory, there is a shear correction factor, k, to account for nonuniform shear stresses across the cross-section of the beam. Originally it was taken as the ratio of average to maximum shear stress on the cross-section. Thus, for a rectangular cross-section, this procedure yields a value of 2/3 for k. In a subsequent paper[24], Timoshenko proposed a new value, 8/9, for better correlation with the experimental results of Filon[1].

Most of the refined theories that followed are based upon Timoshenko-type beam equations. Uflyand[25] and Mindlin[26] have developed plate theories including the effects of rotatory inertia and transverse shear deformation specifically for dynamic applications. Uflyand's[25] equations are essentially an extension of Timoskenko's beam equations.

Mindlin's[26] plate theory also contains the shear correction factor, k. A unique way of obtaining k is not provided in the theory. It is chosen by an ad-hoc criterion. He suggested two such criteria based on a matching principle. One is to choose k such that the limiting phase velocity for very short flexural waves is made identical with the velocity of Rayleigh's surface waves. The other is to select k so that it gives exact circular

frequency of the first antisymmetric mode of thickness-shear vibration. The result is that k depends on the cross sectional shape and the mode of motion. Values of k for various cross sectional shapes are provided in Reference 27. References 28 and 29 treat the analysis of thickness shear vibration in quartz crystals where Mindlin's shear deformation theory was used. Traill-Nash, and Collar[30] and Goodman and Sutherland[31] have provided analogous theories for beam vibration. In the former, experimental verification was also given.

Following the above mentioned work, there were several attempts to improvise Mindlin-type equations. The differences primarily relate to the selection of shear correction factor, k, according to various ad-hoc criteria. A recent survey by Kaneko[32] gives an excellent description of them. Cowper[33] provided a new formula for k which depends upon Poisson's ratio. His equations appeared to give satisfactory results for static applications and long-wavelength, low frequency deformation of beams. In the analysis, the effects of transverse normal stress were neglected. Leibowitz and Kennard[34] have used an alternative approach to obtain k. Exact bending moment-curvature relation of a beam bent under its own weight was used to redefine k.

A shear deformation theory with two arbitrary constants is presented in Reference 35. The underlying idea was further developed in Reference 36 by combining the contributions of References 33, 34 and 35. Two constants, k_1 and k_2, are introduced and chosen as follows. k_1 is the usual shear correction factor defined by a transverse shear stress-strain relationship. k_2 is associated with bending stiffness and comes from

accounting for transverse normal and lateral stresses in the moment-curvature relation. It is assumed that the stresses during beam vibration can be approximated by those of a beam bent under uniform gravity loading.

The above work of Stephen and Levinson[36] is especially noteworthy. It is the first work to make use of the observations and insights of Goodier[15]. Good agreement with exact solutions for several flexural wave propagation problems has been demonstrated for overall response properties. The theory requires an exact elasticity solution for St. Venant's bending problem for the beam cross section under consideration for its application, however. It also possesses a shortcoming. The displacement variables are averaged quantities over the cross section. Consequently, no claims are made regarding the pointwise distribution of stresses or displacements.

For static applications, Reissner[37] has derived plate equations that account for shear deformation and transverse normal stresses using an entirely different approach in 1945. Consequently, his shear deformation theory is marked by the presence of transverse normal stress effects. He used assumed stresses and an energy principle to obtain the governing differential equations. He clarified[38] and subsequently improved his earlier work for bending of plates without transverse normal stress[39]. Several analogous theories for plates are surveyed in Panc's book[40]. The notable among them are due to Panc, Hencky and Kromm.

Refined Bending Theories

The classical bending theory and the shear deformation theories can be considered to be related. The former can be obtained by taking the shear modulus in terms associated with the transverse shear deformation to

be very large in the latter. In both theories, the displacement variables contain only linear terms in the thickness coordinate, z. More refined theories can be formulated by taking higher order terms in z in addition to the linear terms. These theories are sometimes called higher order theories.

The usual procedure for developing this type of theory has been a displacement formulation. The displacements are assumed as a power series in the thickness coordinate, z. The governing differential equations and the appropriate boundary conditions are then obtained using energy principles. References 41 and 42 formed the basis for subsequent works. Whitney and Sun[43] and Nelson and Lorch[44] have proposed refined theories for laminated plates and shell structures. A class of contact problems in beams is solved in Reference 45. An excellent survey of various higher order theories and a comparative study of relative differences is given in Reference 46. Lo, Christensen and Wu[46,47] have proposed recently a theory for isotropic and laminated composite plates specifically for dealing with problems which involve rapidly fluctuating loads with a characteristic length of the order of thickness.

Displacement formulations of the above types begin with kinematically admissible displacements, but the stress equilibrium equations are violated. In Reference 48, a systematic approach to obtain solutions of the three-dimensional elasticity equations is given for beams subjected to arbitrary loading. It is generally true, however, that assumed displacement approaches result in stresses which are not in equilibrium and which provide poor design stress estimates. To obtain stresses, alternative means may have to be sought as pointed out in Reference 49.

Reissner's[37,38,39] plate theory and the theory proposed in the Reference 36 should also be classified as refined theories of bending. This is because effects besides those due to transverse shear deformation are accounted for.

Synopsis

Although engineering bending theory has a long and successful history, there are issues that remain surrounded in uncertainty. Beyond the classical theories, there are no unique or clearly superior refined or shear deformation theories. A thorough exploration of the effects enumerated by Goodier[15] in addition to those of transverse shear has not been undertaken. Are there relationships among the various theories that have been proposed and are some "better" than others? Problems and opportunities associated with composite structures require that these issues be resolved.

CHAPTER III

PRELIMINARY ANALYSIS

Introductory Remarks

As a first, important step in an analysis of bending behavior, a plane stress elasticity solution for a simply supported beam under uniformly distributed loading is studied. It is possible to identify the individual contributions due to various factors affecting beam response. An assessment of their relative importance, therefore, can be made.

Problem Definition and Solution

The two-dimensional elasticity solution for a simply supported beam under uniformly distributed loading is given in the text by Timoshenko and Goodier[22]. It is valid for very thin rectangular beams in the plane stress form. For infinitely wide plates, the same solution remains valid if a transformation of elastic constants for plane strain is employed.

The beam and coordinate system are shown in Figure 1. The length of the beam is 2ℓ and the depth is 2c. The width of the beam is taken as unity for convenience. The beam is bent by a uniformly distributed load of intensity q applied to its upper surface. The midspan of the beam centroidal axis is chosen as the origin for the coordinate axes x and z. $z = +c$ and $z = -c$ correspond to the bottom and top surfaces of the beam. The notation and convention are shown.

For the stresses, the usual convention and notation are followed. Accordingly, σ_{xx} is the axial stress, σ_{zz} is the transverse normal stress

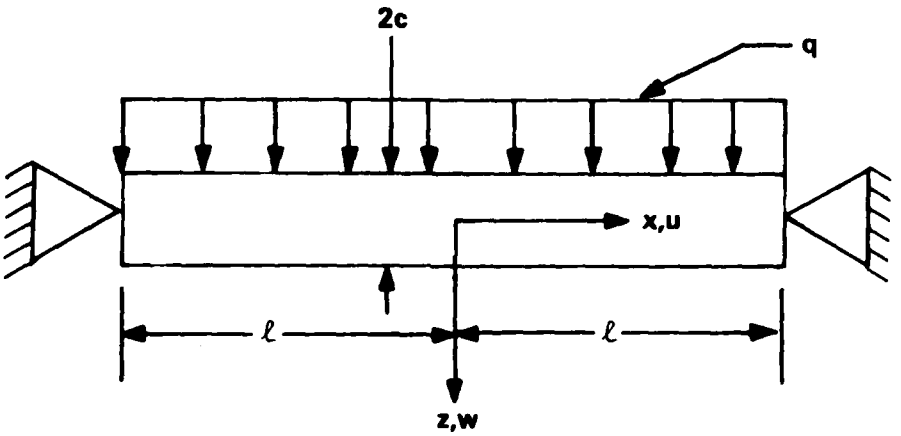

Figure 1. Uniformly Loaded Simply Supported Beam and Coordinate System

and σ_{xz} is the transverse shear stress. They are given by the following expressions:

$$\sigma_{xx} = \frac{q}{2I}(\ell^2 - x^2)z + \underline{\frac{q}{2I}\left(\frac{2z^3}{3} - \frac{2c^2z}{5}\right)} \tag{1}$$

$$\sigma_{zz} = -\frac{q}{2I}\left(\frac{z^3}{3} - c^2z + \frac{2c^3}{3}\right) \tag{2}$$

$$\sigma_{xz} = -\frac{q}{2I}(c^2 - z^2)x \tag{3}$$

I is the second moment of the cross sectional area and is $2c^3/3$ for the rectangular section under consideration. These stresses satisfy all the governing differential equations and the stress boundary conditions on the upper and lower surfaces. On the ends $x = \pm\ell$, the stress boundary conditions are satisfied in an overall Saint Venant sense.

As an aid in this analysis, three tracer constants, α_a, α_n and α_s, are introduced. They are defined and used so as to facilitate keeping track of three distinct contributions to the response. The first term of Equation (1) corresponds to the bending stress given by classical Bernoulli-Euler theory. The underlined term is a stress contribution which will be called the "nonclassical axial stress". It produces no resultant force or moment and is, therefore, a self equilibrating stress. α_a is the tracer constant associated with this contribution. If $\alpha_a = 1$, this contribution is fully accounted for. If $\alpha_a = 0$ in the following, however, it is ignored and the Bernoulli - Euler axial stress distribution is recovered. For example, the axial stress is written using this convention

in the form

$$\sigma_{xx} = \frac{q}{2I}(\ell^2 - x^2)z + \alpha_a \frac{q}{2I}(\frac{2}{3}z^3 - \frac{2}{5}c^2 z) \tag{1A}$$

α_n and α_s are defined analogously and are associated with contributions due to σ_{zz} and σ_{xz}, respectively.

The displacement components u and w are shown in Figure 1. Expressions for them can be obtained by using Hooke's law and the strain displacement relations. For plane stress, Hooke's law for an isotropic material is

$$\epsilon_{xx} = \frac{1}{E}(\sigma_{xx} - \nu\sigma_{zz}) \tag{4}$$

$$\epsilon_{zz} = \frac{1}{E}(\sigma_{zz} - \nu\sigma_{xx}) \tag{5}$$

$$\gamma_{xz} = \frac{\sigma_{xz}}{G} \tag{6}$$

E is Young's modulus, ν is Poisson's ratio and G is the shear modulus. ϵ_{xx} and ϵ_{zz} are the extensional strains in the longitudinal and the transverse directions and γ_{xz} is the shear strain. The strain-displacement relations are

$$u_{,x} = \epsilon_{xx};\ w_{,z} = \epsilon_{zz};\ u_{,z} + w_{,x} = \gamma_{xz} \tag{7}$$

With the aid of Equations (1) - (6), u and w can be obtained by direct integration of Equations (7). The following boundary conditions at the ends $x = +\ell, -\ell$ are imposed:

$$w(\ell,0) = w(-\ell,0) = 0 \tag{8}$$

They represent support conditions applied at the beam axis. Also, from the symmetry requirement

$$u(0,z) = 0 \tag{9}$$

These conditions are sufficient to prevent rigid body motion.

The expressions for u and w are

$$u(x,z) = \frac{q}{2EI}\left[(\ell^2 x - \frac{x^3}{3})z + \alpha_a(\frac{2}{3}z^3 - \frac{2c^2 z}{5})x + \alpha_n \nu(\frac{z^3}{3} - c^2 z + \frac{2c^3}{3})x\right] \tag{10}$$

$$w(x,z) = w(x,0) - \frac{q}{2EI}\left[(\frac{z^4}{12} - \frac{c^2 z^2}{2} + \frac{2c^3 z}{3})\alpha_n + \nu(\ell^2 - x^2)\frac{z^2}{2} + \nu\alpha_a(\frac{z^4}{6} - \frac{c^2 z^2}{5})\right] \tag{11}$$

In Equation (11), w(x,0) is the vertical deflection of the beam centroidal axis due to bending. It is given by the Equation

$$w(x,0) = \delta - \frac{q}{2EI}\left[\frac{\ell^2 x^2}{2} - \frac{x^4}{12} + \left[(1+\nu)\alpha_s - (\frac{\alpha_a}{5} + \frac{\alpha_n \nu}{2})\right]c^2 x^2\right] \tag{12}$$

$$\text{where} \quad \delta = \frac{5q\ell^4}{24EI}\left[1 + \frac{12c^2}{5\ell^2}\left[(1+\nu)\alpha_s - \frac{\alpha_a}{5} - \frac{\alpha_n \nu}{2}\right]\right] \tag{13}$$

δ is the deflection at the midspan of the beam.

An Analysis of Beam Response

The major differences between the classical Bernoulli-Euler theory and the elasticity solution can be clearly identified in Equation (13). The underlined term represents the correction to the former due to the presence of contributions identified by the tracer constants α_s, α_a and α_n. Note that the contributions due to all three effects - transverse shear, nonclassical axial stress and transverse normal strain - are of the same order of magnitude. A static version of Timoshenko's theory[23] includes only the terms associated with α_s.

The corrections shown in Equation (13) were known to earlier authors[13,14]. However, they did not differentiate among the various contributions. This differentiation provides the key ingredient for the establishment of a rational engineering theory. Goodier[15] suspected that the other influences beside transverse shear were important, but offered no means of estimating them quantitatively and no concrete examples of their contribution to beam response. The approach adopted here makes the matter transparent and settles the issue for this example.

If ν is taken to be 0.3 and $\alpha_n = \alpha_s = \alpha_a = 1$ in Equation (13), then

$$\delta = \frac{5q\ell^4}{24EI}\left[1 + 2.28\,\frac{c^2}{\ell^2}\right] \qquad (14)$$

A corresponding result from Timoshenko's original shear deformation theory[23] can be obtained by setting $\alpha_n = \alpha_a = 0$, and $\alpha_s = 1$ in Equation

(13). For $\nu = 0.3$, the result is

$$\delta_{\text{Timoshenko}} = \frac{5q\ell^4}{24EI}\left[1+ 3.12\,\frac{c^2}{\ell^2}\right] \qquad (15)$$

A popular alternative is to use Timoshenko theory with $\alpha_s = \frac{4}{5}$. This approximately corresponds to result obtained if Reissner's approach is adopted. This leads to

$$\delta_{\text{Timoshenko}} = \frac{5q^4}{24EI}\left[1 + 2.496\,\frac{c^2}{\ell^2}\right] \qquad (15A)$$

Conclusions

On the basis of the foregoing analysis, the following conclusions are reached:

1. A Timoshenko-type transverse shear theory does not contain the necessary physical ingredients to treat problems with distributed loadings.

2. Transverse shear, nonclassical axial stress and transverse normal strain make contributions to the response that are of the same order of magnitude. A theory that is purported to be more accurate or complete than classical theory must, therefore, correctly account for all of these influences.

CHAPTER IV

FOUNDATIONS OF A NEW THEORY

Objectives

The primary objective of this work is the development of a foundation for an engineering bending theory which is consistent, reliable, and simple to use. The theory should provide more reliable information than existing ones. Furthermore, it must account for the three effects that were clearly identified previously --- transverse shear strain, nonclassical axial stress and transverse normal strain.

An engineering theory is one in which assumptions or approximations are introduced in order to simplify the governing equations or facilitate their solution. Hopefully only a little accuracy is sacrificed for a considerable reduction in computational labor. The intent is to encompass the heart of the problem under consideration. Consistency and rationality are desirable, but mathematical rigor is meaningless in this context. An engineering theory is judged solely on the basis of the results obtained from its use.

The standard of comparison for results that is used herein is rigorous solution to the equations of elasticity theory for the problem in question.

A second objective is to obtain stress estimates that are improvements over those provided by classical bending theory. This must be accomplished if the influence of nonclassical axial stress is to be

properly accounted for.

Statically Equivalent Stresses

Equilibrium of a beam element is governed by overall equations containing resultant axial force, shear force and bending moment. The sign convention and notation for these appear in Figure 2. The equilibrium equations are

$$N_{,x} = 0 \tag{16}$$

$$Q_{,x} + q = 0 \tag{17}$$

$$M_{,x} - Q = 0 \tag{18}$$

The force and moment resultants are defined in terms of stresses as

$$N = \int_{-c}^{c} \sigma_{xx}\, dz \tag{19}$$

$$Q = \int_{-c}^{c} \sigma_{xz}\, dz \tag{20}$$

$$M = \int_{-c}^{c} \sigma_{xx} z\, dz \tag{21}$$

In the above, a rectangular cross section of unit width is assumed as before. In addition, the beam is assumed to be of uniform depth.

According to classical theory, the stresses are

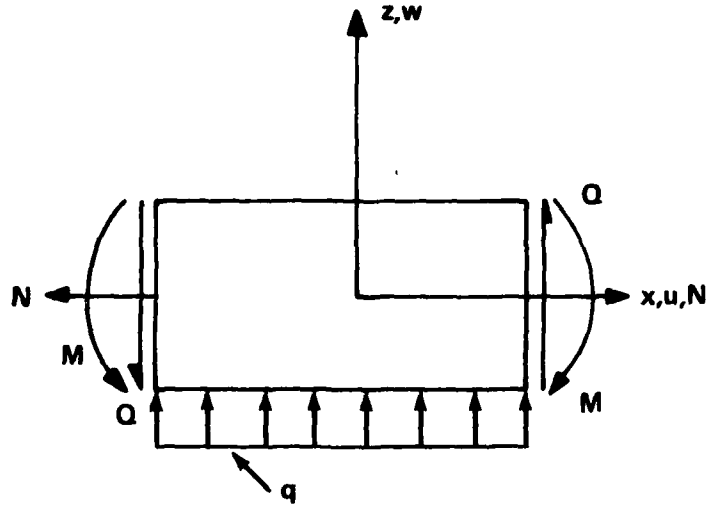

Figure 2. Sign Convention

$$\sigma_{xx} = \frac{N}{A} + \frac{Mz}{I} \tag{22}$$

$$\sigma_{xz} = \frac{Q}{2I}(c^2 - z^2) \tag{23}$$

$$\sigma_{zz} = \frac{Q_{,x}}{2I}\left(\frac{z^3}{3} - c^2 z + \frac{2}{3}c^3\right)$$

A is the cross sectional area, which is 2c for the rectangular cross section under consideration. These stresses are statically equivalent to the applied loads and satisfy the stress equations of equilibrium:

$$\sigma_{xx,x} + \sigma_{xz,z} = 0 \tag{25}$$

$$\sigma_{zz,z} + \sigma_{xz,x} = 0 \tag{26}$$

In addition, Equations (19)-(21) are satisfied, as are appropriate stress conditions at $z = c$ and $z = -c$.

The above stresses, although not exact, serve as a first approximation. This stress field is statically equivalent to applied loads, however, it does not satisfy compatibility requirements. It will be used subsequently to develop approximations for the displacement components.

Kinematics

Classical Bernoulli-Euler theory is based upon a kinematic assumption that is equivalent to ignoring, and hence setting to zero, transverse normal strain and transverse shear strain. Timoshenko-type shear deformation theories account for transverse shear strain but still do not permit transverse normal strain. On the basis of the previous analysis

of the simply supported beam example, it appears necessary to completely abandon the Bernoulli-Euler kinematic assumption. In order to obtain some simplification from the complete elasticity equations, an assumption that facilitates the analysis is required, however.

The central assumption that replaces the Bernoulli-Euler hypothesis in the present development is that the statically equivalent stresses in Equations (22)-(24) can be used to estimate the transverse normal strain and transverse shear strain. Note that this is an assumption regarding stresses. It is not a kinematic assumption. This is in sharp contrast to classical and Timoshenko-type shear deformation theories.

The development will be carried out for orthotropic materials with principal material directions corresponding to axes of the beam. The appropriate form of Hooke's Law for plane stress (beams of thin rectangular cross section) is

$$\epsilon_{xx} = \frac{1}{E_{11}} (\sigma_{xx} - \nu_{13} \sigma_{zz}) \tag{27}$$

$$\epsilon_{zz} = \frac{\sigma_{zz}}{E_{33}} - \frac{\nu_{13}}{E_{11}} \sigma_{xx} \tag{28}$$

$$\gamma_{xz} = \sigma_{xz}/G_{13} \tag{29}$$

ϵ_{xx}, ϵ_{zz}, and ϵ_{xz} are the axial strain, transverse normal strain and transverse shear strain, respectively. E_{11} and E_{33} are elastic moduli associated with the x and z directions. ν_{13} is Poisson's ratio and G_{13} is the transverse shear modulus.

Although it is impossible to obtain a unique displacement field from the incompatible stress field, a selective use of strain displacement relations and Hooke's Law permits an approximate form for the displacement field to be determined. The error involved in this process will be estimated in Chapter VII.

On the basis of the above, Equations (7), (22), (24) and (28) permit the transverse normal strain to be approximated as

$$w_{,z} \cong -\frac{\nu_{13}}{E_{11}}\left(\frac{N}{A}+\frac{Mz}{I}\right)+\frac{Q_{,x}}{2E_{33}I}\left(\frac{z^3}{3}-c^2z+\frac{2}{3}c^3\right) \qquad (30)$$

Integration of this equation results in the following expression for the lateral displacement component, w:

$$w = W(x)-\frac{\nu_{13}}{E_{11}}\left(\frac{Nz}{A}+\frac{Mz^2}{2I}\right)+\frac{Q_{,x}}{2E_{33}I}\left(\frac{z^4}{12}-\frac{c^2z^2}{2}+\frac{2}{3}c^3z\right) \qquad (31)$$

W(x) is the lateral deflection of the beam axis (z = 0), which is an unknown function to be determined.

The axial component of displacement u can be estimated as follows. Equations (7), (16), (18), (23), (29), and (31) permit $u_{,z}$ to be expressed in terms of the shear stress and w.

$$u_{,z} = \sigma_{xz}/G_{13} - w_{,x}$$

$$= \frac{Q}{2G_{13}I}(c^2-z^2) - W_{,x}$$

$$+ \frac{\nu_{13}}{2E_{11}I} Qz^2 - \frac{Q_{,xx}}{2E_{33}I}\left(\frac{z^4}{12} - \frac{c^2z^2}{2} + \frac{2}{3}c^3z\right)$$

This expression is integrated to yield

$$u = U(x) - zW_{,x} + \frac{\nu_{13}}{E_{11}I} Q \frac{z^3}{6}$$

$$+ \frac{Q}{2G_{13}I}\left(c^2z - \frac{z^3}{3}\right) - \underline{\frac{Q_{,xx}}{2E_{33}I}\left(\frac{z^5}{60} - \frac{c^2z^3}{6} + \frac{1}{3}c^3z^2\right)} \qquad (32)$$

U(x) is the axial deflection of the beam axis, which is an unknown function to be determined.

The static displacement field is completely described by Equations (31) and (32). U and W, the axis displacement components, emerge as natural kinematic variables. If $\nu_{13} \to 0$ and $E_{33} \to \infty$ in (31) and (32), a tranverse shear theory is obtained which includes the effects of cross section warping. If, in addition, $G_{13} \to \infty$, then the classical Bernoulli-Euler kinematic assumption is recovered.

Considerable simplification is achieved if the underlined terms in Equations (31) and (32) are neglected. These terms are associated with higher derivatives of the shear force Q than the remaining terms. This simplification is adopted here. Its full implication will be discussed in Chapter VII. The accuracy of this approximation is related to how rapidly the applied load q varies with x.

Refined Axial Stress Distribution

The axial stress σ_{xx} is the largest and most important stress component. An accurate knowledge of it is often all that is needed in a practical application. A refined estimate which improves Equation (22) is central, therefore, to the improvements that are sought.

Equations (7), (24), (27) and (32) can be utilized to produce a refined axial stress expression.

$$\sigma_{xx} = E_{11}\, u_{,x} + \nu_{13}\, \sigma_{zz}$$

$$= E_{11}\left[U_{,x} - z\, W_{,xx} + \frac{\nu_{13}}{E_{11}I}\, Q_{,x}\, \frac{z^3}{6}\right.$$

$$\left. + \frac{Q_{,x}}{2G_{13}I}\left(c^2 z - \frac{z^3}{3}\right)\right] + \nu_{13}\, \frac{Q_{,x}}{2I}\left(\frac{z^3}{3} - c^2 z + \frac{2}{3}\, c^3\right) \qquad (33)$$

In the above, contributions due to the underlined terms in Equation (32) are not included. Notice that the stress distribution throughout the thickness is not linear as in the classical approximation (22).

Relationships for the axial force and bending moment are obtained by using Equations (19), (21) and (33). The results are

$$N = \left(E_{11}\, U_{,x} + \frac{\nu_{13} c^3}{3I}\, Q_{,x}\right)A \qquad (34)$$

$$M = -\, E_{11} I W_{,xx} + \left(\frac{4}{5}\, k_x + \frac{\nu_{13}}{2}\right)c^2\, Q_{,x} \qquad (35)$$

The parameter k_x is $(E_{11}/2G_{13} - \nu_{13})$; it is unity for an isotropic material. Equations (34) and (35) permit (33) to be rewritten as

$$\sigma_{xx} = \frac{N}{A} + \frac{Mz}{I} + \underline{\frac{Q_{,x}}{3I} k_x \left(\frac{3}{5} c^2 z - z^3\right)} \qquad (33A)$$

The underlined term is the nonclassical axial stress contribution, which is the desired refinement.

Summary

The governing equations for the new theory can be summarized now. They encompass four categories. Overall beam-type equations consist of the equilibrium equations (16)-(18) and the constitutive equations (34) and (35). In addition, two sets of equations provide the distributions of stresses and displacements throughout the structure. The first set for stresses consists of Equations (33A), (23) and (24). The second for displacements is composed of Equations (31) and (32) with the underlined terms omitted.

The above collection of equations requires the specification of boundary conditions. The classical boundary condition options are to specify N or U, Q or W, and M or ϕ at the ends of the beam. ϕ is a rotation-related variable.

Three commonly used rotation-related variables are considered below. The first is the rotation of the cross section at the beam, ϕ_1

$$\phi_1 = u_{,z}\,(x,o) = \frac{Qc^2}{2G_{13}I} - W_{,x} \qquad (36)$$

Another is the rotation-related variable, ϕ_2, which is defined by the following equation:

$$\phi_2 = \frac{1}{I} \int_{-c}^{c} uz \, dz$$

$$= -W_{,x} + \frac{3}{10A} \left(\frac{\nu_{13}}{E_{11}} + \frac{4}{G_{13}}\right) Q \tag{37}$$

This variable naturally arises in Reissner's development of plate bending theory[38] based upon the complementary energy principle.

The third is the mean rotation of the cross section, ϕ_3.

$$\phi_3 = \frac{1}{2c} \int_{-c}^{c} u_{,z} dz = \frac{1}{2c} \left[u(x,c)-u(x,-c)\right]$$

$$= \frac{Qc^2}{3I} \left(\frac{1}{G_{13}} + \frac{\nu_{13}}{2E_{11}}\right) - W_{,x} \tag{38}$$

In a Timoshenko-type theory, since u is linear in z, all of the above definitions are equivalent. Equation (36) is the actual definition used in the original paper.[23] These variables permit different models for simulating clamped end conditions to be defined.

Discussion

The development of the equations requires no ad hoc kinematic assumptions or use of a variational principle. The central assumption is that the transverse normal and shear strain components can be estimated from classical stresses. A selective use of strain displacement relations

is utilized to establish the approximate form of the displacements. The equations have the following properties:

1. Stress and displacement distributions throughout the structure are found in terms of the response variables associated with the axis;

2. Nonclassical axial stress and cross section warping effects, transverse shear strain and transverse normal strain are all accounted for in a rational manner;

3. The equations can be shown to yield exact results for the case of uniformly distributed lateral loading;

4. For nonuniform loading, some of the equations are approximate -- the stresses are not exactly in equilibrium and the stresses and displacements are not exactly compatible; and

5. The equations are as simple to apply as static Timoshenko-type shear deformation theories.

Items 1-3 and 5 are strong points in favor of the new equations. Item 4 imposes some limitations on the validity of the theory, which will be thoroughly discussed in Chapter VII, but it is responsible for the simplicity that is achieved. The level of stress approximation which results is analogous to that suggested by Seewald[14] for isotropic materials.

In the process of solving a particular bending problem, the only

apparent difference from application of a static Timoshenko-type shear deformation theory is the value for the coefficient of the $Q_{,x}$ - term in Equation (35). As the applications will demonstrate, this seemingly minor difference, together with the use of Equations (31), (32) and (33A), produces significantly improved results.

CHAPTER V

STATIC APPLICATIONS

Introductory Remarks

In order to illustrate the benefits of the new theory, several elementary applications for uniform beams subjected to uniformly distributed loading applied to the upper surface analogous to the situation shown in Figure 1, will be presented. One special case of a linearly varying load is studied to illustrate a particular point. Comparisons are made with the exact elasticity solution, classical Bernoulli-Euler theory and the original Timoshenko theory[23] in each case. The two dimensional elasticity solution, for the present purposes, is considered an exact solution, although the plane stress approximation requires the width to depth ratio of the beam to be small. A discussion of this issue is given in Reference 23, page 274.

Solutions are derived for orthotropic beams, and corresponding results for isotropic beams are obtained by specialization. Poisson's ratio is taken to be 0.3 throughout. For orthotropic beams, E_{11}/G_{13} is taken to be 30; this is a typical value for a modern graphite/epoxy composite material.

In presenting results, appropriate response variables are non-dimensionalized with respect to the corresponding values obtained from

Bernoulli-Euler theory. This practice permits easy recognition of departures from classical theory predictions.

Response can be separated into bending and stretching. Stretching is governed by Equations (16) and (34), bending by Equations (17), (18), and (35). The bending problem involving M, Q and W must be solved first. N and U, stretching variables, are determined secondarily. For the present purposes, only the bending portion of the response is discussed.

Simply Supported Beam

The exact solution for a simply supported (SS) isotropic beam was presented earlier. The precise boundary conditions that have been imposed at the ends are

$$\text{SS:}\quad M = 0,\ W = 0 \tag{39}$$

Such a beam is shown in Figure 1. It is a statically determinate structure, so the moment and shear distributions are known.

The response of the beam is defined if the axis lateral deflection W(x) is found. For this type of end restraint, W can be expressed as

$$W = \delta - \frac{q}{4E_{11}I}\left[\left(\ell^2 x^2 - \frac{x^4}{6}\right) + \frac{K}{2} H^2 x^2\right] \tag{40A}$$

In the above, the constant K is

$$K = \frac{1}{2}\left(\alpha_s \frac{E_{11}}{G_{13}} - \alpha_n \nu_{13}\right) - \alpha_a \frac{k_x}{5} \tag{41}$$

The tracer constants introduced earlier are utilized to identify the origin of the various contributions to K. δ is the maximum or midspan deflection,

which is

$$\delta = \frac{5q\ell^4}{24E_{11}I}\left[1 + \frac{12}{5}K\left(\frac{H}{L}\right)^2\right] \tag{42}$$

$L = 2$ is the total length of the beam and $H = 2c$ is the depth of the cross section. The stress distribution at midspan is given by

$$\sigma_{xx} = \frac{qL^2z}{8I}\left\{1 + \alpha_a\, 4k_x \frac{H^2}{L^2}\left(\frac{2z^2}{3H^2} - \frac{1}{10}\right)\right\} \tag{40B}$$

The solution by the present theory correspond to $\alpha_a = \alpha_n = \alpha_s = 1$ in (41); it is exact for this problem. If K is set to zero in Equations (40) and (42), then the Bernoulli-Euler result is obtained. If $\alpha_a = \alpha_n = 0$ and $\alpha_s = 1$ in (41), the static Timoshenko theory prediction is recovered. Note that Timoshenko theory overestimates the midspan deflection in this case.

Cantilever Beam

For a cantilever beam, it is convenient to take the origin of coordinates, $x = 0$, at the free end. $x = L$, corresponds to the clamped end. Unlike the more elementary theories, the present theory does not suggest a unique, simple model for a clamped or fixed end. Three rotation variables were introduced earlier in Equations (36)-(38). Three definitions of clamping, therefore, will be discussed.

All results can be cast in a common format. The three types of clamping are denoted C1, C2, and C3. They correspond to the following definitions:

$$C1: \quad W = 0, \ \phi_1 = 0 \tag{43}$$

$$C2: \quad W = 0, \ \phi_2 = 0 \tag{44}$$

$$C3: \quad W = 0, \ \phi_3 = 0 \tag{45}$$

The cantilever beam is statically determinate with M and Q vanishing at the free end. At the fixed end, one of the above definitions of clamping must be imposed. The rotation variables can be expressed in the common form

$$\phi_i = K_i \frac{Qc^2}{E_{11}I} - W_{,x}; \ i = 1, 2, 3. \tag{46}$$

The constants K_1-K_3 are

$$K_1 = \frac{\alpha_s}{2} \frac{E_{11}}{G_{13}} \tag{47}$$

$$K_2 = \frac{1}{2} \left[\alpha_s \frac{E_{11}}{G_{13}} - \frac{\alpha_a}{5} \left(\frac{E_{11}}{G_{13}} - \nu_{13} \right) \right] \tag{48}$$

$$K_3 = \frac{1}{2} \left[\alpha_s \frac{E_{11}}{G_{13}} - \frac{\alpha_a}{3} \left(\frac{E_{11}}{G_{13}} - \nu_{13} \right) \right] \tag{49}$$

Since the structure is statically determinate, the axial stress distribution can be readily obtained by appropriate substitution for N, M and Q in Equation (33A). The result for the fixed end is

$$\sigma_{xx} = - \frac{qL^2 z}{2I} \left\{ 1 + \alpha_a \frac{2}{3} k_x \frac{H^2}{L^2} \left(\frac{3}{20} - \frac{z^2}{H^2} \right) \right\} \tag{33B}$$

The lateral deflection can be conveniently expressed as follows.

$$W = \delta_i - \frac{q}{E_{11}I}\left[\left(\frac{L^3}{6} + (K_i - K)c^2L\right)x + \frac{KH^2}{8}x^2 - \frac{x^4}{24}\right]; \quad i = 1, 2, 3. \tag{50}$$

The constants δ_i (i = 1, 2, 3) are the beam tip deflections; they are found from

$$\delta_i = \frac{qL^4}{8E_{11}I}\left[1 + (2K_i - K)\left(\frac{H}{L}\right)^2\right]; \quad i = 1, 2, 3. \tag{51}$$

The constant K is defined in Equation (41).

The present solutions correspond to setting all the tracer constants to unity; they are exact for the end conditions imposed. The designation C1, C2 and C3 has been chosen to correspond to the order of increasing stiffness of the end restraint. The coefficients of $(H/L)^2$ for C1, C2 and C3 are 18.08, 12.15 and 8.19, respectively, for the orthotropic material chosen.

If K_i and K are set to zero in the above equations, the Bernoulli-Euler results are obtained. This approximation, of course, overestimates stiffness. The Timoshenko theory result is obtained from the C1 case by setting $\alpha_s = 1$ and $\alpha_a = \alpha_n = 0$ in Equations (41) and (47). The coefficient of $(H/L)^2$ is 15 for the same material considered earlier. It is interesting to note that Timoshenko theory underestimates maximum deflection in this case.

Bernoulli-Euler theory tends to always overestimate stiffness. Timoshenko theory, however, in light of the results presented here, may either provide an overestimate or underestimate of the maximum deflection,

depending upon the problem under consideration. It is therefore, "unreliable" in this sense.

A related problem is a cantilever beam subjected to a linearly varying distributed load that varies from zero at the free end to q at the fixed end. The exact solution is given in Reference 22. For an isotropic beam with Cl restraint at the fixed end, the tip deflection is

$$\delta = \frac{qL^4}{30EI}\left\{1 + \frac{H^2}{4L^2}\left[2\alpha_a + 5\alpha_n + 5\alpha_s\,(1+\nu)\right] \underline{- \frac{\alpha_s}{4}\,(1+\nu)\,(\frac{H}{L})^4}\right\} \qquad (52)$$

If the present theory is used, the underlined term is not obtained. For $L/H > 2$, this term is negligible. For practical purposes, therefore, the present theory results are indistinguishable from the exact ones.

Clamped Beam

Unlike the previous examples, the clamped beam is statically indeterminate. Three solutions were found corresponding to the three definitions of clamping given in Equations (43)-(45). They may be expressed in a common form. It is convenient to place the origin of coordinates at midspan and use the semi-length ℓ. The bending moment distribution is

$$M = \frac{q}{2}\,(\ell^2 - x^2) - M_o \qquad (53)$$

M_o is the end fixing moment, which is positive if it tends to reduce the end rotation due to the uniform load.

The expression for the lateral axis deflection is

$$W = \frac{1}{E_{11}I}\left[\frac{q}{4}\left(\frac{5}{6}\ell^4 - \ell^2x^2 + \frac{x^4}{6}\right)\right.$$

$$\left. + \left(\frac{KH^2q}{8} - \frac{M_o}{2}\right)(\ell^2 - x^2)\right] \qquad (54A)$$

The redundant end fixing moment is different for each type of clamping. It can be written in the common form

$$M_o = \frac{qL^2}{12}\left[1 + 3\left(\frac{H}{L}\right)^2 (K - K_i)\right] \; ; \; i = 1, 2, 3. \qquad (55)$$

The axial stress distribution is also different for each type of clamping.

$$\sigma_{xx} = \frac{qL^2z}{4I}\left\{\frac{1}{6} - \frac{x^2}{2\ell^2} - (K - K_i)\frac{H^2}{L^2} + k_x\frac{H^2}{L^2}\left(\frac{4z^2}{H^2} - \frac{3}{5}\right)\right\} \qquad (54B)$$

As before, L is the total beam length and K_1-K_3 are defined in Equations (47)-(49). The occurrence of different end moment values is due to the statically indeterminate nature of the structure. The present theory yields the exact solutions to this problem for each form of clamping.

An end moment ratio as a function of beam slenderness is plotted in Figures 3 and 4 for isotropic and orthotropic materials, respectively.The subscript "B-E" refers to the value from Bernoulli-Euler theory. Bernoulli-Euler and Timoshenko theories give identical predictions. The present theory, however, which is exact, predicts fundamentally different behavior that differs for each type of clamping. Departures from classical

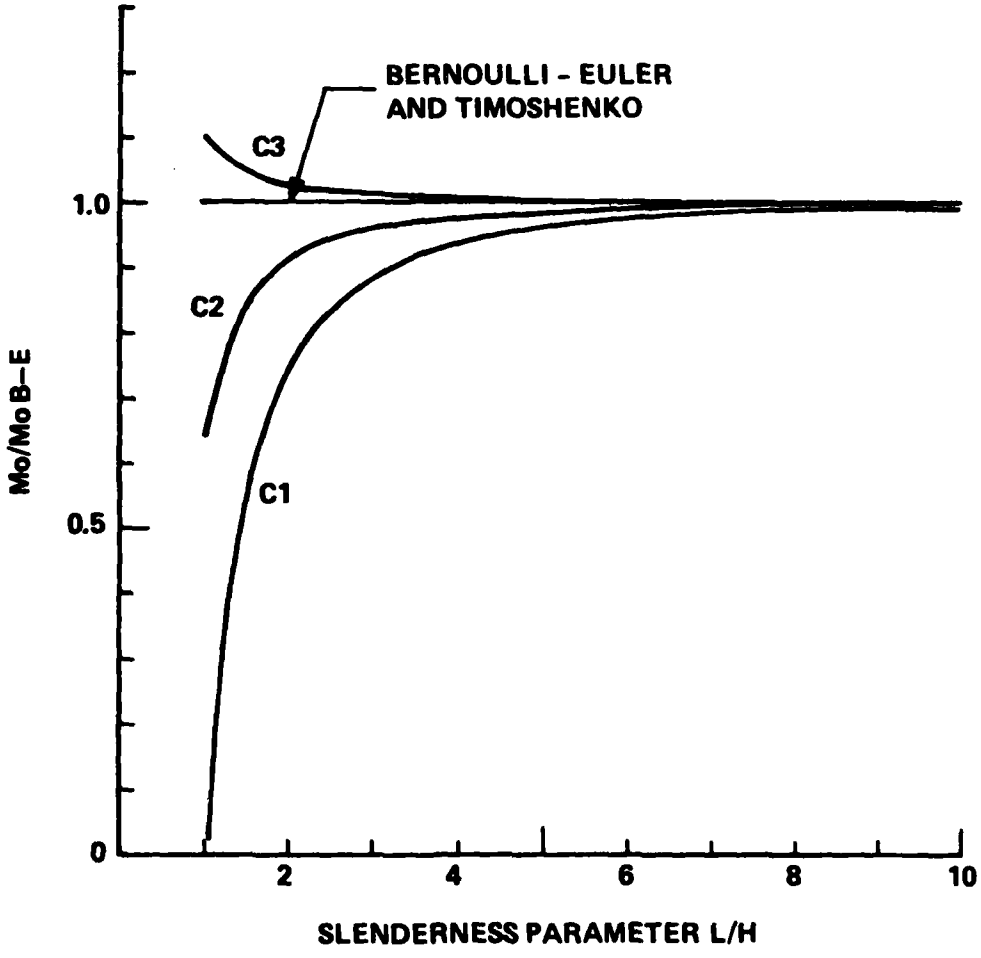

Figure 3. End Moment Ratio for a Clamped Isotropic Beam

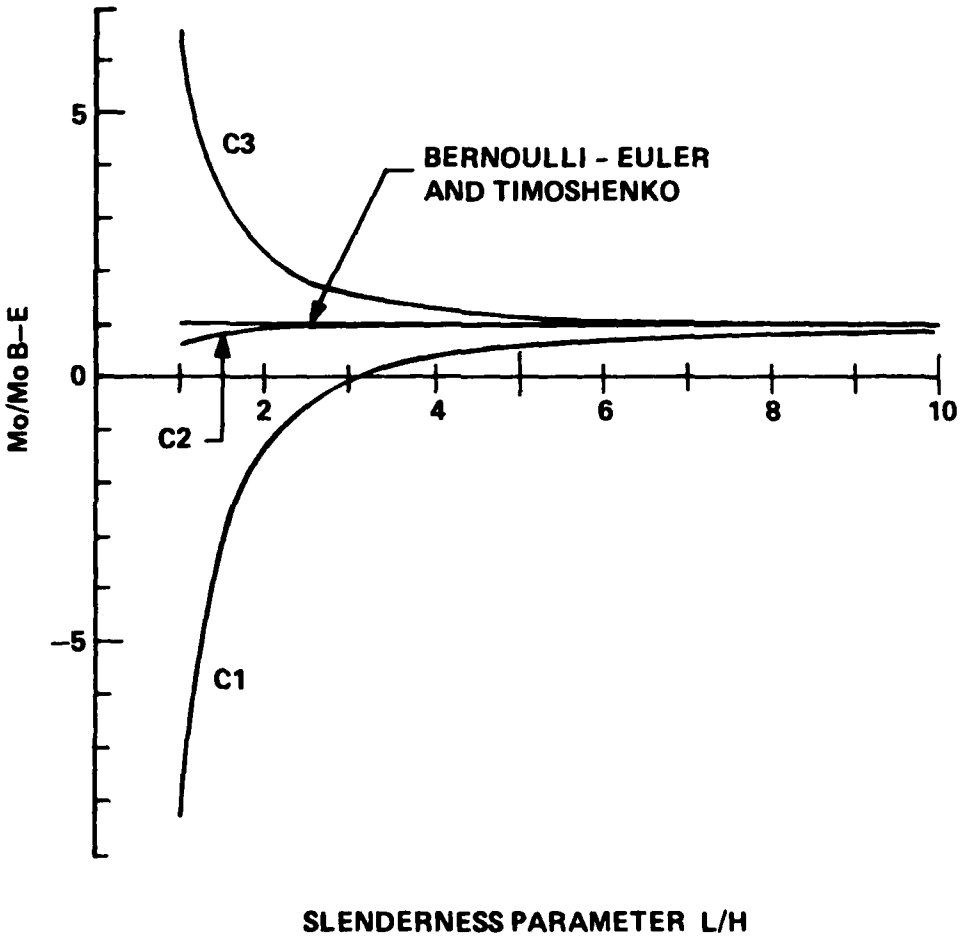

Figure 4. End Moment Ratio for a Clamped Orthotropic Beam, $E_{11}/G_{13} = 30$

theory are much greater for beams made of the typical orthotropic material.

An interesting phenomenon occurs for C1 restraint of orthotropic beams. The end fixing moment acutally reverses sign for relatively deep beams. This intriguing situation is explained by the fact that the end rotation is forced to zero by a combination of shear force and bending moment. By virtue of symmetry of loading and structure, the end shear force is fixed by vertical force equilibrium considerations alone. Consequently, only the end moment is available for controlling rotation. Since the transverse shear stiffness to extensional stiffness ratio is quite low for this material, a reversal of moment is required to offset the large shear strain at the axis for shorter C1-supported beams. A countertrend for C3-supported beams reflects the increased relative difficulty of achieving this rigid type of fixity as shorter beams are considered.

Propped Cantilever Beam

Let the origin of coordinates be the simply supported end of a propped cantilever beam and $x = L$ be the clamped end. Three cases corresponding to the three types of clamping have been considered. The bending moment is

$$M = Q_o x - q \frac{x^2}{2} \tag{56}$$

Q_o is the shear force (reaction) at the propped end $x = 0$. It can be expressed in common form as follows for each type of clamping.

$$Q_o = \frac{qL}{8}\left[1 + 2\frac{H^2}{L^2}\left(K_i - \frac{K}{2}\right)\right] / \left(\frac{1}{3} + \frac{K_i}{4}\frac{H^2}{L^2}\right);\ i=1,2,3. \quad (57)$$

The lateral axis deflection and the axial stress distribution are given by

$$W = \frac{1}{E_{11}I}\left[\frac{Q_o x}{6}(L^2 - x^2) - \frac{qx}{24}(L^3 - x^3) + \frac{K}{8}H^2 qx(L - x)\right] \quad (58)$$

$$\sigma_{xx} = \frac{qLxz}{I}\left[\frac{\left(\frac{1}{8} - \frac{x}{6L}\right) + \frac{1}{8}\frac{H^2}{L^2}\left\{2K_i - K - \frac{x}{L}K_i\right\}}{\left(\frac{1}{3} + \frac{K_i}{4}\frac{H^2}{L^2}\right)}\right] \quad (56A)$$

$$+ k_x\ q\left(4\frac{z^3}{H^3} - \frac{3}{5}\frac{z}{H}\right)$$

End moment ratio plots appear in Figures 5 and 6 for isotropic and orthotropic beams, respectively. for this indeterminate structural system, Bernoulli-Euler and Timoshenko theories predict different behavioral trends. The present theory predictions are again exact for this problem, as will be the case always for uniformly distributed loadings.

Cl-supported orthotropic beams again exhibit a reversal of sign of the end fixing moment similar to the clamped case. Timoshenko theory, which approximates this end fixity condition, displays a similar trend, but does not predict an actual reversal for values of slenderness parameter shown.

Concluding Remarks

Several representative static applications which illustrate the use

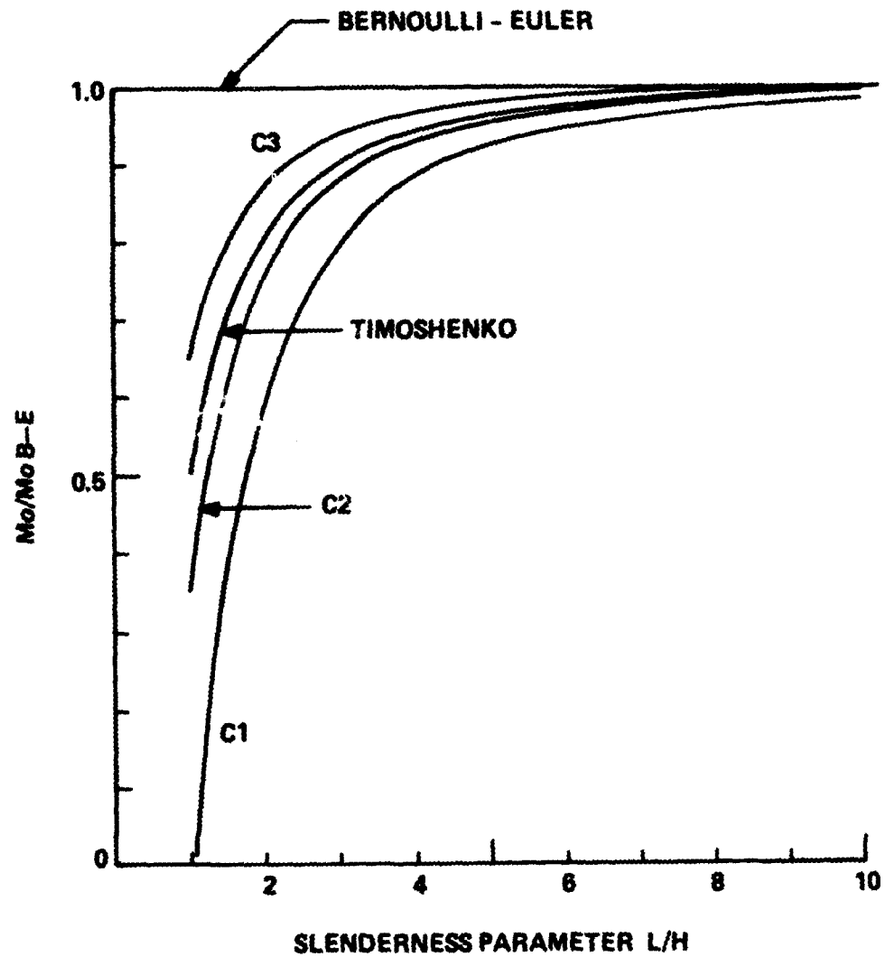

Figure 5. End Moment Ratio for a Propped Cantilever Isotropic Beam

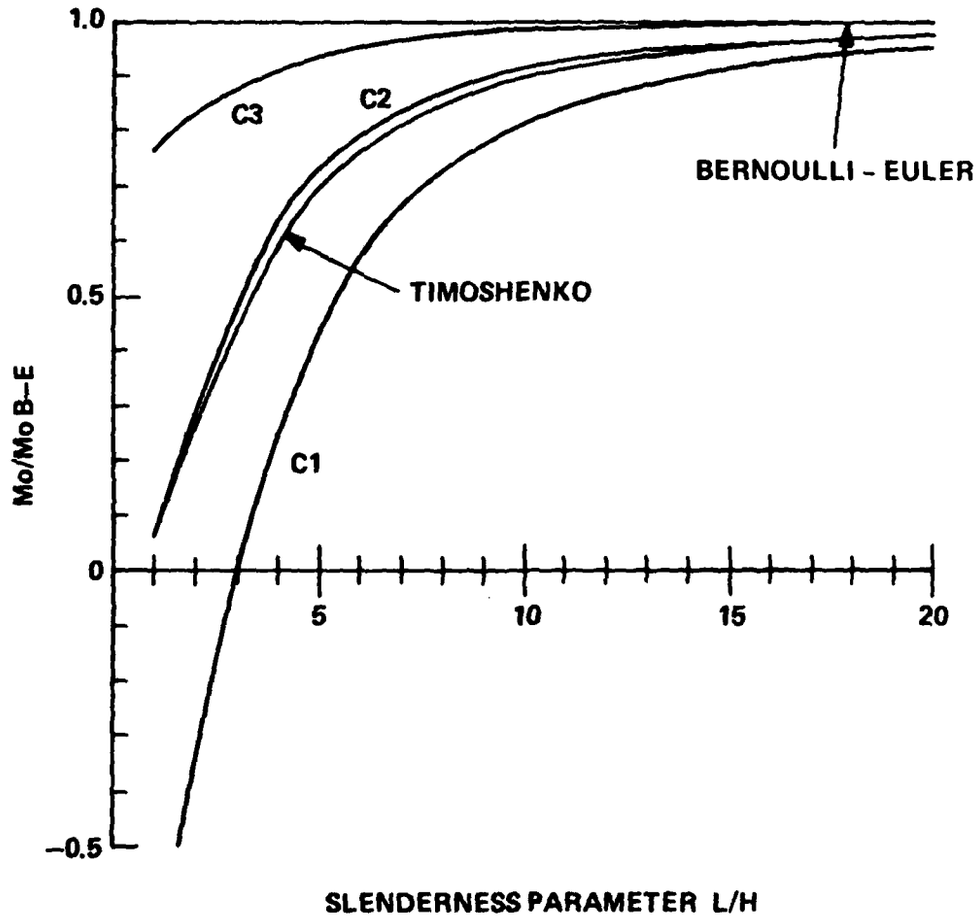

Figure 6. End Moment Ratio for a Propped Cantilever Orthotropic Beam, $E_{11}/G_{13} = 30$

of the new equations have been studied. The additional effects are seen to be more pronounced for statically indeterminate and orthotropic structures. Furthermore, the three elementary clamping model solutions indicate that care must be devoted to matching mathematical descriptions of boundary restraint with practical end restraint achieved in tests or structural assemblies. The sensitivity of the response to boundary restraint modeling is substantial for orthotropic structures. Consequently, the next chapter is devoted to a study of this issue.

CHAPTER VI

AN APPROACH TO ACHIEVE IDEAL CLAMPING

Preliminary Remarks

The static response of a clamped beam under uniformly distributed loading is extremely sensitive to the precise definition of the boundary conditions. This sensitivity is more pronounced if the beam is orthotropic. None of the three elementary models for the clamped end satisfy exactly the generally accepted definition of zero displacement at the fixed end. This fact is illustrated in Figure 7. It shows clamped end cross section warping for a typical orthotropic beam with L/H = 4. In this Chapter, an approach to eliminate the warping at the ends, thereby achieving ideal clamping, is described.

Analysis

The analysis is based on the principle of superposition. The first part of the solution is taken to be one of the elementary clamping models. To this solution a second solution for the beam bent by prescribed end displacements is added. The boundary displacements are chosen such that they nullify the warping due to the elementary clamping model. Any of the three elementary models may be chosen as the starting point. However, for the purpose of illustration, the C1 clamping model solution is taken here as a starting point. According to this solution, the clamped end axial displacement components are

$$u_1 = u(x = \pm \ell) = \frac{Q_o z^3}{6E_{11}I}\left(\nu_{13} - \frac{E_{11}}{G_{13}}\right)$$

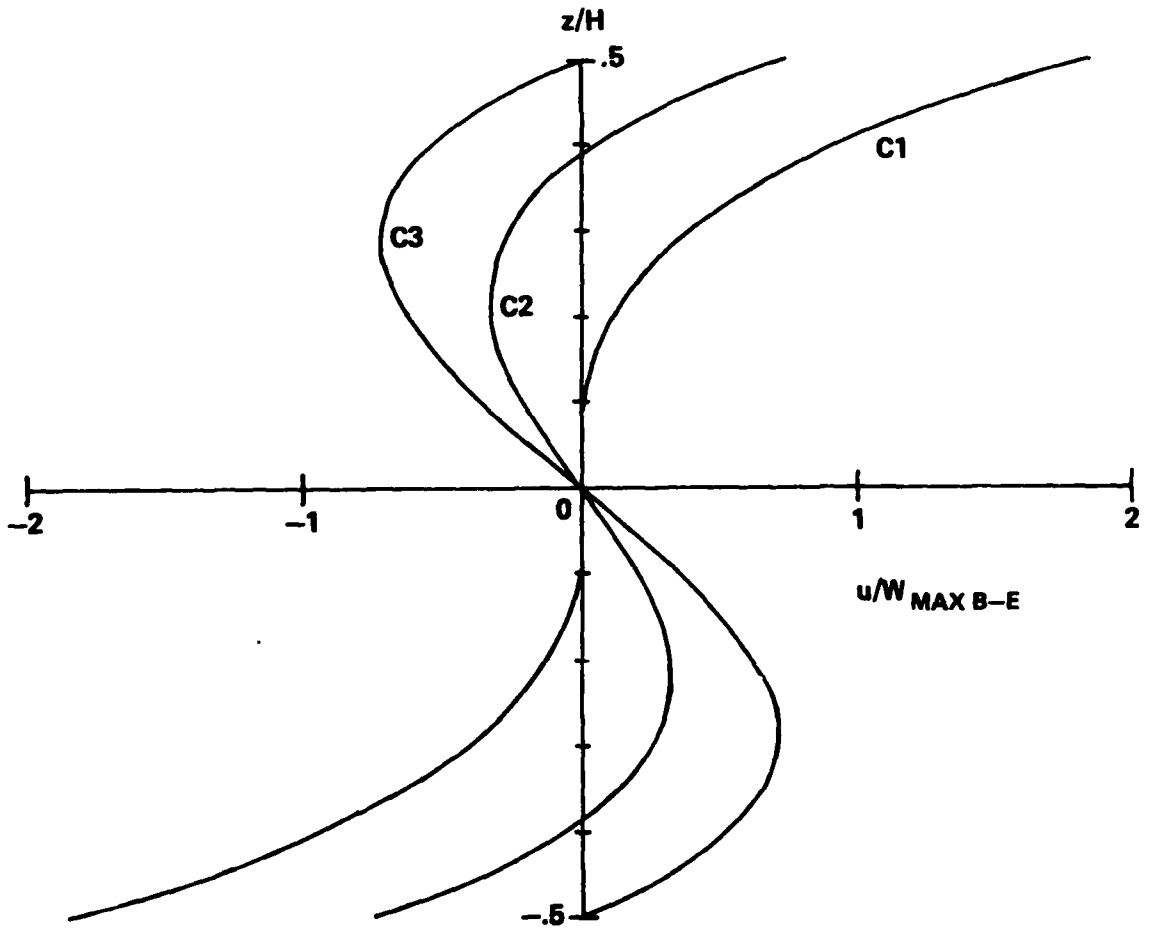

Figure 7. Cross Section Warping at the Fixed End for a Clamped Orthotropic Beam, E_{11}/G_{13} = 30, L/H = 4

$$w_1 = w(x = \pm \ell) = -\frac{\nu_{13} M_o z^2}{2E_{11} I} \tag{59}$$

The second part is a solution to the following boundary value problem:

$$\begin{aligned} \bar{u} + u_1 &= 0 \qquad \text{at } x = \pm \ell \\ \bar{w} + w_1 &= 0 \qquad \text{at } x = \pm \ell \end{aligned} \tag{60}$$

$\bar{u}$ and $\bar{w}$ are prescribed boundary displacements.

$$\sigma_{xz} = \sigma_{zz} = 0 \qquad \text{on} \quad z = \pm c \text{ for all } x \tag{61}$$

The addition of the two solutions leads to a refined clamping model which will be referred as C4.

This boundary value problem is solved with the aid of the principle of virtual complementary work. This principle is appropriate for problems with prescribed displacement boundary conditions. The statement is

$$\int_{-\ell}^{\ell} \int_{-c}^{c} \left\{ \varepsilon_{xx} \, \delta\sigma_{xx} + \varepsilon_{zz} \, \delta\sigma_{zz} + \gamma_{xz} \, \delta\sigma_{xz} \right\} dx dz$$

$$- \int_{-c}^{c} \bar{u} \, \delta\sigma_{xx} \Big|_{-\ell}^{\ell} dz - \int_{-c}^{c} \bar{w} \, \delta\sigma_{xz} \Big|_{-\ell}^{\ell} dz = 0 \tag{62}$$

The principle requires stresses which satisfy the equilibrium equations

and stress boundary conditions. The following stress field is selected.

$$\sigma_{xx} = Bz + f_2(x)\,(z^3 - \frac{3}{5}\,c^2 z) \tag{63}$$

$$\sigma_{xz} = \frac{f_{2,x}}{20}\,(6c^2z^2 - c^4 - 5z^4)$$

$$\sigma_{zz} = \frac{f_{2,xx}}{20}\,z(z^2 - c^2)^2$$

B is an arbitrary constant and $f_2(x)$ is an arbitrary function to be determined by application of the principle. The distribution of σ_{xx} has been selected based on the physical nature of the problem. σ_{xz} and σ_{zz} are then obtained by using the equilibrium equations (25) and (26) and the boundary conditions given in Equations (61). The use of assumed solutions employing free functions is due to Kantorovich[50].

Substitution of Equations (59) and (63) into (62) leads to the following functional:

$$\int_{-\ell}^{\ell}\int_{-c}^{c}\left[\left\{\frac{Bz}{E_{11}} + \frac{f_2}{E_{11}}\,(z^3 - \frac{3c^2z}{5}) - \frac{\nu_{13}}{E_{11}}\,\frac{f_{2,xx}}{20}\,z(z^2 - c^2)^2\right\}\left\{z\delta B + (z^3 - \frac{3c^2z}{5})\delta f_2\right\}\right.$$

$$\left. + \left\{\frac{f_{2,xx}}{20E_{33}}\,z(z^2 - c^2)^2 - \frac{\nu_{13}}{E_{11}}\,Bz - \frac{\nu_{13}}{E_{11}}\,f_2(z^3 - \frac{3c^2z}{5})\right\}\left\{\delta f_{2,xx}\,\frac{z(z^2 - c^2)^2}{20}\right\}\right.$$

$$+\left\{\frac{f_{2,x}}{20G_{13}}(6c^2z^2-c^4-5z^4)\right\}\left\{\frac{\delta f_{2,x}}{20}(6c^2z^2-c^4-5z^4)\right\}\Bigg]\,dx\,dz$$

$$-\int_{-c}^{c}\frac{Q_o}{6E_{11}I}\left(\frac{E_{11}}{G_{13}}-\nu_{13}\right)z^3\left\{z\,\delta B+\left(z^3-\frac{3}{5}c^2z\right)\delta f_2\right\}\Bigg|_{-\ell}^{\ell}dz$$

$$-\int_{-c}^{c}\frac{\nu_{13}M_o z^2}{2E_{11}I}\left\{\frac{\delta f_{2,x}}{20}(6c^2z^2-c^4-5z^4)\right\}\Bigg|_{-\ell}^{\ell}dz=0 \qquad (62A)$$

Simplification and rearrangement of the terms of Equation (62A) results in

$$\int_{-\ell}^{\ell}\left\{\frac{8c^7f_2}{175E_{11}}-\frac{32c^9k_x}{7875}f_{2,xx}+\frac{16c^{11}}{86625E_{33}}f_{2,xxxx}\right\}\delta f_2dx$$

$$+\left[\frac{2\pi c^3B}{3E_{11}}-\frac{16c^7\nu_{13}}{2100}f_{2,x}+\frac{2}{5}\left(\nu_{13}-\frac{E_{11}}{G_{13}}\right)\frac{Q_o}{6E_{11}I}c^5\right]\delta B\Bigg|_{-\ell}^{\ell}$$

$$+\left[\frac{16c^{11}}{86625E_{33}}f_{2,xx}-\frac{16}{2100}\frac{\nu_{13}c^7B}{E_{11}}+\frac{16\nu_{13}f_2c^9}{7875}-\frac{4\nu_{13}M_o}{525E_{11}I}c^7\right]\delta f_{2,x}\Bigg|_{-\ell}^{\ell}$$

$$+\left[\frac{-16c^{11}}{86625E_{33}}f_{2,xxx}-\frac{16\nu_{13}c^9}{7875}f_{2,x}+\frac{16c^9f_{2,x}}{7875G_{13}}\right.$$

$$\left.+\frac{8c^7}{175}\cdot\frac{Q_o}{6E_{11}I}\left(\nu_{13}-\frac{E_{11}}{G_{13}}\right)\right]\delta f_2\Bigg|_{-\ell}^{\ell}=0 \qquad (64)$$

The above functional yields the Euler equations

$$\mu c^4 f_{2,xxxx} - 22 k_x c^2 f_{2,xx} + \frac{990}{4} f_2 = 0 \qquad (65)$$

$$B + \frac{3c^2}{5\ell} \frac{Q_o}{6I} \left(\nu_{13} - \frac{E_{11}}{G_{13}}\right) - \frac{2}{175} \frac{\nu_{13} c^4}{\ell} f_{2,x} = 0 \qquad (66)$$

where μ is the ratio E_{11}/E_{33}.

The *natural boundary conditions are*

$$\mu f_{2,xx} c^2 - \frac{165}{4} \frac{B}{c^2} \nu_{13} + 11\nu_{13} f_2 - \frac{165}{4} \frac{\nu_{13} M_o}{Ic^2} = 0 \qquad (67)$$

$$\mu f_{2,xxx} \frac{c^4}{\ell} + 11\left(\nu_{13} - \frac{E_{11}}{G_{13}}\right) \frac{c^2}{\ell} f_{2,x} - \frac{990}{4\ell} \left(\nu_{13} - \frac{E_{11}}{G_{13}}\right) \frac{Q_o}{6I} = 0 \qquad (68)$$

Equations (65)-(68) have precise physical significance. The Euler Equations are the relations to be satisfied for the kinematic compatibility of the strains. Equations (67)-(68) are displacement type boundary conditions. The first represents transverse shear strain. The second represents axial strain.

The solution to Equation (65) may be chosen as $e^{\frac{mx}{\ell}}$, which yields the following characteristic equation

$$\mu\left(\frac{c}{\ell}\right)^4 m^4 - 22k_x \left(\frac{c}{\ell}\right)^2 m^2 + \frac{990}{4} = 0 \qquad (65A)$$

Consequently

$$m^2 = \left\{ \frac{22k_x \mp \sqrt{484k_x^2 - 990\mu}}{2\mu} \right\} \frac{\ell^2}{c^2} \qquad (65B)$$

The roots are real, equal or complex depending on whether

$$k_x^2/\mu > 2.045, = 2.045, < 2.045$$

In terms of elastic constants the above is

$$\left\{ \frac{E_{11}}{2G_{13}} - \nu_{13} \right\}^2 /(E_{11}/E_{33}) > 2.045, = 2.045, < 2.045$$

For an orthotropic material with properties $E_{11}/G_{13} = 30$, $E_{11}/E_{33} = 15$ and $\nu_{13} = 0.3$, $k_x^2/\mu = 14.406$. Consequently, the roots are real and the most general form of solution to Equation (65) may be written as

$$f_2 = C \cosh \frac{m_1 x}{\ell} + D \cosh \frac{m_2 x}{\ell} + C' \sinh \frac{m_1 x}{\ell} + D' \sinh \frac{m_2 x}{\ell}$$

Since σ_{xx} is symmetric with respect to x, the above reduces to

$$f_2 = C \cosh \frac{m_1 x}{\ell} + D \cosh \frac{m_2 x}{\ell} \qquad (69)$$

m_1 and m_2 are to be obtained from

$$m_1, m_2 = \left\{ \frac{22k_x \mp \sqrt{484k_x^2 - 990\mu}}{2\mu} \right\}^{\frac{1}{2}} \frac{\ell}{c} \tag{70}$$

For an isotropic material $k_x^2/\mu = 1$. The roots are $(\pm 3.656 \frac{\ell}{c} \pm 1.528 \frac{\ell}{c})$. The solution form is, therefore selected as

$$f_2 = C \cosh \frac{m_1 x}{\ell} \cos \frac{m_2 x}{\ell} + D \sinh \frac{m_1 x}{\ell} \sin \frac{m_2 x}{\ell} \tag{71}$$

where m_1 and m_2 are given by

$$m_1 = 3.656 \frac{\ell}{c}$$

$$m_2 = 1.538 \frac{\ell}{c} \tag{70A}$$

It is interesting to note that for isotropic materials, the solution is independent of the material constants E, G and ν. Also, there exists a possibility of complex and equal roots for orthotropic materials as indicated by Equation (65B). However, this situation is not usually encountered in practical situations. The practical ranges for the parameters k_x and μ are 20-50 and 10-25, respectively.

Results and Discussion

The axial stress distribution in C4 restraint beam is

$$\sigma_{xxC4} = \left[\frac{q(\ell^2 - x^2)}{2} - M_{o1} \right] \frac{z}{I} + \frac{k_x q}{3I} \left(z^3 - \frac{3}{5} c^2 z \right)$$

$$+ Bz + f_2 (z^3 - \frac{3}{5} c^2 z) \qquad (71)$$

M_{o1} is the end moment due to C1 clamping. From Equation (55) it may be written as

$$M_{o1} = \frac{q\ell^2}{3} \left[1 - 3 \frac{c^2}{\ell^2} \left(\frac{\nu_{13}}{2} + \frac{k_x}{5} \right) \right] \qquad (72)$$

Equations (71), (72) and (66) can be combined to cast σ_{xxC4} into the following convenient form:

$$\frac{\sigma_{xxC4}}{\sigma_{B-E}} = \frac{\sigma_{xxC2}}{\sigma_{B-E}} + \underline{\left[\frac{2}{175} \nu_{13} \frac{c^4}{\ell} f_{2,x} z + f_2 (z^3 - \frac{3}{5} c^2 z) \right] \Big/ \sigma_{B-E}} \qquad (73)$$

σ_{B-E} is the maximum axial stress at the center according to Bernoulli-Euler theory and σ_{xxC2} is the axial stress distribution in C2 restraint beam. They are given by

$$\sigma_{B-E} = \frac{q\ell^2 c}{6I} \qquad (74)$$

$$\sigma_{xxC2} = \frac{z}{I} \left[\frac{q(\ell^2 - x^2)}{2} - \frac{q\ell^2}{3} \left(1 - \frac{6}{5} \nu_{13} \frac{c^2}{\ell^2} \right) \right] + \frac{k_x q}{3I} (z^3 - \frac{3}{5} c^2 z) \qquad (75)$$

The underlined term in Equation (73) represents a correction to be added to C2 stress distribution. This will be referred as local disturbance parameter in the subsequent text.

It is possible to show, for large values of L/H, that f_2 can be represented approximately by

$$f_2 = \bar{C}\, L/H\, e^{-m_1\bar{\xi}} + \bar{D}L/H\, e^{-m_2\bar{\xi}} \qquad (76)$$

$\bar{C}$ and $\bar{D}$ are constants and $\bar{\xi}$ is the dimensionless distance measured from the end.

$$\bar{\xi} = 1 - \frac{x}{\ell} \qquad (76A)$$

Equations (73) and (76) allow the following to be written

$$LDP = \frac{12}{175}\frac{c^3}{\ell^3}\left(\frac{z}{c}\right)\left\{\bar{C}m_1 e^{-m_1\bar{\xi}} + \bar{D}m_2 e^{-m_2\bar{\xi}}\right\} + 6\,\frac{c}{\ell}\left\{\bar{C}\, e^{-m_1\bar{\xi}} + \bar{D}e^{-m_2\bar{\xi}}\right\}\left\{\left(\frac{z}{c}\right)^3 - \frac{3}{5}\left(\frac{z}{c}\right)\right\} \qquad (77)$$

LDP refers to the local disturbance parameter.

An important conclusion can be reached by observation of the Equation (77). The local disturbance decays exponentially from the ends; for relatively slender beams, therefore, the solution due to C4 approaches C2 results in the interior zone. This decay phenomenon is well understood and is usually termed as an end effect or boundary layer effect[51]. The maximum value of the local disturbance parameter is shown graphically in Figure 8 for several length-to-depth ratios. Results are obtained from the complete expression (69). Another point of interest is the maximum axial stress at the edges and the influence of the orthotropicity on it. Figure

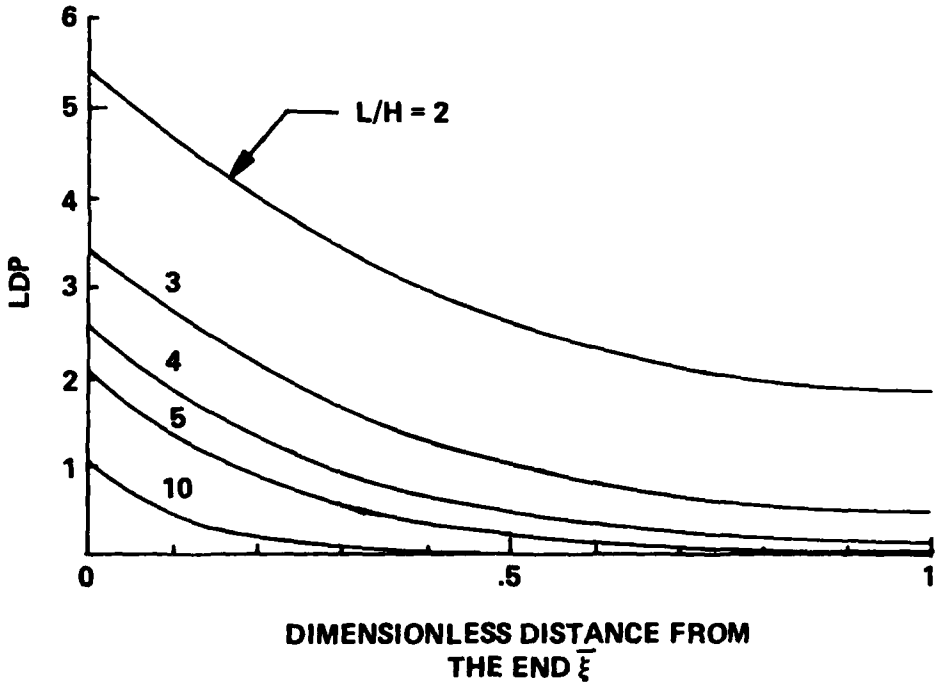

Figure 8. Local Effect Decay in a Clamped Orthotropic Beam, $E_{11}/G_{13} = 30$

9 provides this comparison. In the calculations, the ratio E_{11}/E_{33} is taken to be equal to $E_{11}/2G_{13}$ and E_{11}/G_{13} is varied between 10 to 50. The isotropic value is also shown for comparison.

The presence of a boundary zone near ends limits validity of the elementary theory to the interior zone. The lower of the two exponents m_1 and m_2 primarily governs the extent of the boundary zone. An approximate estimate of a decay length, or the dimension of the boundary zone, can be obtained by equating the corresponding term to e^{-3}, which is approximately 0.05 in value. The lower of the two roots m_1, is given by

$$m_1 = \left(\frac{22k_x - \sqrt{484k_x^2 - 990\mu}}{2\mu}\right)^{\frac{1}{2}} \frac{\lambda}{c} \qquad (78)$$

for orthotropic materials. The calculation of decay length is illustrated below.

$$e^{-\left\{\frac{22k_x - \sqrt{484k_x^2 - 990\mu}}{2\mu}\right\}^{\frac{1}{2}} \frac{x_d}{c}} = e^{-3} \qquad (79)$$

x_d is decay length and is obtained as 1.682 H. For isotropic materials, an approach similar to the above is followed starting from Equation (72). x_d is obtained as 0.410 H. It is independent of material constants.

Equation (79) indicates a strong dependence of the decay length on the material properties. The decay length defines limits for application of a decay type solution of the form given in Equation (76). A minimum of two decay lengths is required for the beam to be considered long so that corrections of the type in Equation (77) are applicable. Beams with

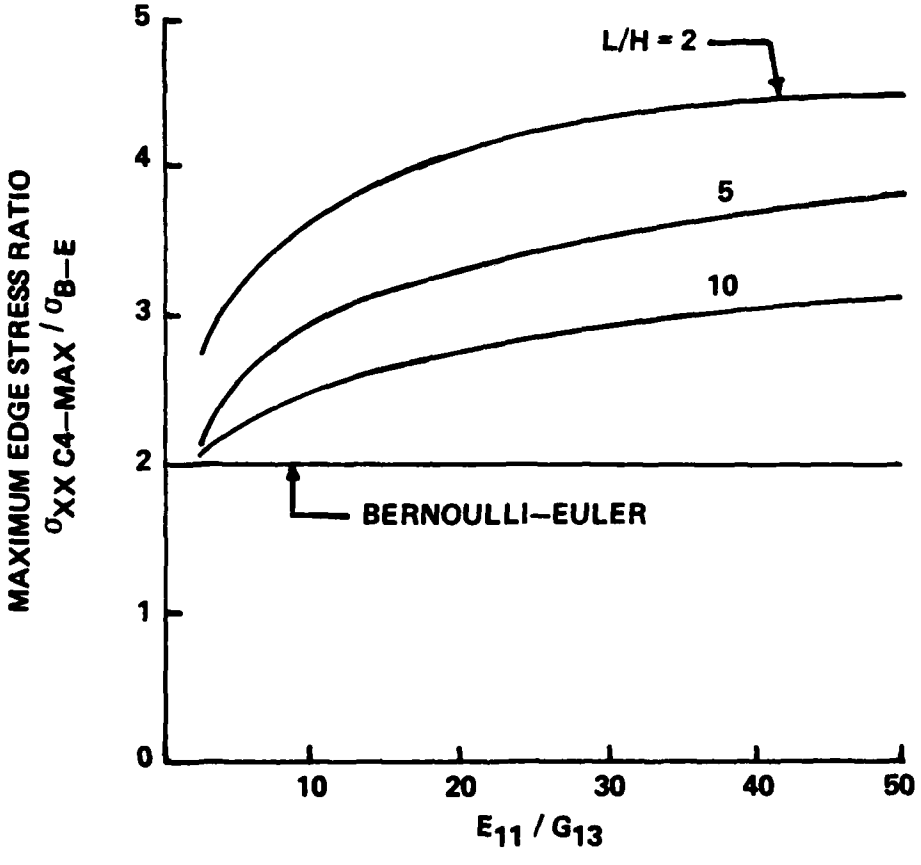

Figure 9. Maximum Edge Axial Stress Ratio in a Clamped Beam

lengths less than $2x_d$ must be considered short and a full solution of the type in Equation (71) should be used in the computations of refined clamping model solution.

An estimate of the clamped end warping displacement may be obtained by integration of the constitutive relation

$$u_{,x} = \frac{\sigma_{xx}}{E_{11}} - \frac{\nu_{13}}{E_{33}} \sigma_{zz} \tag{80}$$

u is nondimensionalized with respect to maximum deflection at the center according to Bernoulli-Euler theory for convenience and is expressed as

$$\frac{u(\xi,z)}{W_{\max B-E}} = \frac{u_{C2}}{W_{\max B-E}} + 48 \frac{H}{L} \left[\frac{2}{175} \left(\frac{H}{L}\right)^4 \nu_{13} \frac{z}{H} F_2 + 4 \frac{H^2}{L^2} \left(\frac{z^3}{H^3} - .15 \frac{z}{H}\right) \right.$$

$$\left. \left\{ \frac{C_1}{m_1} \sinh m_1 + \frac{D_1}{m_2} \sinh m_2 \right\} \frac{40_{13}}{5} \frac{H^4}{L^4} \frac{z}{H} \left(\frac{z^2}{H^2} - .25\right) \left(C m_1 \sinh m_1 + D m_2 \sinh m_2\right) \right] \tag{81}$$

u_{C2} is the axial displacement at the clamped end due to C2 restraint.

$$\frac{u_{C2}}{W_{\max B-E}} = 48 \frac{H}{L} \left\{ (K - K_2) \frac{z}{H} + \frac{2}{3} \left(\frac{E_{11}}{G_{13}} - \nu_{13}\right) \frac{z^3}{H^3} \right\}$$

$W_{\max B-E}$ is the maximum deflection at the center according to Bernoulli-Euler theory and is given by

$$W_{\max B-E} = \frac{qL^4}{384 E_{11} I} \tag{83}$$

The clamped end transverse displacement w is of secondary importance for the present study. It is usually Poisson's effect and therefore much smaller. It may be obtained, in a similar manner, by integrating

$$w_{,z} = \frac{\sigma_{zz}}{E_{33}} - \frac{\nu_{13}}{E_{11}} \sigma_{xx} \qquad (84)$$

The result is

$$\frac{w(\ell, z)}{W_{\max B-E}} = 16 \nu_{13} \frac{H^2}{L^2} \cdot \frac{z^2}{H^2} \cdot \left\{1 - 3 \frac{H^2}{L^2}\left(\frac{\nu_{13}}{2} + \frac{k_x}{5}\right)\right\}$$

$$+\frac{24}{5} \nu_{13} \frac{H^4}{L^4} \left(\frac{E_{11}}{G_{13}} - \nu_{13}\right) \frac{z^2}{H^2}$$

$$- \frac{96}{175} \nu_{13}^2 \frac{z^2}{H^2} \frac{H^6}{L^6} (C m_1 \sinh m_1 + D m_2 \sinh m_2)$$

$$-384 \nu_{13} \frac{H^4}{L^4} \left(\frac{z^4}{4H^4} - \frac{3}{40} \frac{z^2}{H^2}\right)(C \cosh m_1 + D \cosh m_2)$$

$$+ \frac{384}{5} \frac{E_{11}}{E_{33}} \cdot \frac{H^6}{L^6} \left(\frac{z^6}{6H^6} - \frac{z^4}{8H^4} + \frac{z^2}{32H^2}\right) (C m_1^2 \cosh m_1 + D m_2^2 \cosh m_2) \qquad (85)$$

The clamped end displacement components are shown in Table 1. It

can be concluded that the approach adopted in the present study provides a simple, reliable model for ideal clamping.

Since the stresses do not satisfy compatibility relations exactly, the above approach is not a unique way of determining the displacement components. It is, however, rational and the most direct.

Concluding Remarks

On the basis of the results presented above the following conclusions are reached.

1. A way of determining the boundary zone stresses is presented which indicates that the interior solution is best represented by C2 model.

2. It is demonstrated with confirmatory results that C4 model clamping is extremely good.

3. An estimate of end zone correction for long beams is provided through LDP. The region of local effects is quantified with the aid of the decay length; it is shown to be a strong function of material properties.

Table 1. Clamped End Displacements for an Orthotropic Beam with $E_{11}/G_{13} = 30$ and $L/H = 4$

z/H	$u/W_{max\ B-E}$		$w/W_{max\ B-E}$	
	C2	C4	C2	C4
- 0.5	- .7425	- 0.0018	.0315	0.0230
- 0.4	- .0594	0.0013	.0202	- 0.0212
- 0.3	- .2673	0.0006	0.0114	- 0.0293
- 0.2	- .3267	- 0.0004	0.0050	- 0.0190
- 0.1	- .2079	- 0.0006	0.0013	- 0.0057
- 0.0	- .0000	0.0000	.0000	0.0000

CHAPTER VII

VALIDATION OF THE THEORY

Preliminary Remarks

It is demonstrated in Chapter V that the new equations yield exact results or results that are indistinguishable from exact for the static examples considered. The loading is uniform in all but one case. A linearly varying load is considered in the exceptional case. The validity of the theory for arbitrarily varying load remains to be established. This is accomplished by completing the following three tasks:

(1). A thorough analysis to determine error estimates for the equations is presented.

(2). Reissner plate equations, specialized for planar bending, are demonstrated to be obtainable from the present equations.

(3). A quantitative demonstration for a classic benchmark problem is provided.

The benchmark problem is the response of a simply supported beam tc a sinusoidally distributed loading. Exact solutions for this problem appear in References 52 and 53, which facilitate a critical comparison. This is a generic problem which has been used as a test case by others. Predictions of the present theory are compared with the exact solutions using an approach which yields the range of validity of the theory as a function of beam length-to-depth ratio. Consequently, a direct indication of the applicability of the theory in this nonuniform loading situation is obtained for specific geometrical and stiffness characteristics.

A Consistency Analysis

Analytical Approach

The stresses given by the present theory are approximate for nonuniformly distributed loadings. It is desirable for the errors in the equations of equilibrium, compatibility equations and displacements to be consistent with the level of approximation of the stresses. To study this issue, a systematic order of magnitude analysis has been undertaken. The approach adopted and the underlying philosophy of the arguments presented are similar to those employed by Koiter[54, 55] in conjunction with a critical study of shell theory equations.

The magnitudes of spatial derivatives are estimated in the following way: a wavelength for the deformation is defined such that

$$\left| \frac{d\phi}{dx} \right| \approx O\left[\frac{\phi_m}{\lambda} \right] \tag{86}$$

ϕ_m is the maximum absolute value of the quantity ϕ in the region under consideration. λ is associated with the wavelength of load variation and the wavelength of deformation. Derivatives with respect to z are dealt with in a similar way.

$$\left| \frac{d\phi}{dz} \right| = O\left[\frac{\phi_m}{H} \right] \tag{87}$$

This implies that the smallest wavelength of deformation to be considered in the z direction is of O(H).

Let L be the measure of beam length. For applications of interest here, $L = O(\lambda)$ and H/λ is small.

In bending, σ_{xx} is the largest stress and is chosen as a convenient reference. Let σ be its maximum value. With the aid of Equations (22), (16)-(18), the following estimates are obtained:

$$|M| = O(\sigma H^2) \tag{87}$$

$$|Q| = O(\sigma H^2/\lambda) \tag{88}$$

$$|\sigma| = O(\frac{q\lambda^2}{H^2}) \tag{89}$$

Equations (23), (24) and (88) permit the estimation of σ_{xz} and σ_{zz}.

$$|\sigma_{xz}| = O(\sigma H/\lambda) \tag{90}$$

$$|\sigma_{zz}| = O(\sigma H^2/\lambda^2) \tag{91}$$

The nonclassical axial stress is represented by the underlined term in (33A). From the result (88), this may be estimated as

$$\sigma_{xxNC} = O(k_x \sigma H^2/\lambda^2) \tag{92}$$

The subscript "NC" refers to the nonclassical part of the stress.

Error Estimates for the Equilibrium Equations

In the classical theory, the stress equilibrium equations are satisfied identically. Due to the nonclassical bending stress in the present theory, stress equilibrium is not satisfied exactly for nonuniform loading. In order to facilitate the argument that follows, the stresses

σ_{xx} and σ_{xz} are written as

$$\sigma_{xx} = \sigma_{xxC} + \sigma_{xxNC} \tag{93}$$

$$\sigma_{xz} = \sigma_{xzC} + \sigma_{xzNC} \tag{94}$$

The subscript "C" refers to the classical part of stresses. It has been shown by Seewald[14] that σ_{xxNC} contains higher order terms in addition to the term used in the present theory for nonuniform loading. The representation for σ_{xx} is, therefore, valid up to terms of $O(\sigma \frac{H^2}{\lambda^2} k_x)$. The nonclassical term is seen to be a function of beam geometry and the relative stiffness represented by k_x. Equation (33A) for σ_{xx} provides a good approximation for small values of the combination $k_x H^2/\lambda^2$. The nonclassical axial stress effects are more significant for orthotropic materials with large k_x values.

Introduction of Equations (93) and (94) into (25) leads to

$$\sigma_{xzNC,z} + Q_{,xx} \frac{k_x}{I} (z^3 - \frac{3}{5} c^2 z) = 0 \tag{95}$$

The above permits to estimate the nonclassical shear stress to be of $O(k_x \sigma H^3/\lambda^3)$ and the error in equilibrium is of $O(\sigma \frac{H^2}{\lambda^3} k_x)$. It can be concluded, therefore, that the error in the stress field is at most of $O\sigma \frac{H^3}{\lambda^3} k_x)$. This is consistent with the original approximation for σ_{xx}.

Error Estimates in the Compatibility Equations

The relevant compatibility equation expressed in strains for planar bending is given by

$$\varepsilon_{xx,zz} + \varepsilon_{zz,xx} - \gamma_{xz,xz} = 0 \qquad (96)$$

It is convenient to express Equation (96) in terms of stresses.

$$\frac{1}{E_{11}} \left[\sigma_{xx,zz} + \frac{E_{11}}{G_{13}} \sigma_{zz,xx} - 2\left(\frac{E_{11}}{2G_{13}} - \nu_{13}\right) \sigma_{xz,xz} \right] = 0$$

Substitution of Equations (33A), (94), (23) and (24) into (96A) leads to

$$\frac{2\left(\frac{E_{11}}{2G_{13}} - \nu_{13}\right)}{E_{11}} \sigma_{xzNC,xz} + \underline{\frac{E_{11}}{E_{33}} \frac{Q_{,xxx}}{2E_{11}I} \left\{ \frac{z^3}{3} - c^2 z + \frac{2}{3} c^3 \right\}} = 0 \qquad (97)$$

The error represented by the underlined term is of $O\left[\frac{\sigma}{E_{33}} \frac{H^2}{\lambda^4}\right]$ and

the nonclassical shear stress is of $O\left(\sigma \frac{H^3}{\lambda^3} \frac{E_{11}}{E_{33}\left(\frac{E_{11}}{2G_{13}} - \nu_{13}\right)}\right)$.

It is concluded, therefore, that the error in the stress field is at most of $O\left\{\sigma \frac{H^3}{\lambda^3} \frac{E_{11}}{E_{33}\left(\frac{E_{11}}{2G_{13}} - \nu_{13}\right)}\right\}$. This is consistent with the original approximation for σ_{xx} in Equation (33A) and with the error estimate found for the equilibrium equations based upon Equation (95).

Error Estimates in Displacements

The error in u due to the error in stresses may be estimated from

equations (7) and (27).

$$u_{,x} = \left(\frac{\sigma_{xx}}{E_{11}} - \frac{\nu_{13}}{E_{11}}\,\sigma_{zz}\right) \tag{27A}$$

The error in W may be estimated from Equations (7) and (29)

$$w_{,x} = -u_{,z} + \frac{\sigma_{xz}}{G_{13}} \tag{29A}$$

The error in the stresses is of $0(\sigma \frac{H^3}{\lambda^3} k_x)$. Consequently, from Equations (27A) and (29A)

$$|\text{Error in } u| = 0(\frac{\sigma}{E_{11}} \frac{H^3}{\lambda^2} k_x) \tag{98}$$

$$|\text{Error in } w| = 0(\frac{\sigma}{E_{11}} \frac{H^3}{\lambda^2} k_x) \tag{99}$$

In view of Equations (98) and (99), it is justified to omit terms of the order indicated or higher in the expressions for displacements in Equations (31) and (32). The underlined terms in these equations are of $0(\frac{\sigma}{E_{11}} \frac{H^3}{\lambda^2})$ and $0(\frac{\sigma}{E_{11}} \frac{H^4}{\lambda^3})$, respectively. It is consistent to ignore these terms on the basis of the above discussion, so the approximations made are consistent.

Summary

The study of the order of magnitude of the errors in stresses, displacements, equilibrium equations and compatibility equations has demonstrated that the present equations are self-consistent and provides a valid approximation when the error terms are negligible. This implies (H/λ) is sufficiently small.

Relation to Reissner Theory

Reissner's plate theory equations are derived by using a complementary energy principle[37,38]. The definitions of the kinematic variables are clarified in the latter paper. Weighted kinematic variables naturally arise due to the approach used to develop the theory. For planar bending, they are given by

$$\tilde{W} = \frac{1}{2I} \int_{-c}^{c} w(c^2 - z^2)\, dz \tag{100}$$

$$\tilde{\phi} = \frac{1}{I} \int_{-c}^{c} uz\, dz \tag{101}$$

In the following derivation, the Reissner variables are constructed using present theory displacement expressions. Equations (100) and (31) permit w to be written as

$$\tilde{W} = W - \frac{3\nu_{13}M}{10E_{11}A} \tag{102}$$

$\tilde{\phi}$ is identical to ϕ_2 given in Equation (37).

$$\tilde{\phi} = -W_{,x} + \frac{3}{10A}\left(\frac{\nu_{13}}{E_{11}} + \frac{4}{G_{13}}\right) Q \tag{37A}$$

Equations (104), (37A) and (18) allow the following to be written.

$$\tilde{\phi} = -\tilde{W}_{,x} + \frac{6Q}{5G_{13}A} \tag{103}$$

The above is the Reissner relation for transverse shear strain. Intro-

duction of Equation (102) into (37A) and the use of Equation (18) results in

$$M = -E_{11} I \tilde{W}_{,xx} + \frac{2Q_{,x}c^2}{5}\left[\frac{E_{11}}{G_{13}} - \nu_{13}\right] \qquad (104)$$

By virtue of Equation (103), (104) may be rewritten in the following familiar form:

$$\tilde{\phi}_{,x} = \frac{M}{E_{11} I} + \frac{6}{5}\frac{Q_{,x}\nu_{13}}{E_{11} A} \qquad (105)$$

The above demonstrates that Reissner equations can be obtained from the present theory, a fact which further establishes the validity of the new equations. Also, it can be observed that all of the essential physical effects do not appear in the Reissner theory. This is because a knowledge of Reissner's variables does not permit the determination of the response throughout the structure. The effect of nonclassical axial stress on response is totally lost in the averaging process. However, by the use of the relations presented above, the response in terms of Reissner variables can be converted to obtain the response throught the structure

Beam Under Sinusoidal Loading

The problem under consideration is described in Figure 10. The two dimensional elasticity solution for it is given in Reference 52 for an isotropic material and in Reference 53 for an orthotropic material. A solution to the above problem has been obtained by using the present theory.

One half wavelength of the deformed beam is isolated for consideration and is treated as being simply supported. Although only one half wave length is considered the results are applicable to the case of general loading of the form $\sin \frac{n\pi x}{\lambda}$. This follows from the fact that each half wavelength may be considered separately with an appropriate reduction in beam length. The coordinate axes and notation are also given in Figure 10.

The boundary conditions to be enforced are given in Equations (39). In addition, the following are also satisfied:

$$\sigma_{xx}(0,z) = \sigma_{xx}(L,z) = 0 \tag{106}$$

The transverse displacement component W for the above boundary conditions is obtained by integrating Equation 35. The result is

$$W = -\frac{q_o \lambda^4}{16\pi^4 E_{11} I} \sin \frac{2\pi x}{\lambda} \left[1 + 4\pi^2 \frac{H^2}{\lambda^2} \left(\frac{4}{5} k_x + \frac{\nu_{13}}{2}\right)\right] \tag{107}$$

The stresses σ_{xx}, σ_{xz} and σ_{zz} at any section x, are given by

$$\sigma_{xx} = \left[-\frac{q_o \lambda^2 z}{4\pi^2 I} - \frac{q_o k_x}{3I}\left(z^3 - \frac{3}{5} c^2 z\right)\right] \sin \frac{2\pi x}{\lambda} \tag{108}$$

$$\sigma_{xz} = -\frac{\lambda q_o}{4\pi I}\left(c^2 - z^2\right) \cos \frac{2\pi x}{\lambda} \tag{109}$$

$$\sigma_{zz} = \frac{q_o}{I}\left(\frac{z^3}{6} - \frac{c^2 z}{2} - \frac{c^3}{3}\right) \sin \frac{2\pi x}{\lambda} \tag{110}$$

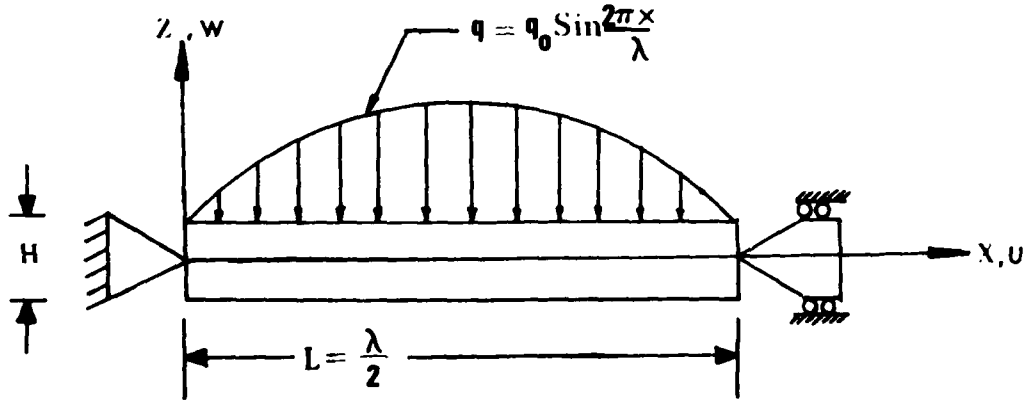

Figure 10. Simply Supported Beam under Sinusoidally Distributed Loading and Coordinate System

It is possible to obtain further refinements to the present theory by retaining the underlined terms in Equations (31) and (32). The constitutive relations are obtained as

$$N = E_{11} AU_{,x} + \frac{\nu_{13} c^3 A Q_{,x}}{3I} - \underline{\frac{\mu c^3}{6} Q_{,xxx}} \qquad (34A)$$

$$M = - E_{11} I W_{,xx} + (\frac{4}{5} k_x + \frac{\nu_{13}}{2}) c^2 Q_{,x} + \underline{\frac{13\mu}{280} Q_{,xxx} c^4} \qquad (35A)$$

The axial stress distribution is given by

$$\sigma_{xx} = \frac{Mz}{I} - \frac{Q_{,x} k_x}{3I} (z^3 - \frac{3}{5} c^2 z) + \underline{\frac{\mu Q_{,xxx}}{I} \left\{ - \frac{c^5}{18} - \frac{13c^4 z}{280} - \frac{z^5}{120} + \frac{c^2 z^3}{12} + \frac{c^3 z^2}{6} \right\}} \qquad (111)$$

The corresponding transverse deflection is given by

$$W = - \frac{q\pi^4}{16\pi^4 E_{11} I} \sin \frac{2\pi x}{\lambda} \left[1 + \frac{\pi^2 H^2}{\lambda^2} \left(\frac{4k_x}{5} + \frac{\nu_{13}}{2} \right) - \underline{\frac{13\mu}{280} \frac{\pi^2 H^4}{\lambda^4}} \right] \qquad (112)$$

The underlined terms in Equations (111) and (112) are the refinements to the present theory. Equations (109)-(110) will be called Approximation I and Equations (111) and (112) are Approximation II in the following discussion. The purpose of the above refinements is to determine the influence of the underlined terms in Equations (31) and (32) for this

problem.

Results and Discussion

The results are presented in a common format and appear in Figures 11-18. For the orthotropic beam, the following properties are chosen: $E_{11} = 25$, $E_{33} = 1$, $G_{13} = 0.5$ and $\nu_{13} = 0.25$. These are the material constants used in computing the exact solution in Reference 53.

The relative merits of each theory under consideration are assessed on the basis of the percentage error with respect to the exact solution. For the present purposes, a five percent error is assumed to be an acceptable limit. The range of beam length-to-depth ratio in which the error is less than five percent is considered the range of validity for the theory. The point at which a theory just exceeds the limit is a cut off or limit value of beam length-to-depth ratio.

The salient features of the results are listed below.

(1) Present approximations provide superior predictions for the response.

(2) The improvements are more significant for orthotropic beams.

(3) The Approximation II appears to be only marginally better than Approximation I. Approximation I is fully adequate for most applications, therefore.

In Figure 11 a curve that corresponds to Reissner theory equations (103) and (105) is also shown for comparison. The Reissner theory prediction appears to be in excellent agreement with the exact solution. However, this is illusory as the quantities under comparison are not the same. Reissner's displacement variable is a weighted average.

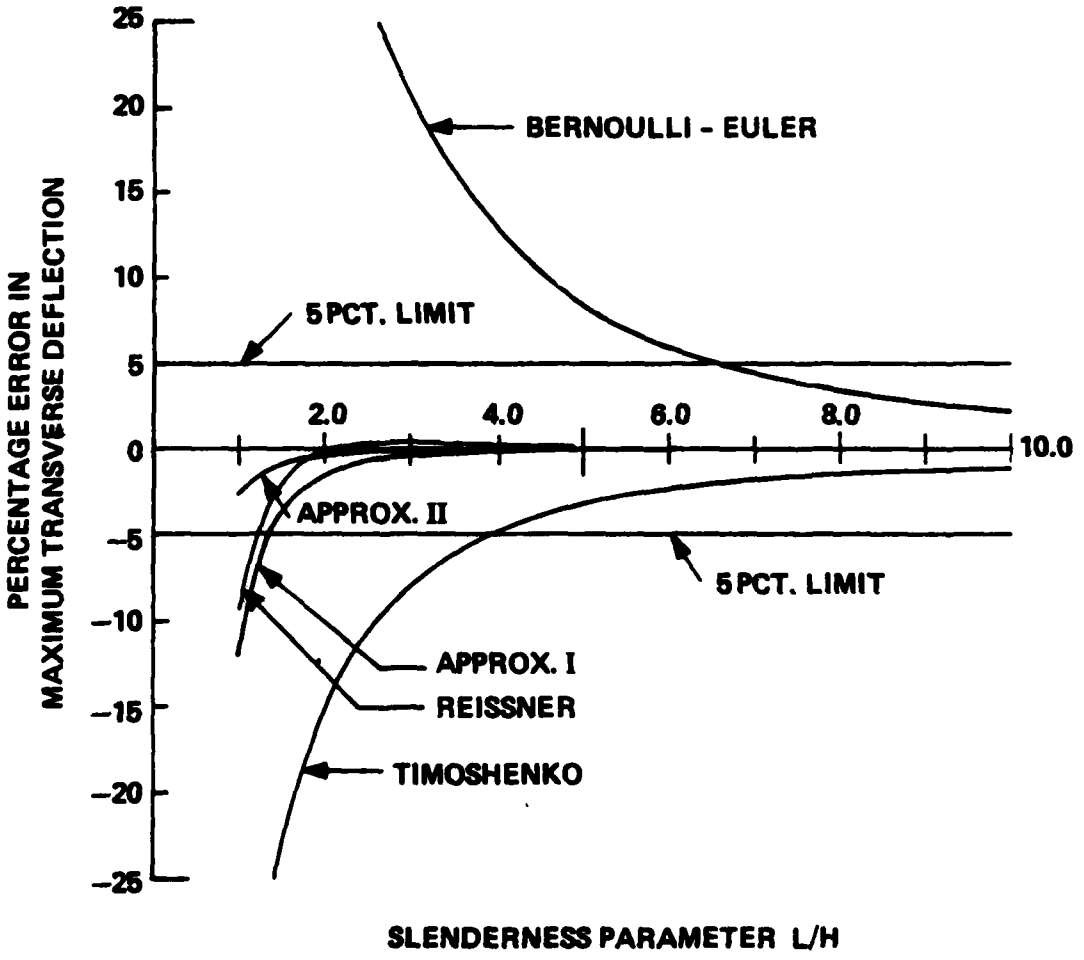

Figure 11. Percentage Error in Maximum Transverse Deflection for a Sinusoidally Loaded Isotropic Beam

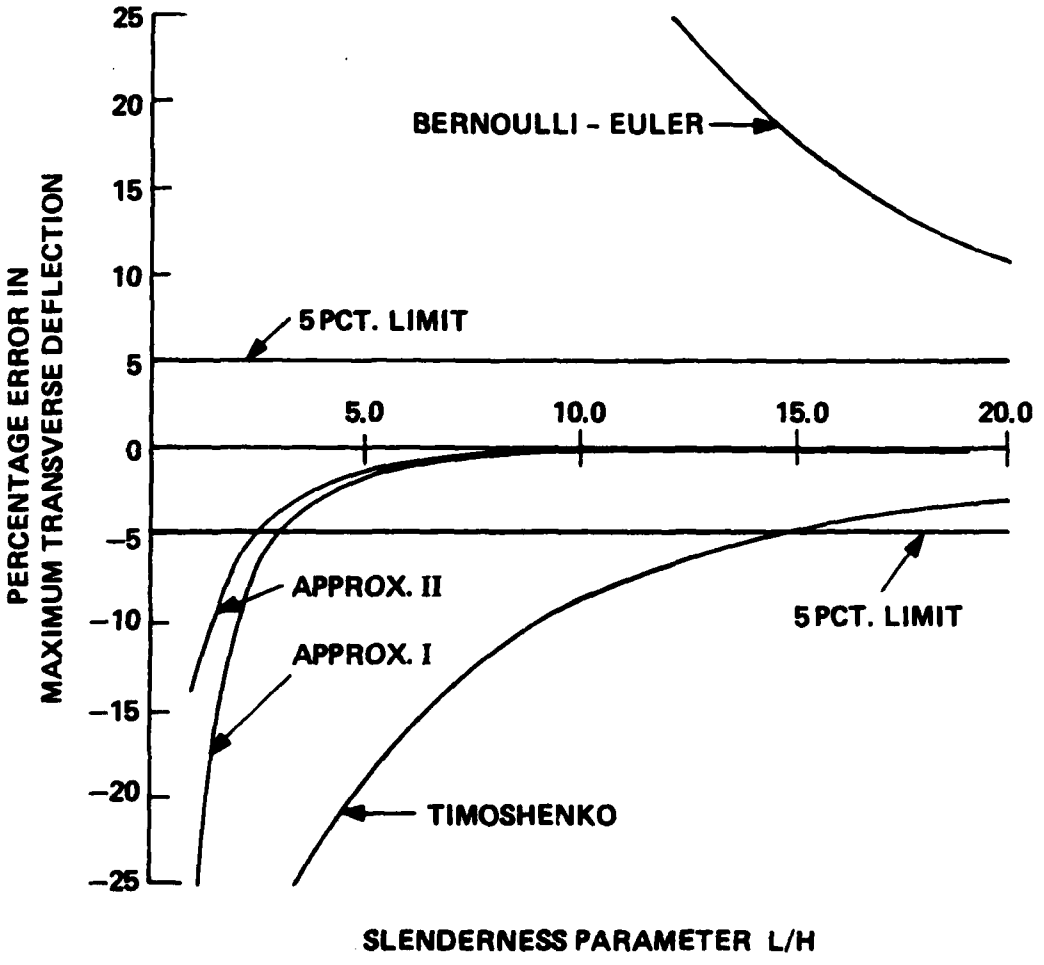

Figure 12. Percentage Error in Maximum Transverse Deflection for a Sinusoidally Loaded Orthotropic Beam, $E_{11}/G_{13} = 50$, $E_{11}/E_{33} = 25$

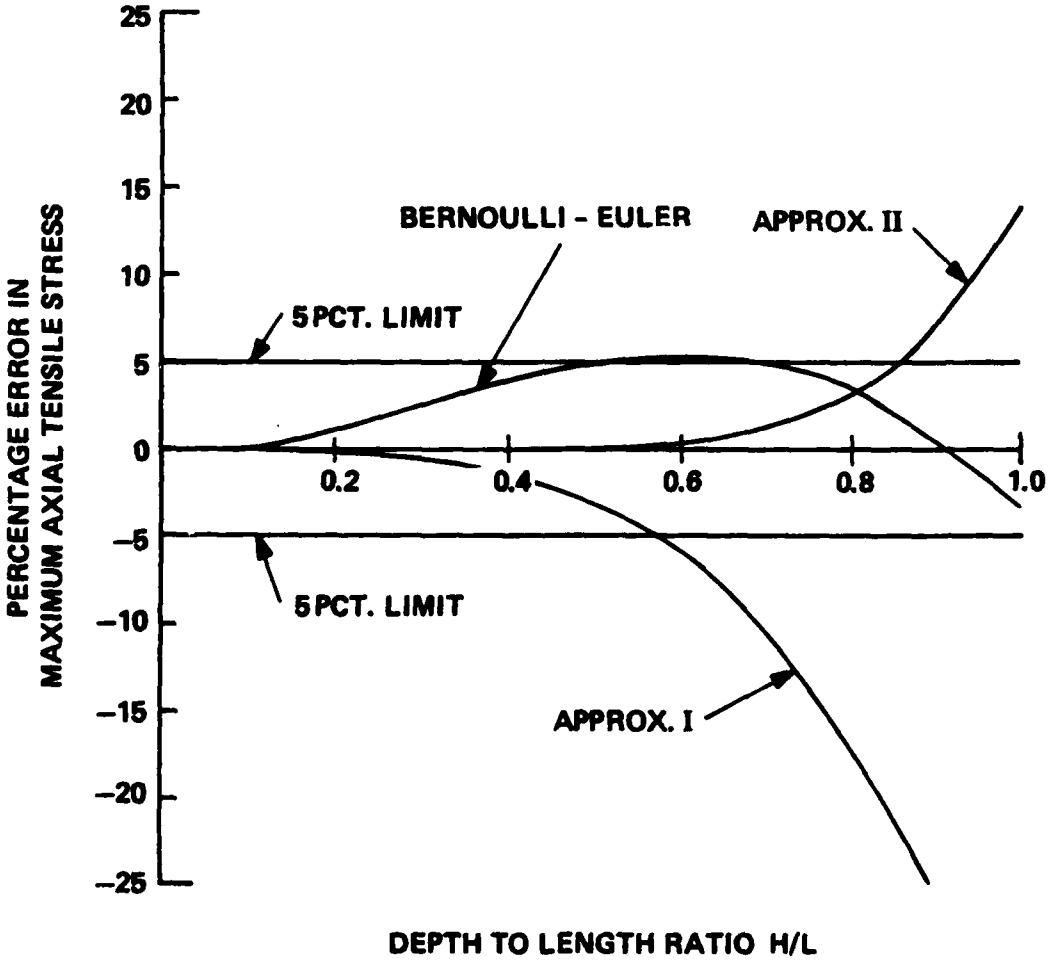

Figure 13. Percentage Error in Maximum Axial Tensile Stress for a Sinusoidally Loaded Isotropic Beam

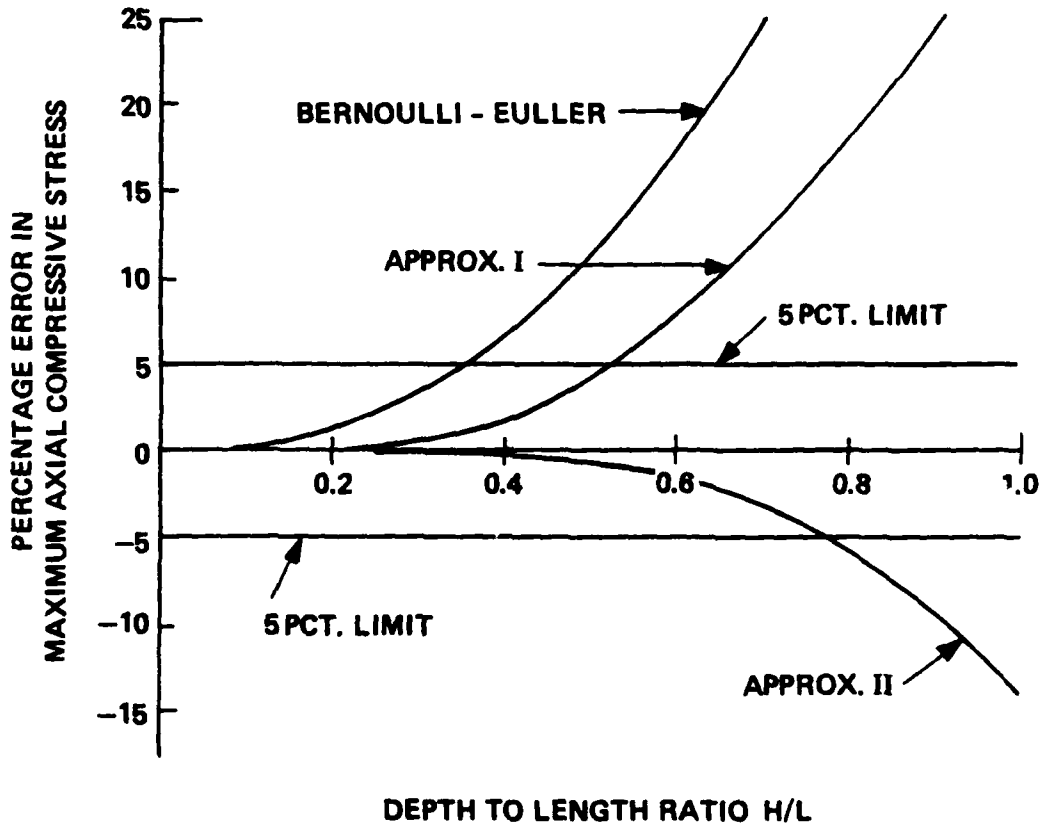

Figure 14. Percentage Error in Maximum Axial Compressive Stress for a Sinusoidally Loaded Simply Supported Isotropic Beam

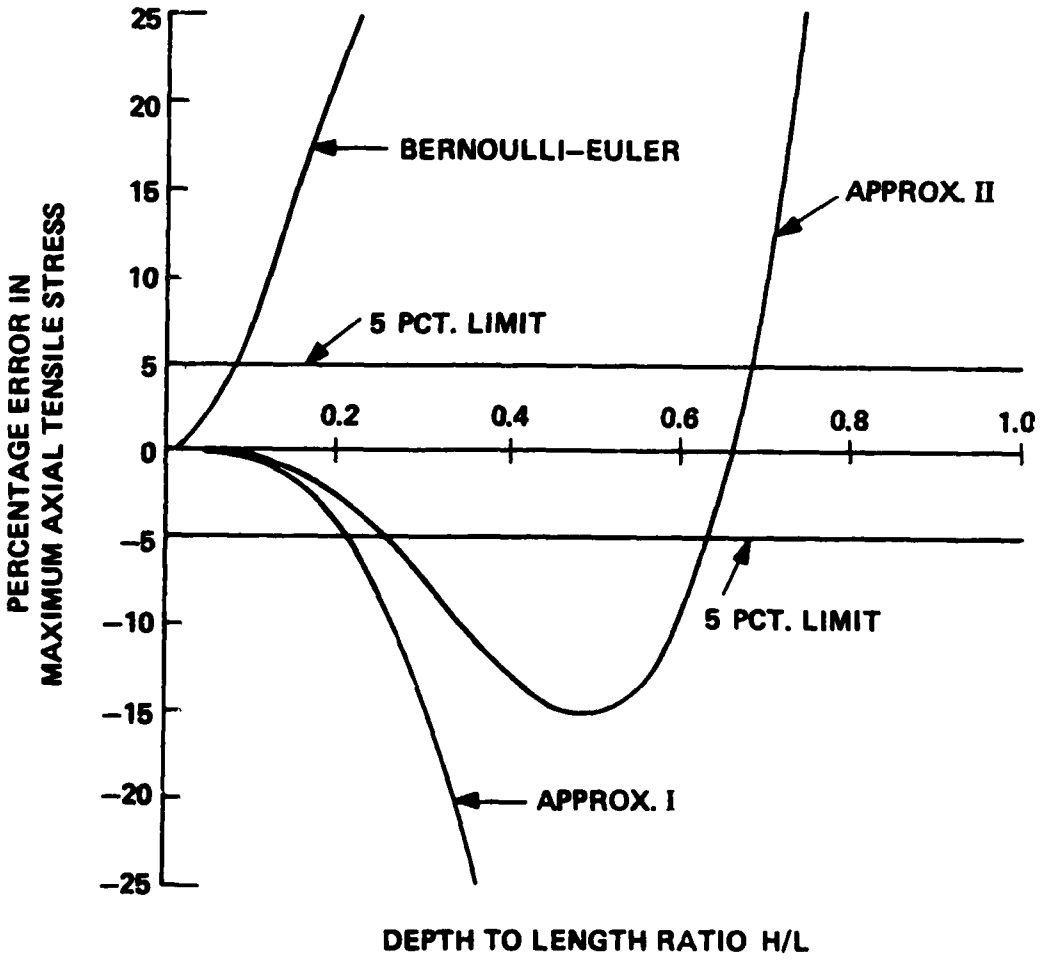

Figure 15. Percentage Error in Maximum Axial Tensile Stress for a Sinusoidally Loaded Simply Supported Orthotropic Beam, $E_{11}/G_{13} = 50$, $E_{11}/E_{33} = 25$

AD-A121 461 A NEW ENGINEERING THEORY OF PLANAR BEND[illegible]
APPLICATIONS(U) GEORGIA INST OF TECH ATLANT SCHOOL OF
AEROSPACE ENGINEERING P L MURTHY ET AL. JAN 82
UNCLASSIFIED AFOSR-TR-82-0960 AFOSR-81-0056 F/G 12/1 NL

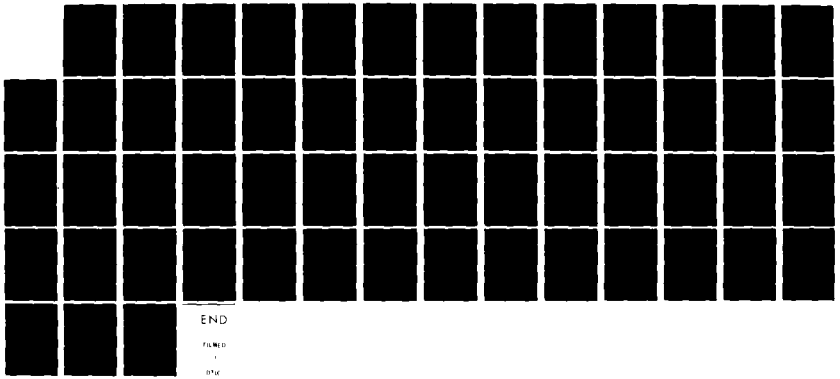

END

FILMED

DTIC

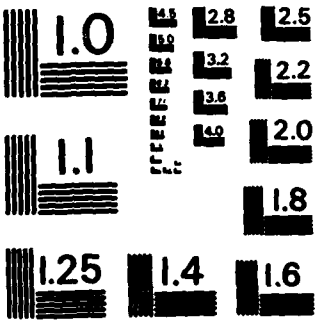

MICROCOPY RESOLUTION TEST CHART
NATIONAL BUREAU OF STANDARDS - 1963 - A

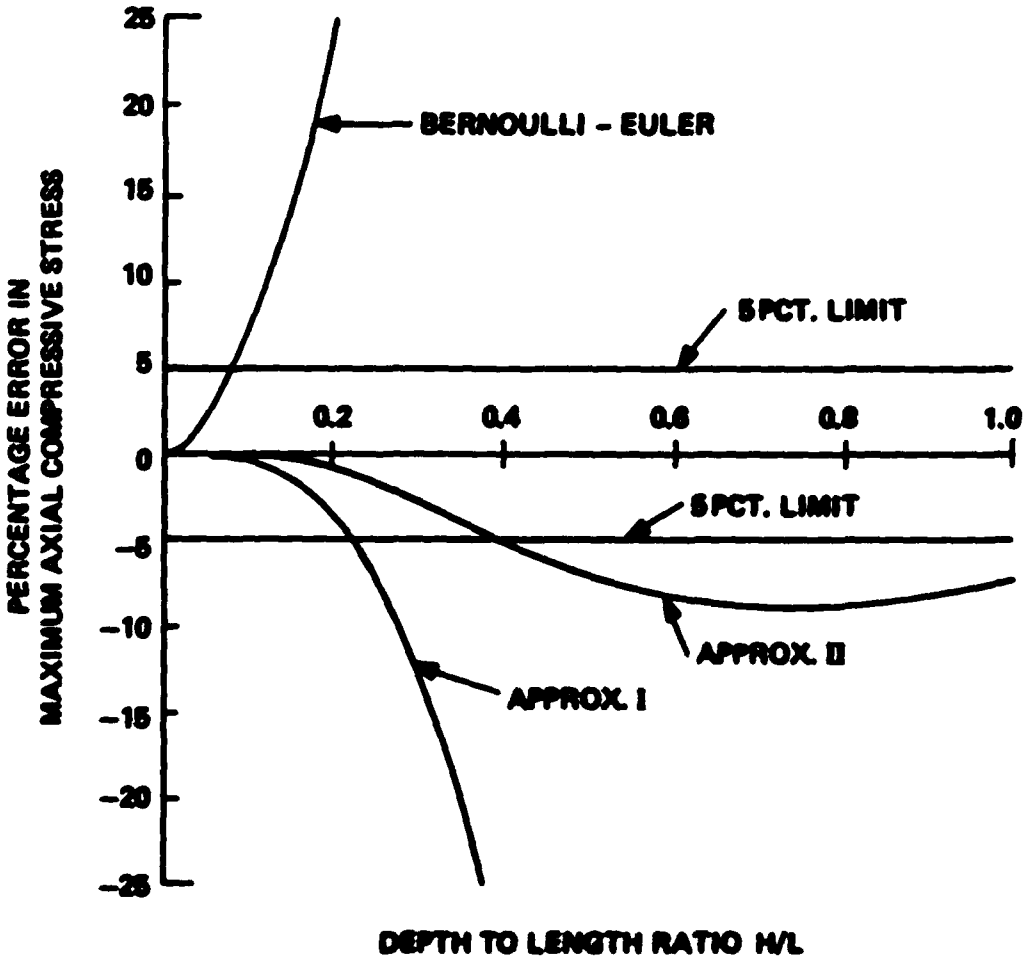

Figure 16. Percentage Error in Maximum Axial Compressive Stress for a Sinusoidally Loaded Simply Supported Orthotropic Beam, $E_{11}/G_{13} = 50$, $E_{11}/E_{33} = 25$

Figures 17 and 18 show the axial stress distribution through the depth of beam at midspan. The agreement of Approximation II with the exact is excellent while Approximation I can be considered satisfactory. The effect of nonclassical axial stress is seen to be more pronounced for the orthotropic beam. Tensile stresses are predicted by both Approximation I and Approximation II near the center of the cross section as seen in Figure 18. There are errors in the present approximation in this portion of the cross section. Maximum stresses are predicted quite well.

It is interesting to note that a Reissner or Timoshenko type theory would have given the same result as classical theory. Nonclassical axial stress contribution is not present in those theories.

The transverse shear stress and transverse normal stress distributions at sections where they are maximum are presented in Tables 2 and 3. The agreement with the exact values is satisfactory.

Conclusions

A qualitative validation is provided through a consistency analysis. The theory is further established by showing that Reissner theory of plates, reduced to planar bending, can be developed from the present theory. A quantitative validation is provided through a correlative study with the exact solution to a classic benchmark problem - - the response of a simply supported beam to a sinusoidally distributed loading.

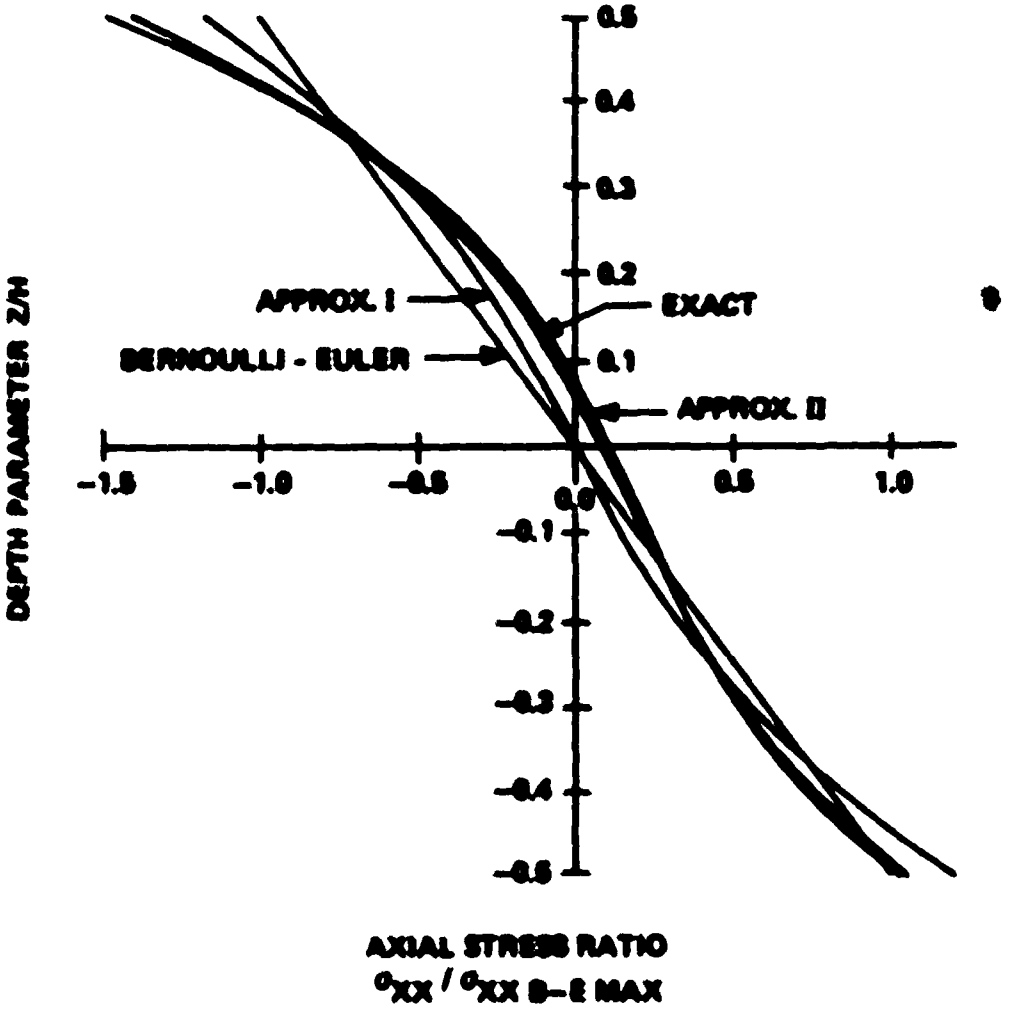

Figure 17. Axial Stress Distribution at the Center for a Sinusoidally Loaded Simply Supported Isotropic Beam, L/H = 1.3

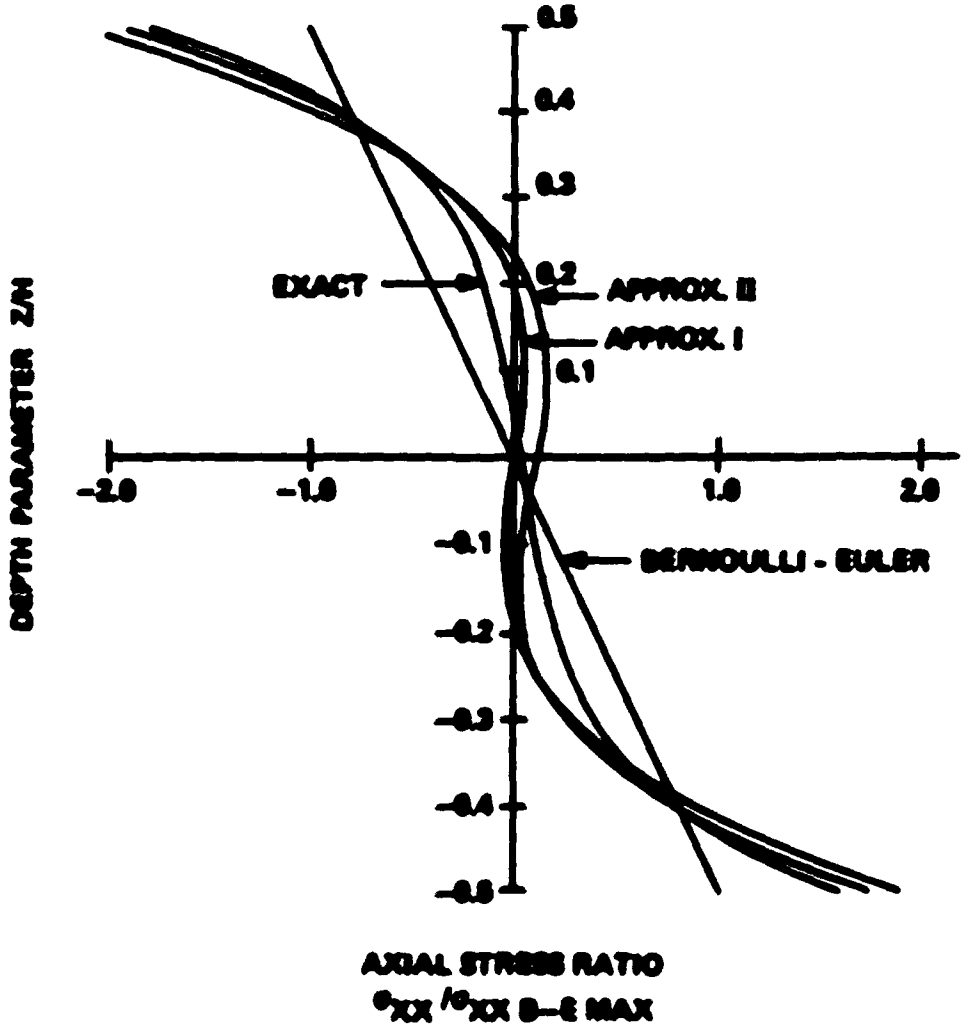

Figure 18. Axial Stress Distribution at the Center for a Sinusoidally Loaded Simply Supported Orthotropic Beam, L/H = 3, $E_{11}/G_{13} = 50$, $E_{11}/E_{33} = 25$

Table 2. Transverse Stresses in Isotropic Beam under Sinusoidally Distributed Loading, L/H = 1.), and ν = 0.)

z/H	$\sigma_{xz}/\sigma_{xz3E\ max}^{*}$		σ_{zz}/q_o	
	Exact	Present	Exact	Present
0.5	0.000	0.000	1.000	1.000
0.4	0.353	0.360	0.963	0.972
0.3	0.601	0.640	0.872	0.896
0.2	0.773	0.840	0.749	0.784
0.1	0.885	0.960	0.610	0.648
0.0	0.944	1.000	0.467	0.500
-0.1	0.949	0.960	0.330	0.352
-0.2	0.887	0.840	0.204	0.216
-0.3	0.735	0.640	0.101	0.104
-0.4	0.458	0.360	0.028	0.028
-0.5	0.000	0.000	0.000	0.000

$$^{*}\sigma_{xz3-E\ max} = \frac{3q_o L}{2HA}$$

Table 3. Transverse Stresses in Orthotropic Beam under Sinusoidally Distributed Loading, $L/H = 4.0$, $E_{11} = 25$, $E_{33} = 1$, $G_{13} = 0.5$ and $\nu_{13} = 0.25$

z/H	σ_{zz}/σ_{zz3}-E max		σ_{zz}/q_o	
	Exact	Present	Exact	Present
0.5	0.000	0.000	1.000	1.000
0.4	0.451	0.360	0.963	0.972
0.3	0.700	0.640	0.875	0.896
0.2	0.832	0.840	0.759	0.784
0.1	0.893	0.960	0.628	0.648
0.0	0.906	1.000	0.493	0.500
-0.1	0.880	0.960	0.359	0.352
-0.2	0.809	0.840	0.231	0.216
-0.3	0.672	0.640	0.119	0.104
-0.4	0.428	0.360	0.035	0.028
-0.5	0.000	0.000	0.000	0.000

CHAPTER VIII

A THEORY FOR DYNAMICS AND APPLICATIONS

Overview

In this chapter, a new dynamic theory for flexural motions is developed, validated and applied. The static bending theory is utilized as a foundation. The pertinent equations are restricted to planar bending as in the static case. The theory proposed by Stephen and Levinson[36], specialized for thin rectangular cross sections, is obtained from the present equations, which is a point of reference for validation. The theory is then applied to flexural wave propagation in slabs and vibration behavior of beams with different end restraints. The accuracy of the theory is demonstrated through a comparative study with exact solutions and an error analysis.

Formulation

The classical theory based on Bernoulli-Euler hypothesis is chosen as the starting point as in the static case. The overall equations of motion are

$$M_{,x} = \bar{\rho}\ddot{\theta} \tag{113}$$

$$Q_{,x} = \bar{\rho}\ddot{w} \tag{114}$$

$$M_{,x} - Q = \bar{\rho}I\ddot{\theta}_{,x} \tag{115}$$

$\bar{\rho}$ is the mass density of the material and ($\dot{}$) denotes differentiation with respect to time.

The key assumption which permits the stress field to be approximated is that the axial stress is given with sufficient precision by Equation (22).

$$\sigma_{zz} = \frac{N}{A} + \frac{My}{I} \tag{22}$$

N and M however, are now functions of both space and time. σ_{xz} and σ_{xx} are obtained by solving the two-dimensional equations of motion.

$$\sigma_{xx,x} + \sigma_{xz,z} = \bar{\rho}\ddot{u} \tag{116}$$

$$\sigma_{xz,x} + \sigma_{zz,z} = \bar{\rho}\ddot{w} \tag{117}$$

The displacement components u and w are assumed to be given by their static counterparts

$$\begin{aligned} u &= U(x,t) - zW_{,x} \\ w &= W(x,t) \end{aligned} \tag{118}$$

Stress free boundary conditions on $z = -c$ and $z = +c$ are imposed on σ_{xz} and σ_{zz}. The results are

$$\sigma_{xz} = \frac{Q(x,t)}{2I}(c^2 - z^2) \tag{23}$$

$$\sigma_{zz} = \frac{Q}{2A}\left(\frac{z^3}{c^2} - z\right) \tag{24A}$$

while σ_{zz} remains the same as in the static case, a different form for σ_{zz} is obtained because of the difference in boundary conditions.

With the aid of Equations (7), (22), (23), (24A), (27), and (28), improved expressions for the displacement components are determined in a manner similar to the static case. The results are

$$w = W(x,t) = \frac{\nu_{13}^{Nx}}{E_{11}A} - \frac{\nu_{13}^{Nx^2}}{2E_{11}I} + \underline{\underline{\frac{Q_{zz}}{2E_{33}A}\left(\frac{z^4}{4c^2} - \frac{z^2}{3}\right)}} \tag{119}$$

$$u = U(x,t) - zW_{,x} = \frac{\nu_{13}Qx^3}{6E_{11}I} + \frac{Q(c^2z - \frac{z^3}{3})}{2G_{13}I}$$

$$+ \frac{\nu_{13}^{N}}{2E_{11}A}z^2 + \frac{\nu_{13}Q}{6E_{11}I}z^3 - \underline{\underline{\frac{Q_{zz}}{2E_{33}A}\left(\frac{z^5}{20c^2} - \frac{z^3}{6}\right)}} \tag{120}$$

In the above the terms which are underlined twice are similar to those present in the static displacements; they arise due to σ_{zz} distribution. The single underlined terms are unique for dynamic situations which come from the inertial forces. All these terms will be ignored in the subsequent analysis. This is similar to the assumption made in the static case and will be justified subsequently on the basis of an order of magnitude analysis.

The constitutive relations and the refined axial stress distribution are obtained in an analogous manner to the static case. The results are

$$N = E_{11} u_{,x} \tag{121}$$

$$M = -E_{11} I w_{,xx} + Q_{,x} c^2 \left(\frac{2}{5}\frac{E_{11}}{G_{13}} + \frac{\nu_{13}}{10}\right) \tag{122}$$

$$\sigma_{xx} = \frac{N}{A} + \frac{My}{I} + \underline{\frac{4Q_{,x}}{3I}\left(\frac{1}{5}c^2 z - z^3\right)} \tag{33A}$$

The expressions for N and M are slightly different from their static counterparts as σ_{zz} is different. The underlined term in Equation (33A) is the nonclassical axial stress contribution and is the same as that of the static case.

A Consistency Analysis

The process just described results in improved expressions for displacements and axial stress. If these are adopted, the equations of motion (116) and (117) are no longer satisfied exactly. In order to arrive at a consistent set of equations, an order of magnitude analysis is needed. The approach adopted is similar to that used in determining the consistent set of static equations. The error in the approximation for stresses is estimated first by utilizing the pertinent compatibility equation. The other equations are established to the same level of approximation.

Derivatives with respect to time are estimated using the definition

$$\left|\frac{\partial w}{\partial t}\right| = O(\omega w_0) \tag{123}$$

The magnitude for ω may be estimated by considering the Bernoulli-Euler relation

$$E_{11} I\, w_{,xxxx} + \bar{\rho} A \ddot{w} = 0 \qquad (124)$$

For flexural motions of present interest, the transverse inertia term is of the same order as the bending stiffness term. In this case, ω is estimated using Equations (86), (123) and (124).

$$\omega = O\left[\frac{E_{11}}{\rho}\ \frac{\pi^2}{\lambda^4}\right] \qquad (125)$$

$\omega \ll \left[\frac{E_{11}}{\rho}\ \frac{\pi^2}{\lambda^4}\right]$ represents a static situation and $\omega \gg \left[\frac{E_{11}}{\rho}\ \frac{\pi^2}{\lambda^4}\right]$ represents impact-type motions; these are excluded from the present discussion.

Substitution of Equations (33A), (23) and (24A) into (96A) permits the estimation of errors in the compatibility equation.

$$\left|\frac{2\nu_{13}}{E_{11}} Q_{,13}^{\,e} - \frac{2\nu_{13}}{E_{11}} Q_{,13}^{\,a} + \frac{Q_{,22}^{\,a}}{G_{13}}\right| = \underline{\frac{Q_{,xxxx}^{max}}{24 E_{33}^{A}} \left(\frac{t^3}{c^2} - t\right)}$$

$$\underline{- \frac{\nu_{13}}{E_{11}} \left(\rho \ddot{w}_{,xx} t + h_a \frac{Q_{,xxxx}^{max}}{3!} \left(t^3 - \frac{3}{5} c^2 t\right)\right)} = 0 \qquad (126)$$

The underlined terms in the above are nonvanishing error terms. The error is at most of $O\left[\frac{\rho}{E_{11}} \frac{\pi^2}{\lambda^4} \frac{E_{11}}{E_{33}}\right]$. It has been shown in Chapter VII that this corresponds to an error of $O\left[\rho \frac{\pi^3}{\lambda^3} \frac{E_{11}/E_{33}}{(E_{11}/2G_{13}) - \nu_{13}}\right]$ in the stresses and, therefore, it is consistent with the level of approximation reflected in Equations (33A), (23) and (24A).

Equations of Motion

Introduction of Equations (119), (120), (37A) and (23) into Equation (116) leads to

$$\frac{M_{,x}z}{I} - k_x \frac{Q_{,xx}}{3I}(z^3 - \frac{3}{5}c^2 z) - \frac{Qz}{I}$$

$$= -\bar{\rho}z(\ddot{W}_{,x} - \frac{3\ddot{Q}}{2G_{13}A}) + \frac{\bar{\rho}\ddot{Q}z^3}{6E_{11}I}(\nu_{13} - \frac{E_{11}}{G_{13}}) \qquad (127)$$

The above cannot be satisfied identically for all z. In view of the approximation inherent in the stresses, it is desirable to satisfy Equation (127) to the same degree of approximation. The terms may be rearranged in the following way

$$\left|\frac{(M_{,x} - Q)z}{I} + \bar{\rho}z\ddot{W}_{,x} - \frac{3\bar{\rho}z\ddot{Q}}{2G_{13}A}\right| - k_x \frac{Q_{,xx}}{3I}(z^3 - \frac{3}{5}c^2 z)$$

$$- \frac{\bar{\rho}\ddot{Q}z^3}{6E_{11}I}(\nu_{13} - \frac{E_{11}}{G_{13}}) = 0 \qquad (127A)$$

By forcing the first term in brackets to zero, the following equation of motion is obtained

$$M_{,x} - Q = \bar{\rho} I\ddot{\phi}_1 \qquad (115A)$$

where ϕ_1 is the rotation related variable given in Equation (36). Since the underlined terms are at most of $O(\sigma \frac{H^2}{\lambda^3} k_x)$, Equation (115A) implies that the approximation inherent in the equation of motion is consistent with that of the stresses and compatibility equation. This is similar to the static situation of Chapter VII. Equation (115A) is the overall equation of motion of the original Timoshenko theory[23]. Equations (23), (117) and (119) yield the second equation of motion as

$$Q_{,x} = \bar{\rho} A\ddot{W} \qquad (114)$$

with an error of $O\left[\nu_{13}\, \sigma \frac{h^3}{\lambda^4}\right]$.

<u>Displacements</u>

The error estimates of displacements due to the approximations in stresses are given by Equations (98) and (99). The underlined term in Equation (119) is of $O(\frac{\sigma}{E_{33}} \frac{h^3}{\lambda^3})$ and the underlined terms in Equation (120) are at most of $O(\frac{\sigma}{E_{11}} \frac{h^4}{\lambda^3})$. This is the justification for neglecting the underlined terms in Equations (119) and (120).

Summary of Dynamic Equations

The dynamic theory equations can be summarized as follows: the overall beam-type equations (113), (114) and (115A) remain the same as in Timoshenko theory. The constitutive relations are given by (121) and (122). Equation (122), with the aid of tracer constant analysis, may also be written as

$$M = -E_{11} I [W_{,xx} - Q_{,x} e^{2'} / \ldots] + \frac{M_{11}}{EC_{11}} - \ldots \frac{2}{5} \ldots - \ldots \frac{\ldots}{7} \qquad (122A)$$

The above facilitates easy recognition of departures from the classical theory and Timoshenko theory as in the static case.

In addition, two sets of equations provide the distribution of stresses and displacements throughout the structure. The first set of equations (33A), (23) and (24A) describe stresses. They retain same form as those in the static case except for the difference in σ_{zz}. The displacements are described by the second set of Equations (119) and (120) with the underlined terms omitted, which are the same functional form as

the static displacements.

Relation to Stephen and Levinson Theory

A dynamic theory for isotropic beams was proposed recently by Stephen and Levinson[36]. The authors' results demonstrate excellent correlation with elasticity solutions for flexural wave propagation. In this section, it is shown that their theory, specialized for plane stress, can be obtained from the present theory.

The Stephen and Levinson theory utilizes averaged kinematic variables $\bar{w}$ and $\bar{\phi}$. They are defined by

$$\bar{w} = \frac{1}{2c}\int_{-c}^{c} w \, dz \tag{128}$$

$$\bar{\phi} = \frac{1}{2I}\int_{-c}^{c} u z \, dz \tag{129}$$

Consequently, the response throughout the structure cannot be predicted. Only the overall response characteristics such as frequency or the averaged variables, for example, can be obtained.

$\hat{w}$ and $\hat{\phi}$ are constructed using the Equations (119) and (120) specialized for isotropic materials:

$$\hat{w} = w - \frac{\nu\beta}{4c} \tag{130}$$

$$\hat{\phi} = -w_{,x} - \frac{c^2}{10I}(\beta + 9v) \tag{131}$$

By virtue of Equations (130) and (131) it is possible to write

$$\bar{w}_{,x} + \bar{\phi} = \frac{Q}{GA}\frac{(12+11\nu)}{10(1+\nu)} + \underline{\frac{\nu c^2 \bar{\phi}_{,1}}{6g}} \qquad (132)$$

Underlined in the above is a rotatory inertia term; it is of $0\left[\frac{\nu\rho}{E}\frac{H^3}{\lambda^3}\right]$. It implies errors of $0(\frac{\nu\rho}{E}\frac{H^3}{\lambda^2})$ in w which were neglected in Equation (128). If this term is neglected, the result is one of the relations of Stephen and Levinson's theory for thin rectangular cross section beams.

Equation (122A) for the isotropic case, reduces to

$$M = -EIw_{,xx} + Q_{,x}c^2\left(\frac{4}{5}+\frac{5}{6}\nu\right) \qquad (133)$$

Equations (115A), (130), (132) and (133) permit a relation between M and $\bar{\phi}$ to be written as

$$\bar{\phi}_{,x} = \frac{M}{EI} - \frac{Q_{,x}\nu}{5EA} \qquad (134)$$

In obtaining the above, underlined terms of the type in Equation (132) are omitted for the same reason mentioned earlier.

Equations (132) and (134) are the central relations of the Stephen and Levinson[36] theory for the dynamics of thin rectangular cross section beams. The overall equations of motion remain similar to (113), (114) and (115A) in the functional form with the kinematic variables replaced by the averaged variables. The above demonstrates that the essence of their theory is included in the new equations. In addition, stresses and displacements are obtained throughout the structure with the present theory.

Dynamic Applications

The following sections provide several examples which illustrate the use of the new dynamic equations. The applications include wave propagation in rectangular slabs of isotropic and orthotropic materials and free vibration of beams.

Flexural Wave Propagation

The study of flexural wave propagation usually consists of determining dispersion curves for sinusoidal disturbances. A dispersion curve relates the phase velocity of waves to their wavelength. The plane strain flexural solution for harmonic waves for an infinitely wide isotropic plate is a classic benchmark for a dynamic theory. The exact solution for this problem was first published by Rayleigh[10] in 1889.

Here a dispersion relation is determined for a thin rectangular orthotropic beam. The isotropic result is obtained by specialization. Two wave velocity parameters, c_s and c_B, are defined for convenience through the following relations:

$$c_s = \sqrt{G_{13}/\bar{\rho}}$$
$$c_B = \sqrt{E_{11}/\bar{\rho}} \qquad (135)$$

c_s is the shear wave velocity. c_B is the velocity of longitudinal waves in uniform bars, which is often referred as the bar velocity. Equations (114), (115A) and (122A) can be combined to obtain the following governing equation:

$$w_{,xxxx} - \ddot{w}_{,xx}\left[\frac{3}{5}\frac{a_0}{c_0^2} + \frac{1}{c_B^2} - \frac{1}{c_B^2}\left(\frac{3}{5}k_x a_a + a_n\frac{\nu_{13}}{2}\right)\right]$$

$$+ \frac{3}{2}\frac{\ddot{w}}{c_B^2 c_0^2}a_0 + \frac{\ddot{w}}{c_B^2 \rho^2} = 0 \qquad (136)$$

ρ is radius of gyration of the cross section.

A solution to Equation (136) can be selected in the form

$$w = w_0 \sin\frac{\pi x}{L}\sin\omega t \qquad (137)$$

w_0 is the amplitude of the motion. A phase velocity parameter ζ and a wave number parameter ξ are introduced through the relations

$$\zeta = \frac{\bar{c}}{c_B}\ ;\quad \xi = \frac{2\pi c}{\lambda} \qquad (138)$$

$\bar{c}$ is the phase velocity and λ is wavelength; they are related to ω and L:

$$\bar{c} = \frac{\lambda}{2\pi}\omega \qquad (139)$$

$$\lambda = 2L$$

Substitution of Equation (137) into (136) leads to the dispersion equation

$$\frac{3}{2}\frac{E_{11}}{G_{13}}\zeta^4 - \left[1 - \left(\frac{3}{5}k_x a_a + \frac{\nu_{13}a_n}{2}\right) + a_0\frac{3}{2}\frac{E_{11}}{G_{13}}\right]\zeta^2 - \frac{3\zeta^2}{\xi^2} + 1 = 0 \qquad (140)$$

The axial stress distribution is obtained with the aid of Equations (13A), (122A), (114) and (137).

$$\sigma_{xx} = \frac{2M_0 E_{11}}{c}\left[\left(\zeta^2 - \frac{\bar{\rho}\omega^2 c^2}{E_{11}} k_1\right)\frac{z}{H} + \frac{4k\bar{\rho}\omega^2 c^2}{E_{11}}\left(\frac{z}{H}^3 - .15\,\frac{z}{H}\right)\right] \tag{141}$$

where

$$k_1 = \alpha_0 \frac{3}{2}\,\frac{E_{11}}{G_{13}} - \alpha_0 \frac{3}{5} k_2 - \alpha_0 \frac{\nu_{13}}{2} \tag{142}$$

As $\xi \to \infty$, Equation (140) gives two asymptotes for the phase velocity parameter ζ. The lower root corresponds to flexural wave velocity for harmonic waves. The lower branch is plotted against the wavelength parameter, ξ in Figure 19, for exact, present and Timoshenko[23] theories, Poisson's ratio is taken as 0.29 in the computations. The exact solution has been reconstructed from the analysis in Reference 56. The curve for Timoshenko theory is based upon the original equations[23], not the later versions which "adjust" the shear correction factor. The exact solution is for an infinitely wide plate. This corresponds to plane strain. E and ν are therefore, replaced by $E/(1-\nu^2)$ and $\nu/(1-\nu)$ in the present equations. Results due to the present theory are in excellent agreement with the exact solution for the range of wavelengths considered. The asymptotic values of the phase velocity parameter are 0.9258, 0.9652 and 0.8165 for exact, present and Timoshenko theories, respectively.

The exact solution leads to infinite branches for the dispersion curve. All the higher branches reach asymptotically the shear wave velocity. Engineering bending theories give only two branches, the second of which is a poor approximation. The second asymptote for the phase velocity parameter is 1.420 and 1.69 for present and Timoshenko theories.

The asymptotes for the phase velocity parameter obtained using

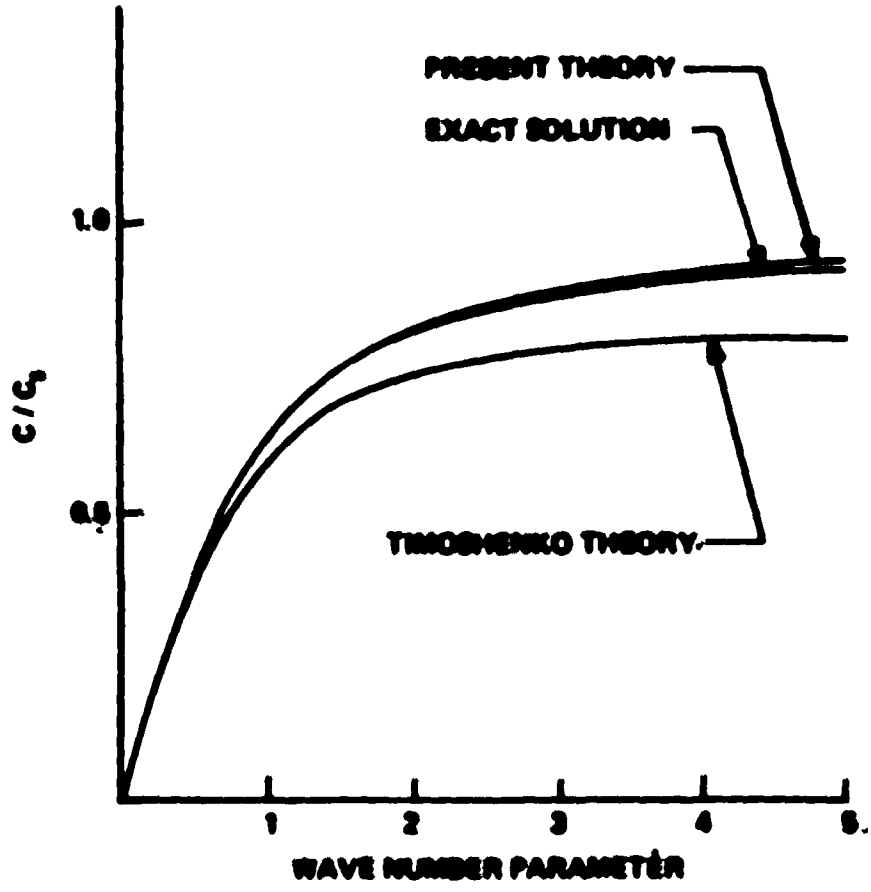

Figure 19. Dispersion Curves for an Isotropic Slab

Stephen and Levinson theory are 0.9412 and 1.6477 for the first and second branch, respectively.

The above results can be used to further validate the new equations. The approach is analogous to the validation study of the static theory. An exact solution to an orthotropic slab is needed for this purpose. It is developed in Appendix A. Isotropic results are obtained by specialization.

Results of the validation study for an isotropic slab appear in Figures 20-22. The percentage errors in phase velocity shown in Figure 20 indicate that the present theory predictions are comparable to Stephen and Levinson theory results; both are valid in the entire range of slenderness parameter considered. Figures 21 and 22 indicate that the present theory bending stress estimates are superior to Bernoulli-Euler and Timoshenko theoretical results; the axial stress distribution through the depth is in excellent agreement with the exact solution. Stephen and Levinson theory, in its present form, cannot provide explicit stress estimates.

Corresponding results for an orthotropic slab are presented in Figures 23-25. Similar behavioral trends to the isotropic case are observed. Present theory predictions, however, show more pronounced improvements over those of Timoshenko and Bernoulli-Euler theories. For example, based upon the percentage error in the axial stress shown in Figure 24, Timoshenko theory is valid up to $L/H \approx 15.5$ whereas the present theory is a good approximation up to $L/H \approx 2.5$. Present theory prediction of the axial stress distribution through depth is in excellent agreement with the exact result. By contrast, as shown in Figure 25, Timoshenko and Bernoulli-Euler predictions, which are linear through the depth, are in very poor agreement with the exact solution.

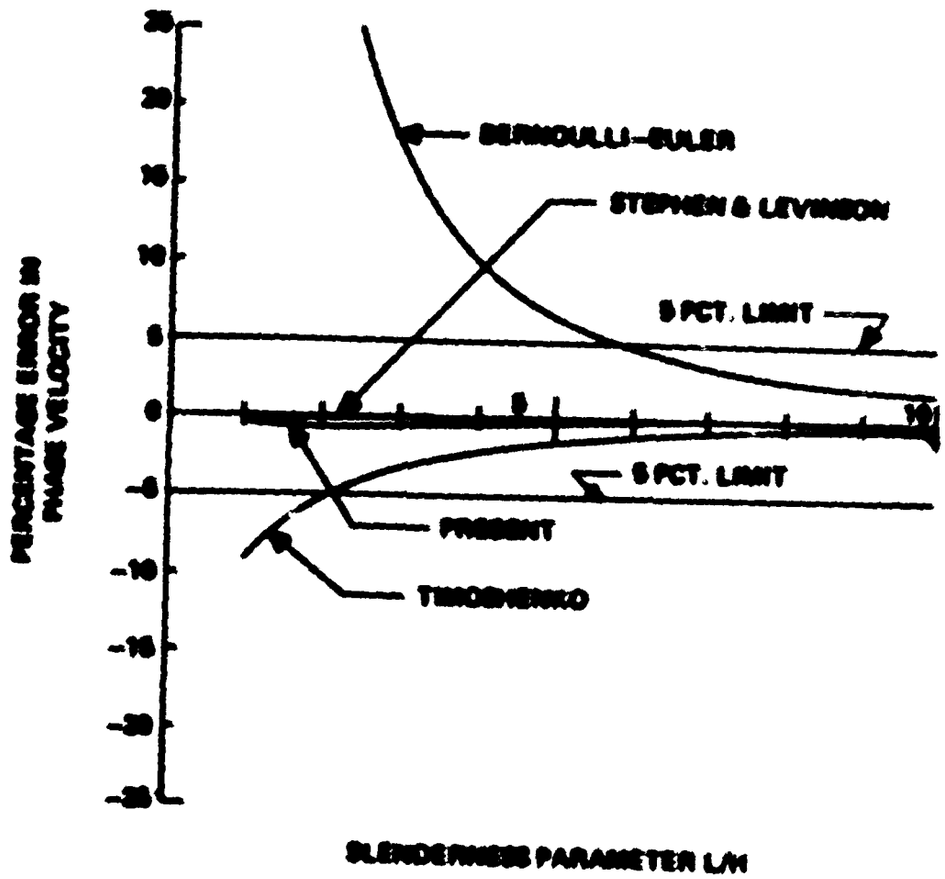

Figure 20. Percentage Error in Phase Velocity for an Isotropic Slab

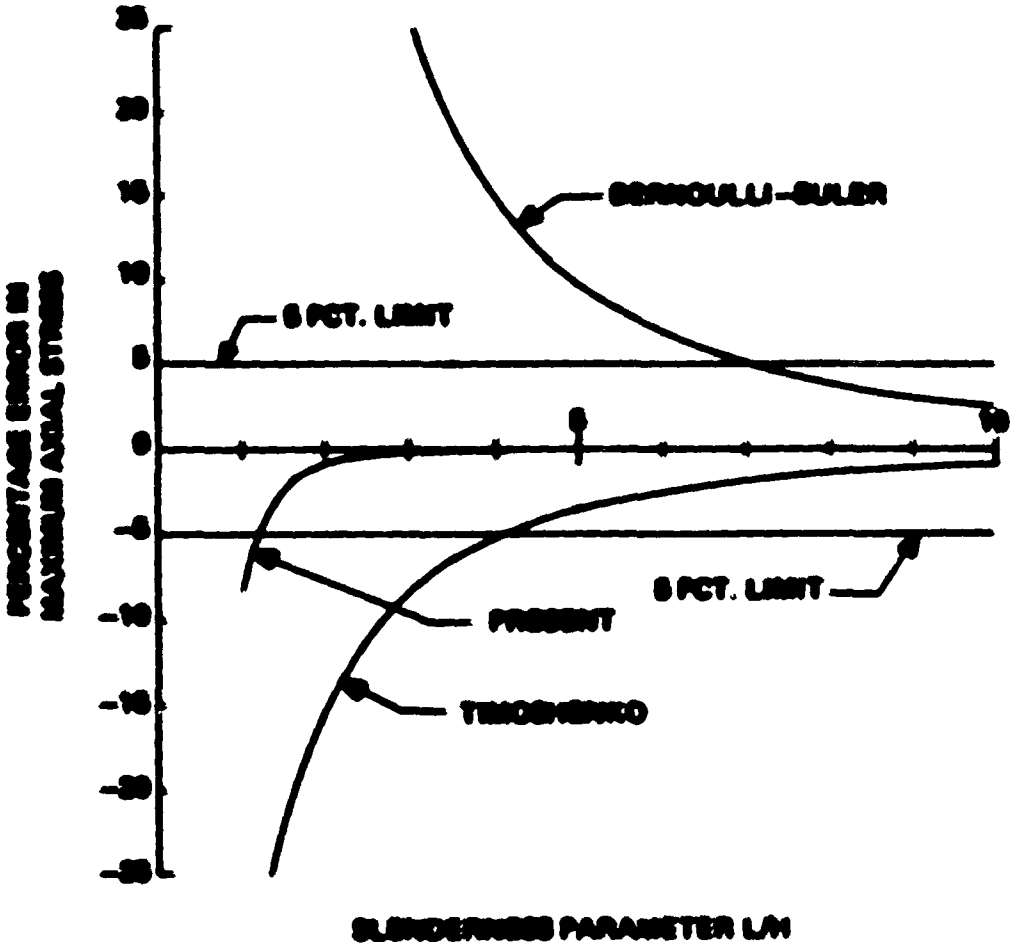

Figure 21. Percentage Error in Maximum Axial Stress for an Isotropic Slab

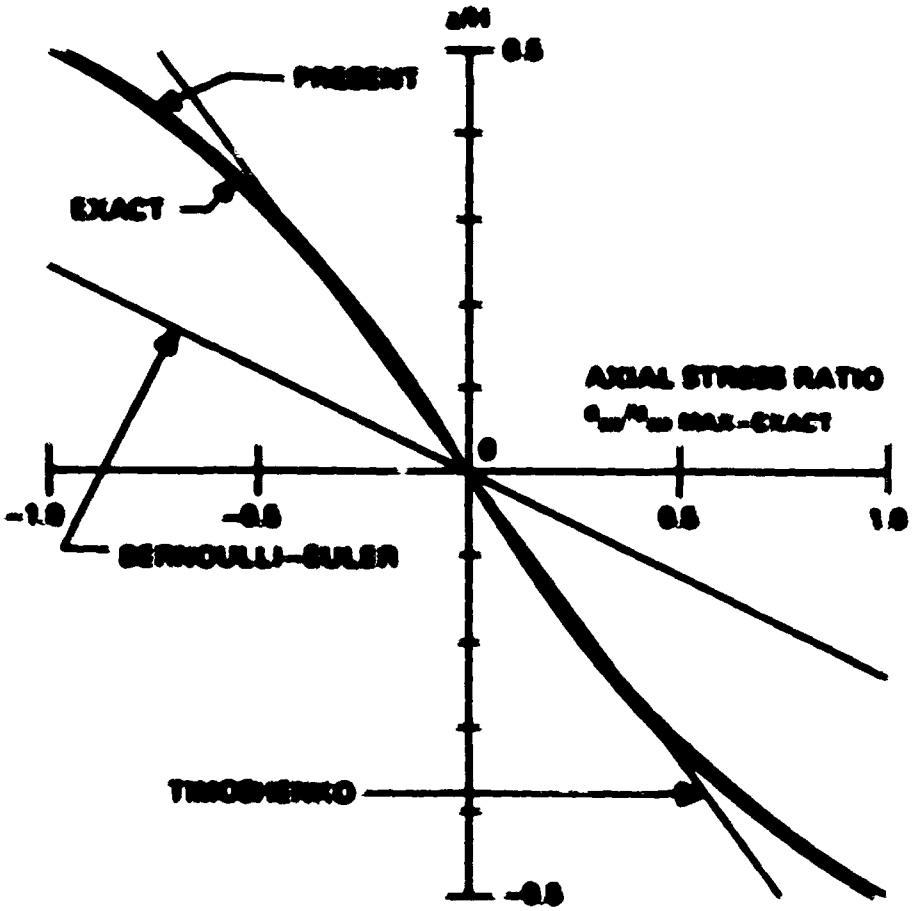

Figure 22. Axial Stress Distribution Through Depth for an Isotropic Slab, L/H = 1.3

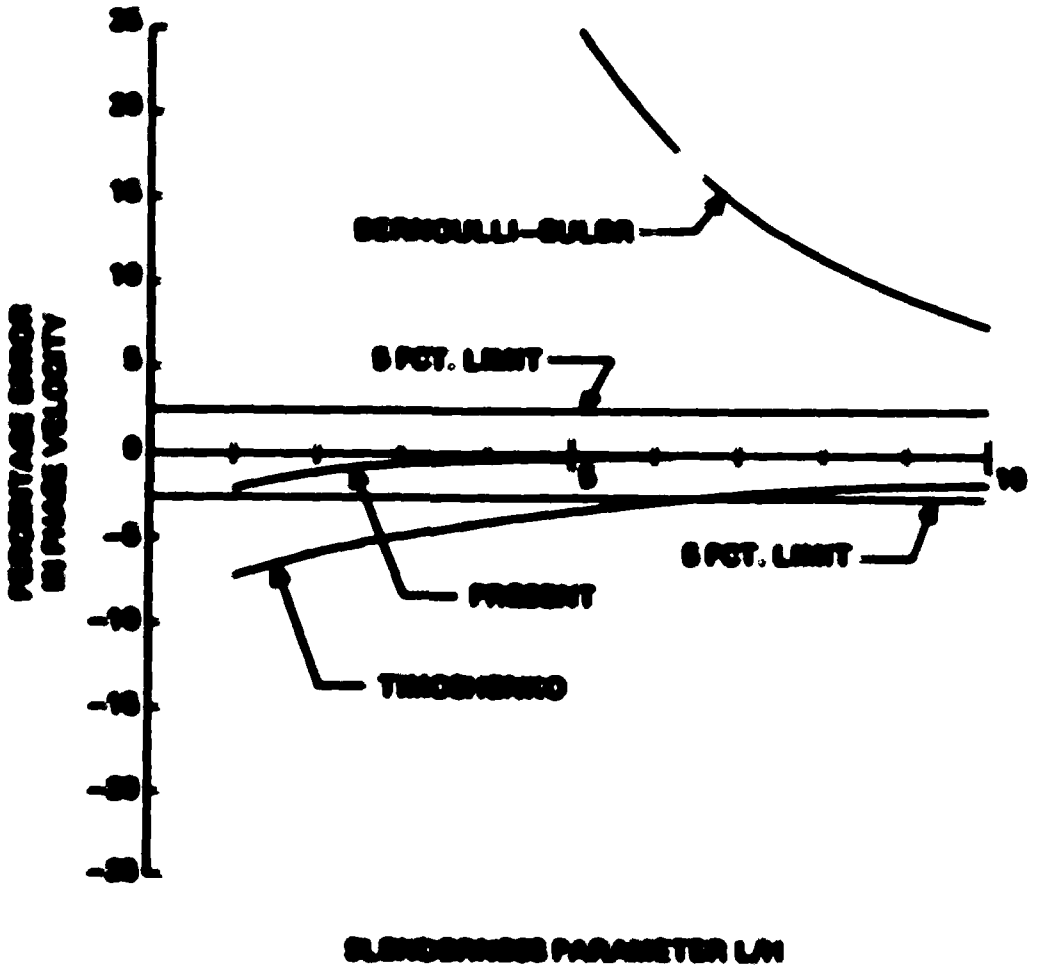

Figure 23. Percentage Error in Phase Velocity for an Orthotropic Slab, $E_{11}/G_{13} = 30$

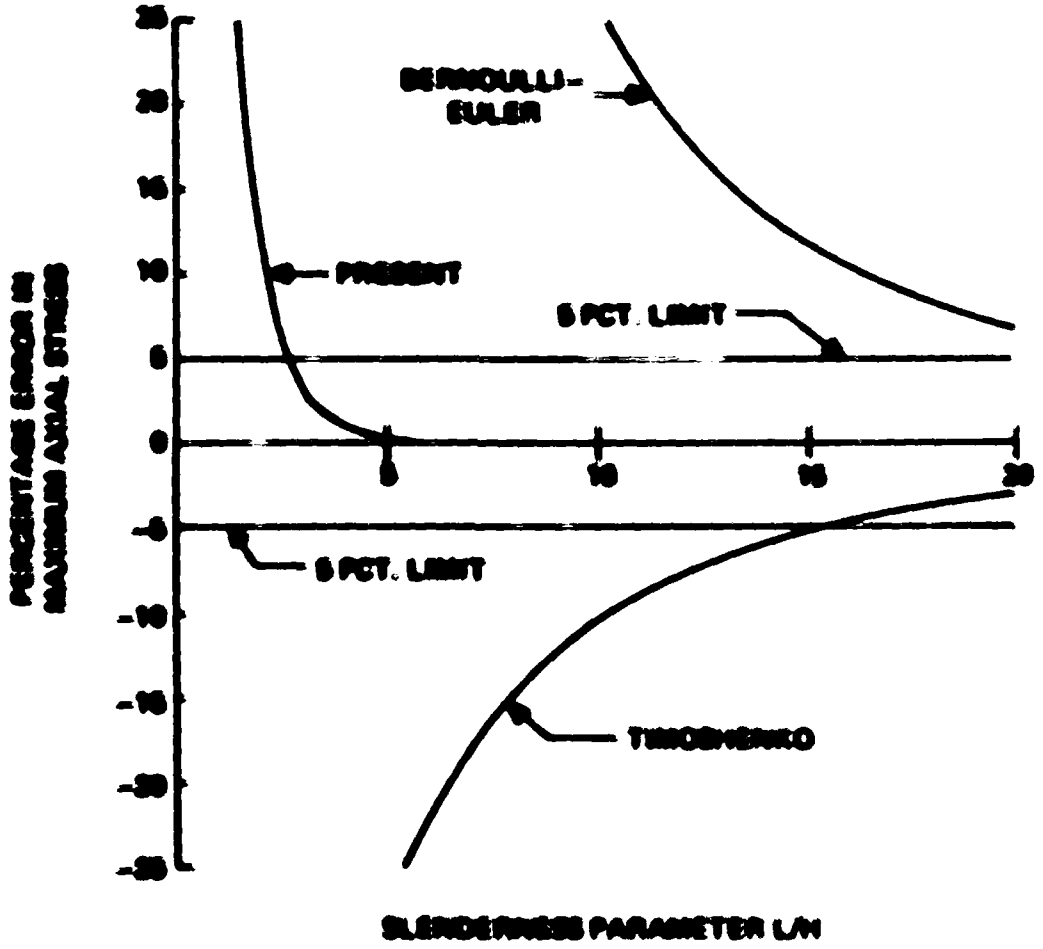

Figure 24. Percentage Error in Maximum Axial Stress for an Orthotropic Slab, $E_{11}/G_{13} = 30$

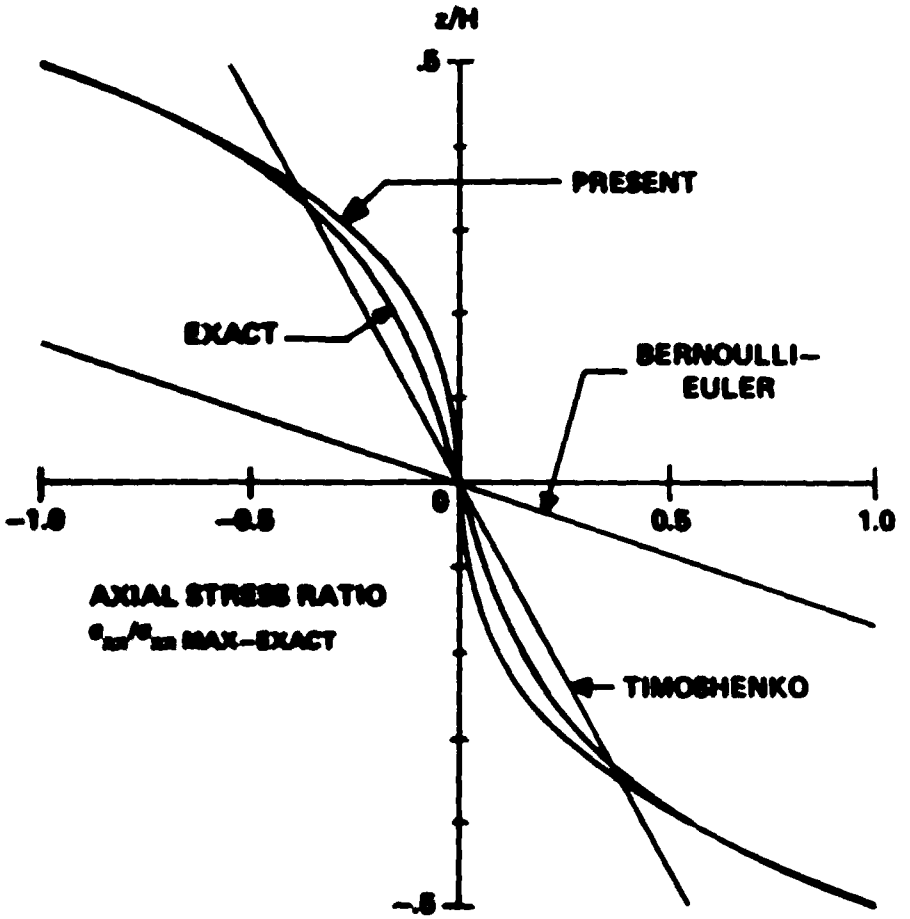

Figure 25. Axial Stress Distribution Through Depth for an Orthotropic Slab, L/H = 3, E_{11}/G_{13} = 30

No results for Stephen and Levinson theory are presented as it has been developed only for isotropic materials.

Vibration Problems

Vibration behavior for beams with various end restraints is obtained using the procedure outlined in References 57 and 58.

Typical results for a clamped orthotropic beam appear in Figures 26 and 27. w_1 refers to the Bernoulli-Euler frequency for a simply supported beam. The differences among the central moment ratio plots are slightly more than those reflected in the frequency ratio graphs.

The results for isotropic beams and for simply supported and clamped restraints also have been obtained. The results have shown general agreement of trends with Timoshenko theory. There is sensitivity to modeling of the boundary restraint, but it is less pronounced than that found in the static applications.

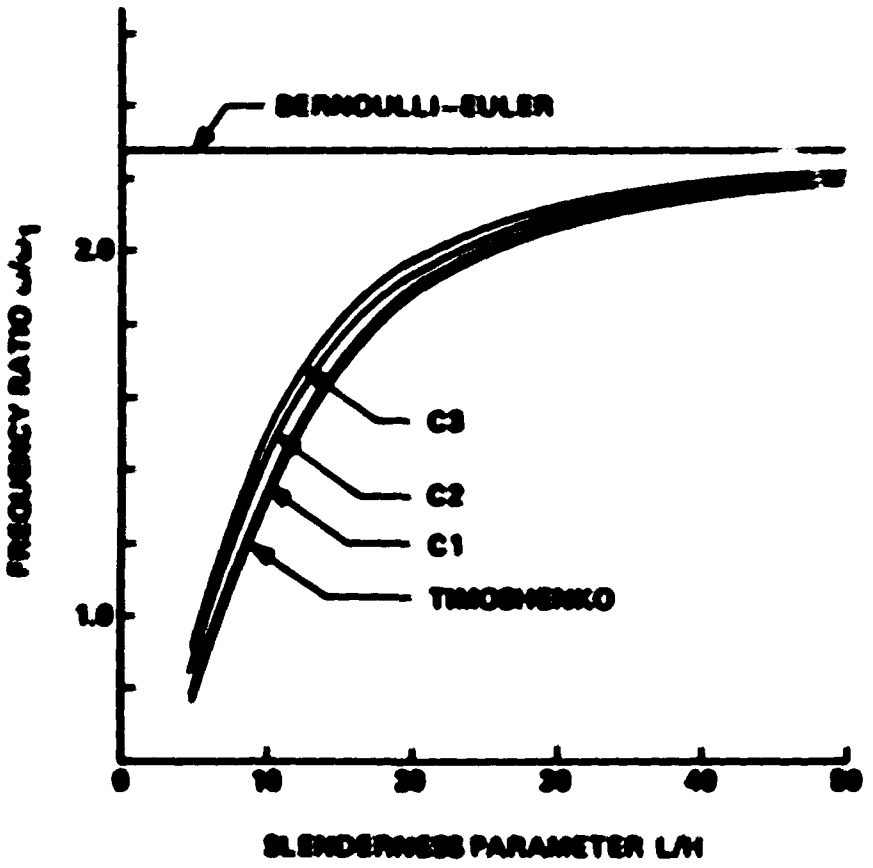

Figure 26. Frequency Ratio for a Clamped Orthotropic Beam, $E_{11}/G_{13} = 30$

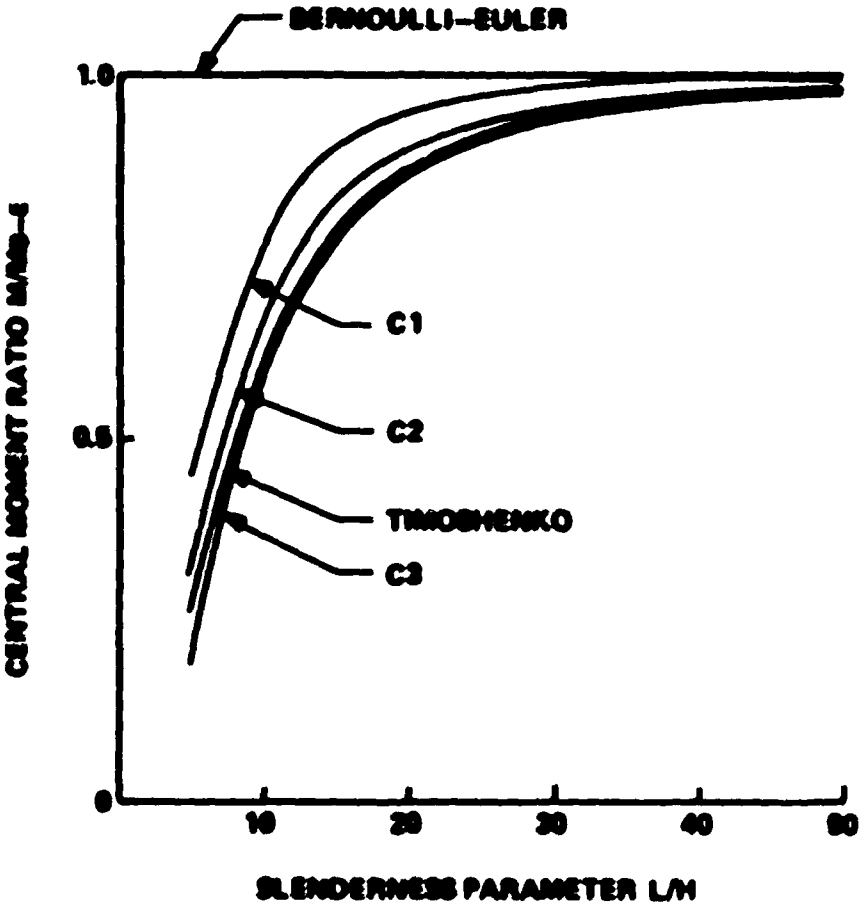

Figure 27. Central Moment Ratio for a Clamped Orthotropic Beam, $E_{11}/G_{13} = 30$

CHAPTER IX

AN ELEMENTARY BUCKLING THEORY

Preliminary Remarks

In this chapter, an elementary buckling theory is developed with the aid of the equations developed in Chapter IV. The primary objective of the present study is to compare buckling load predictions with those of Timoshenko and Bernoulli-Euler theories. Consequently, linearized equations are utilized. A fully nonlinear, large displacement theory is beyond the scope of the present work.

At the onset of buckling, Equation (22) is assumed to provide first approximation to the axial stress. The remaining stresses, which are consistent with this approximation, are taken to be

$$\sigma_{xx} = \frac{M}{2I}(c^2 - z^2) \tag{23A}$$

$$\sigma_{zz} = \frac{M_{xx}}{2A}\left(\frac{z^3}{c^2} - z\right) \tag{24B}$$

The form for σ_{zz} is slightly different from that of the corresponding static distribution because of differences in the boundary conditions. Stress free conditions on $z = \pm c$ surfaces are satisfied. In this respect, it is analogous to the dynamic stress distribution given in Equation (24A). Also, the stresses are expressed in terms of the bending moment M and its derivatives only. This is because Equation (18) is no longer valid, but the spatial distribution of stress over the cross section remains similar

to the classical case.

By following the development used in Chapter IV, the expression for the bending moment is obtained as

$$M = -E_{11}I\,W_{,xx} + M_{,xx}\frac{I}{A}k_b \tag{143}$$

k_b is a parameter defined in Equation (142)

$$k_b = \alpha_s\frac{3}{2}\frac{E_{11}}{G_{13}} - \alpha_s\frac{3}{5}k_x - \alpha_n\frac{\nu_{13}}{2} \tag{142}$$

The Buckling Equation

An overall equilibrium equation is derived from static equilibrium of a deflected beam element according to the adjacent equilibrium approach. Figure 28 shows the forces on a deflected beam element of finite length. The moment equilibrium requires

$$M = PW + M_o \tag{144}$$

M_o is the constant moment at $x = 0$, which is used to satisfy particular boundary conditions. With the aid of Equations (143) and (144), the following equation for the buckled configuration is obtained:

$$W_{,xxxx} + \frac{P}{E_{11}I\left(1 - \frac{I}{A}\frac{k_bP}{E_{11}I}\right)}W_{,xx} = 0 \tag{145}$$

Equation (145) is seen to be of the same form as the classical column equation, which may be obtained by setting $\alpha_s = \alpha_s = \alpha_n = 0$ in the above.

For simply supported ends, the boundary conditions to be enforced

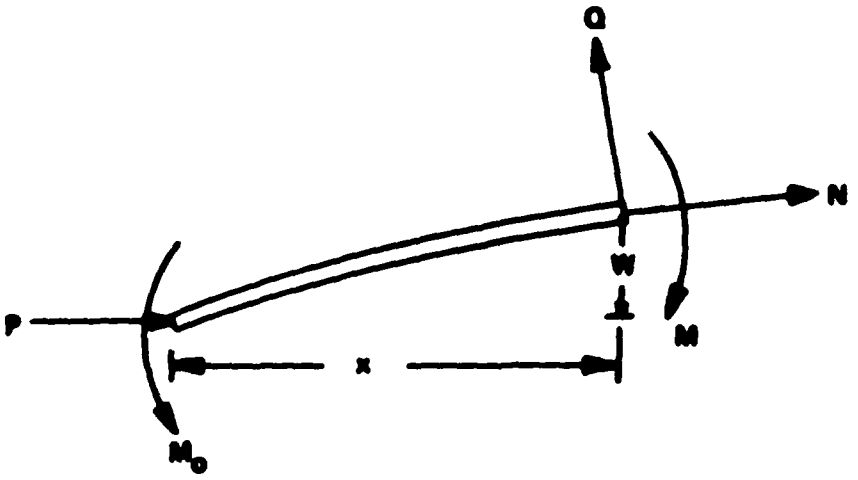

Figure 28. Deflected Beam Element

are given in Equations (39). A buckling load ratio, P_C/P_E, is obtained with the aid of Equations (39) and (145).

$$P_C/P_E = \frac{1}{1 + \pi^2 \frac{\rho^2}{L^2} k_b} \tag{146}$$

P_C is the buckling load and P_E is the classical Euler buckling load for a simply supported column.

$$P_E = \frac{\pi^2 E_{11} I}{L^2} \tag{147}$$

$\rho = \sqrt{I/A}$ is the radius of gyration of the beam cross section. The ratio L/ρ is the slenderness ratio of the column.

Equation (146) offers a convenient means for a definition of slenderness of a column.

$$P_C/P_E = \frac{1}{1 + \pi^2/s^2} \tag{147A}$$

s is a universal slenderness parameter defined by

$$s = \frac{L}{\rho} \sqrt{\frac{1}{k_b}} \tag{148}$$

This parameter is a function of both geometry and stiffness of the column material. As its value increases, classical Euler column behavior is approached. A "short" column, then, implies a departure from classical Euler behavior and is characterized by small values of s.

Results and Discussion

The buckling load ratios are calculated for an orthotropic simply supported column with $E_{11}/G_{13} = 30$ and $\nu_{13} = 0.3$. P_c/P_g predictions according to the present and Timoshenko theory are 0.529 and 0.479 respectively, for $L/\rho = 20$. Timoshenko theory gives a lower value for the buckling load ratio and is, therefore, overly conservative. Departures from classical theory are substantial in this case.

If a five percent departure from classical theory is set as a practical limit to differentiate between slender and short columns, then a threshold value a_L for the universal slenderness parameter can be obtained from Equation (147A). A useful approximation is

$$a_L = 15 \tag{149}$$

The corresponding geometrical slenderness ratio, L/ρ, values for an isotropic material with $\nu = 0.3$ and an orthotropic material with $E_{11}/G_{13} = 30$ and $\nu_{13} = 0.3$ are 26.6 and 90, respectively. These values indicate that geometric slenderness alone is not indicative of column behavior.

CHAPTER X

HYGROTHERMAL EFFECTS

Introductory Remarks

The problems associated with hygrothermal effects in fiber reinforced resin matrix composites have been mentioned earlier. One of the more serious consequences of hygrothermal conditioning is the degradation of stiffness-related and strength-related properties. In the present study, emphasis is placed on property degradation effects in stiffness critical applications. Swelling stresses due to transient moisture distribution are not studied.

Estimates of loss of performance due to hygrothermal conditioning for unidirectional composites are presented in this chapter. Orthotropic solutions derived in previous chapters are utilized to obtain these estimates. The following solutions are applicable to unidirectional layups. The estimates should be viewed as providing qualitative information for insight into potential practical consequences. It is anticipated that composite structures with off axis ply layups will exhibit greater hygrothermal effects.

Mechanical Properties

Three environmental conditions listed below are selected for the study:

Condition A: Dry 200°F

Condition B: 1.05% Moisture Content 200°F

Condition C: 1.6% Moisture Content 200°F

Condition A is for reference. Condition B represents a realistic situation. The typical level of moisture, 1.05% by weight, is an approximation to long-term aircraft service. Condition C is saturation for an AS 3501-6 Graphite/Epoxy and represents the most severe degradation level at the selected temperature. Typical properties have been chosen with the aid of experimental data provided in Reference 59. These are presented in Table 4.

Results and Discussion

The response of an orthotropic beam under sinusoidally distributed loading is computed at the three levels of hygrothermal conditioning. The results are presented in Figures 31 and 32. The response under conditions A and B is a little different, while condition C response exhibits substantial differences from A and B. The axial stress distribution at midspan shown in Figure 32 indicates accentuated nonclassical effects under hygrothermal conditioning. By contrast, the classical or a Timoshenko-type theory fails to predict hygrothermal sensitivity of bending stress. The tensile stresses predicted near the centre of cross section, above the neutral axis are due to errors in the present approximation in this portion of the cross section.

Clamped orthotropic beam results showing the frequency ratio changes due to hygrothermal conditioning appear in Figure 33. The clamping condition corresponds to C2 restraint. The behavioral trends are similar

Table 4. Properties of the Orthotropic Material at Conditions A, B and C.

Property	Condition A 200°F, Dry	Condition B 200°F, 1.05% Wet	Condition C 200°F, 1.6% Wet
E_{11}	19.3×10^6 lbs/in^2	*19.3×10^6 lbs/in^2	*19.3×10^6 lbs/in^2
E_{33}	1.1×10^6 lbs/in^2	$.83 \times 10^6$ lbs/in^2	$.33 \times 10^6$ lbs/in^2
ν_{13}	0.35	0.39	0.41
G_{13}	$.77 \times 10^6$ lbs/in^2	$.64 \times 10^6$ lbs/in^2	$.25 \times 10^6$ lbs/in^2

*In the buckling load ratio computations, a five percent and a 20 percent reduction in E_{11} are assumed for Condition B and Condition C, respectively.

to those of the above. Condition C shows substantial frequency degradation.

Results showing hygrothermal effects on buckling loads of a simply supported orthotropic column appear in Figure 34. The differences between A and B are more significant in this example. Condition C, once again, causes serious stiffness reductions.

The buckling load ratio for a simply supported column is also computed for various levels of moisture absorption and temperature. The material used in this analysis is different and the corresponding properties are estimated with the aid of an analytical model presented in Reference 60. In this model, a particular mechanical property of the matrix material at any use temperature and moisture content is expressed as a function of room temperature dry property and a multiplying factor. This factor depends on the use temperature, percentage of the moisture content and the glass transition temperature. The fiber properties are assumed to remain the same and the gross properties of composite are computed by using micromechanics.

The results are presented in Figure 35. They indicate that hygrothermal effects have minor influences on the buckling load ratio in the range of temperatures 90°F - 190°F for the range of moisture content considered. Accentuated effects due to moisture pick up are observed in the higher temperature ranges. The moisture tolerance limit is substantially reduced at higher use temperatures.

The following are conclusions based on the above study:

1. Use of modern Graphite/Epoxy - type composite materials in the above applications do not pose serious problems in simulated aircraft usage

situation which is represented typically by Condition B.

2. Use of these materials at near saturation conditions should be avoided.

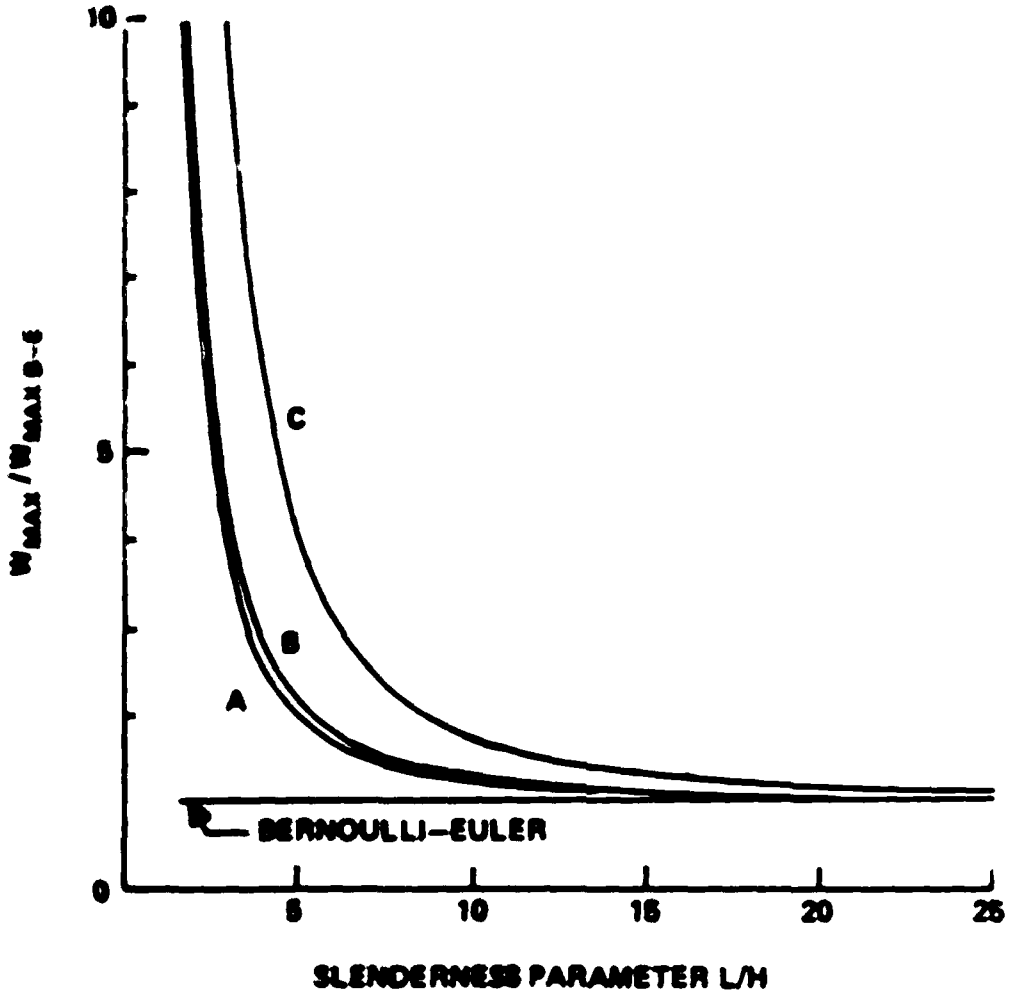

Figure 29. Hygrothermal Effects on the Maximum Deflection for a Simply Supported Orthotropic Beam Under Sinusoidally Distributed Loading

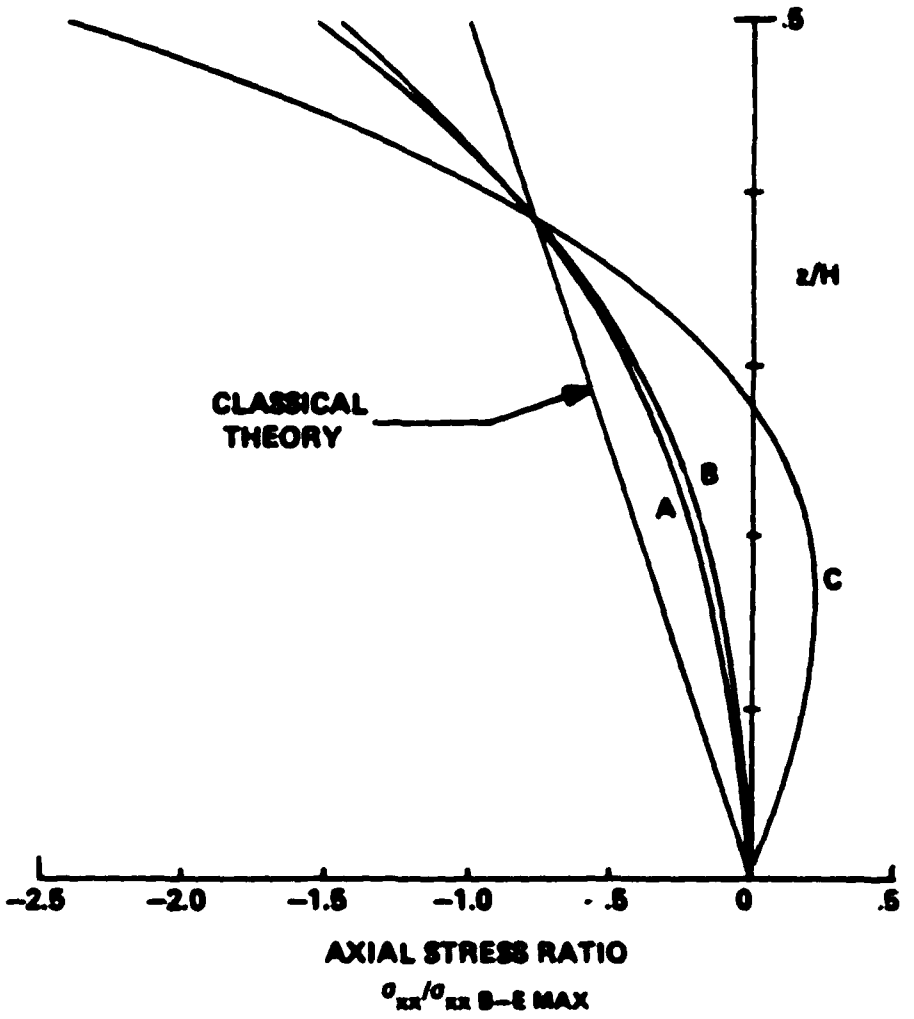

Figure 30. Hygrothermal Effects on the Midspan Axial Stress Distribution for a Simply Supported Orthotropic Beam Under Sinusoidally Distributed Loading, L/H = 3

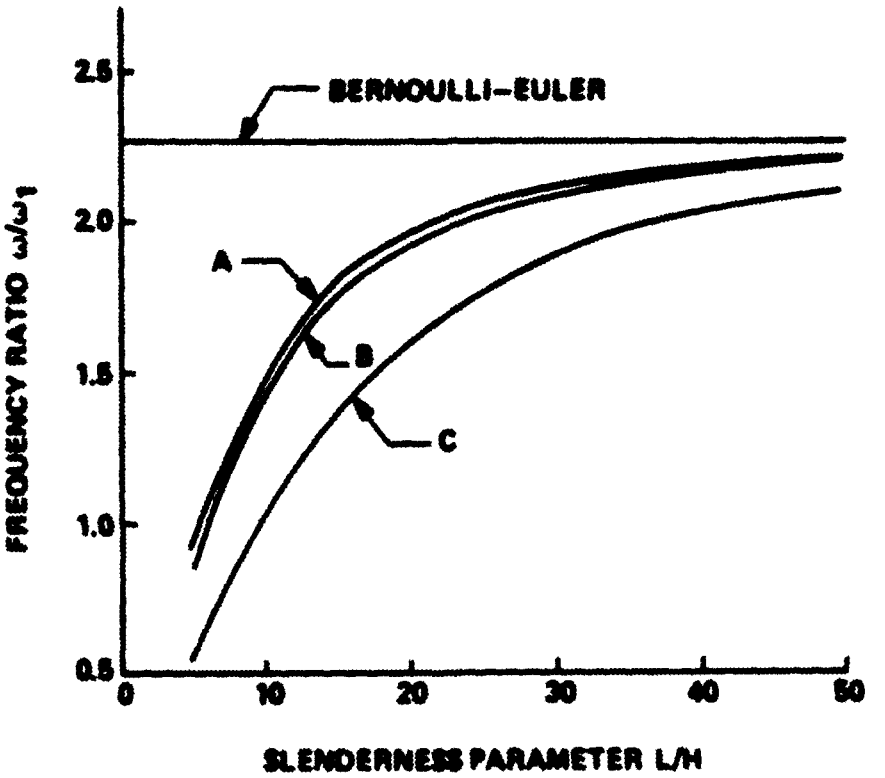

Figure 31. Hygrothermal Effects on Frequency Ratio of C2 Restraint Clamped Orthotropic Beam

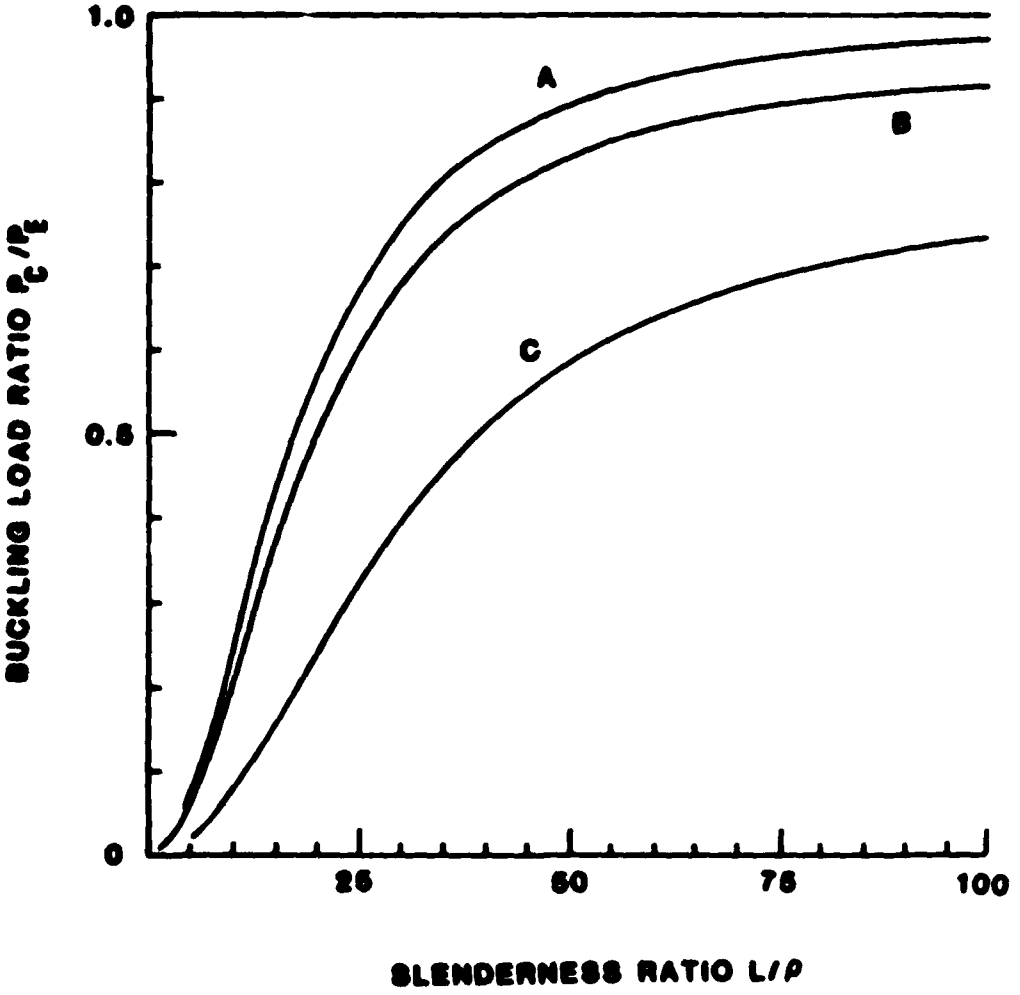

Figure 32. Hygrothermal Effects on the Buckling Load Ratio of a Simply Supported Orthotropic Column

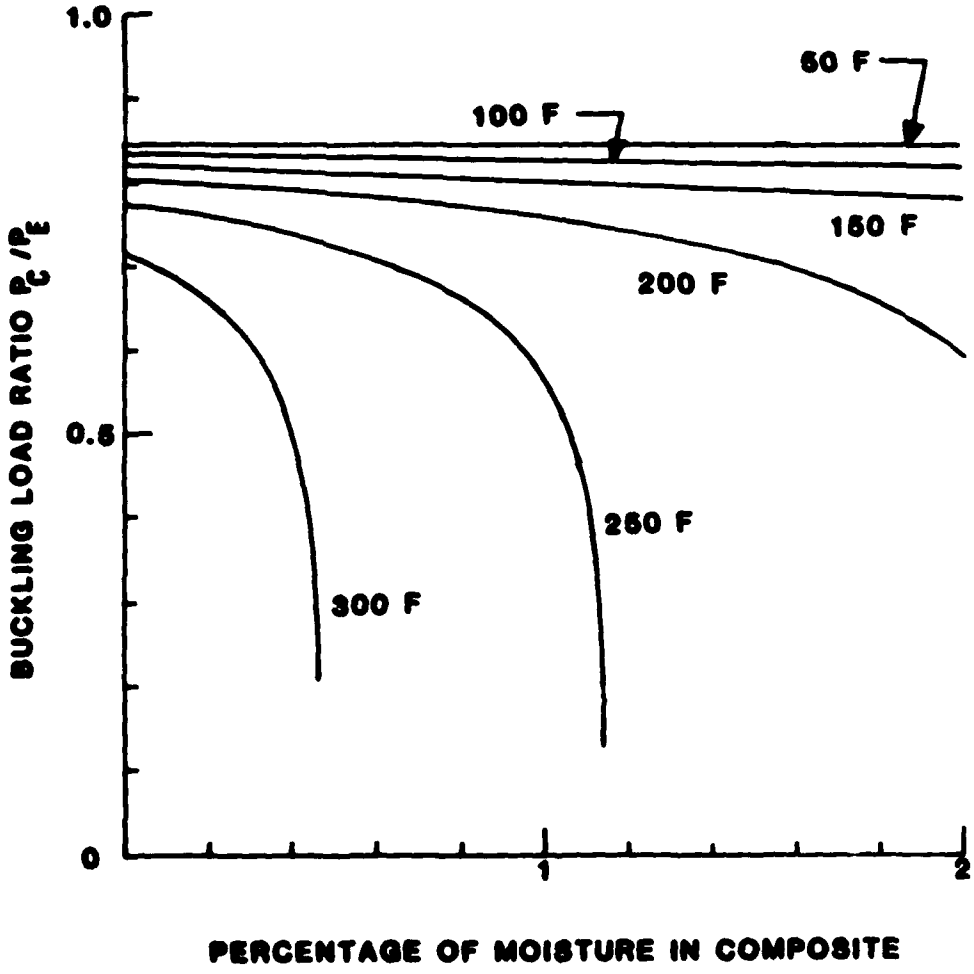

Figure 33. Effects of Moisture and Temperature on the Buckling Load Ratio of a Simply Supported Orthotropic Column, $L/\rho = 50$.

CHAPTER XI

CONCLUSIONS AND RECOMMENDATIONS

A new engineering theory for planar bending has been developed, validated and applied. Its predictive capabilities have been firmly established through correlative studies with exact solutions and a systematic consistency analysis. The theory has been successfully modified so as to apply to dynamics and static buckling. It accounts for three essential physical effects - - - transverse shear strain, transverse normal strain and nonclassical axial stress. The equations are as simple to apply as any transverse shear deformation-type theory yet they provide response throughout the structure.

The present theory predictions are superior to other comparable engineering theoretical predictions. The theory yields exact results for the case of uniformly distributed loading. For nonuniform loading, it has been validated by means of a thorough consistency analysis of a qualitative nature and by quantitative correlative studies with classic benchmark problems.

The theory includes all information contained in Reissner plate theory for planar bending and Stephen and Levinson's dynamic theory specialized to thin rectangular cross section beams.

There is a sensitivity of the predictions to boundary restraint modeling. It is more pronounced in static bending response of statically indeterminate structures. A boundary zone correction approach has been presented and illustrated which permits localized boundary restraint to be

accurately modeled.

Accentuated nonclassical axial stress effects are observed in the response of hygrothermally conditioned orthotropic beams. Other engineering theories fail to predict this interesting behavior.

Based upon the findings of present work, there are logical suggestions for future research.

1. The study of alternative clamping definitions has indicated the presence of an edge zone and decay length. These are much more pronounced in orthotropic structures. A reappraisal of composite materials testing methods when the specimens are relatively short is, therefore, a worthwhile study.

2. Another important area of practical interest is buckling and postbuckling behavior of advanced composite structures. A large displacement theory based upon the new equations is recommended to be developed to pursue the above issue.

3. Finite element models based on the present theory would be useful in the numerical analysis of practical structures.

APPENDIX A

ORTHOTROPIC SLAB SOLUTION

A plane stress solution for flexural wave propagation in an orthotropic beam is developed. This, by suitable modification of elastic constants, can be used to obtain stresses and phase velocity in an infinitely wide slab. The results are used in the dynamic theory validation study.

The Hooke's Law for orthotropic materials may be expressed as

$$\sigma_{xx} = \bar{E}_{11} \{u_{,x} + \nu_{31} w_{,z}\} \tag{A.1}$$

$$\sigma_{zz} = \bar{E}_{33} \{w_{,z} + \nu_{13} u_{,x}\} \tag{A.2}$$

$$\sigma_{xz} = G_{13} \{u_{,z} + w_{,x}\} \tag{A.3}$$

The above are obtained by inverting Equations (27) - (29) and using Equations (7). $\bar{E}_{11}$ and $\bar{E}_{33}$ are given by

$$\bar{E}_{11} = E_{11}/(1 - \nu_{13}\nu_{31}) \tag{A.4}$$

$$\bar{E}_{33} = E_{33}/(1 - \nu_{31}\nu_{13}) \tag{A.5}$$

The equations of motion in two dimensions are

$$\sigma_{xx,x} + \sigma_{xz,z} = \bar{\rho}\ddot{u} \tag{116}$$

$$\sigma_{xz,x} + \sigma_{zz,z} = \bar{\rho}\ddot{w} \tag{117}$$

Let the beam vibrate with circular frequency ω . The lowest mode has one half-wave in the x direction. The displacement components u and w may be taken as

$$u = U_1 \cos \frac{\pi x}{L} \sin \omega t \; e^{\bar{p} \frac{z}{c}} \tag{A.6}$$

$$w = W_1 \sin \frac{\pi x}{L} \sin \omega t \; e^{\bar{p} \frac{z}{c}} \tag{A.7}$$

U_1 and W_1 are arbitrary constants. $\bar{p}$ should be chosen such that the above satisfy Equations (116) and (117). This condition leads to

$$(\bar{p}/c)^4 + (\bar{p}/c)^2 \left[c_p^2 (\mu + \gamma) + \xi^2 (2 \mu \nu_{31} - \gamma + \gamma \nu_{31} \nu_{13}) \right]$$

$$+ c_p^4 \gamma \mu + \xi^4 \mu - \xi^2 c_p^2 \mu (1 + \gamma) = 0 \tag{A.8}$$

where

$$c_p^2 = \frac{\bar{\rho} \omega^2 c^2}{\bar{E}_{11}} \tag{A.9}$$

$$\mu = E_{11}/E_{33} \tag{A.10}$$

$$\gamma = \bar{E}_{11}/G_{13} \tag{A.11}$$

$$\xi = \pi c/L \tag{A.12}$$

Let p_1 and p_2 be the roots of Equation (A.8). Then the solution for u and w may be expressed as

$$u = \cos \frac{\pi x}{L} \sin \omega t \left[A_1 \sinh \frac{p_1 z}{c} + A_3 \sinh \frac{p_2 z}{c} \right] \tag{A.13}$$

$$w = \sin \frac{\pi x}{L} \sin \omega t \left[A_2 \cosh \frac{p_1 z}{c} + A_4 \cosh \frac{p_2 z}{c} \right] \tag{A.14}$$

$A_1 - A_4$ are arbitrary constants. The relations among these are obtained as follows: Substitution of Equations (A.6) and (A.7) into (117) using Equations (A.2) and (A.3) leads to

$$-U_1 \left[\frac{\pi \bar{p}\, G_{13}}{Lc} + \frac{\pi \nu_{13} \bar{E}_{33} \bar{p}}{Lc} \right] + W_1 \left[\bar{E}_{33} \frac{\bar{p}^2}{c^2} - G_{13} \frac{\pi^2}{L^2} + \bar{\rho} \omega^2 \right] = 0 \tag{A.15}$$

Equation (A.15) must be satisfied independently by the solutions for u and w associated with the roots p_1 and p_2. Therefore from (A.15) for the root p_1, it is required

$$A_2 \left[\bar{\rho} \omega^2 + \frac{p_1^2 \bar{E}_{33}}{c^2} - G_{13} \frac{\pi^2}{L^2} \right] = A_1 \left[\frac{\pi p_1 G_{13}}{Lc} + \frac{\pi \nu_{13} \bar{E}_{33} p_1}{Lc} \right] \tag{A.16}$$

Equation (A.16) is expressed in the following form for convenience in the subsequent analysis.

$$A_2 = F_1 A_1 \tag{A.17}$$

where
$$F_1 = \frac{\xi p_1 \left|1 + \frac{\gamma}{\mu} \nu_{13}\right|}{\left(\gamma(c_p^2 + \frac{p_1^2}{\mu}) - \xi^2\right)} \tag{A.18}$$

Similarly

$$A_4 = F_2 A_3 \tag{A.19}$$

where
$$F_2 = \frac{\xi p_2 \left|1 + \frac{\gamma}{\mu} \nu_{13}\right|}{\left(\gamma (c_p^2 + \frac{p_2^2}{\mu}) - \xi^2\right)} \tag{A.20}$$

The arbitrary constants A_1 and A_2 are eliminated to produce a frequency determinant by using the stress boundary conditions given in Equations (61). The results are

$$A_1 \left\{\frac{F_1 p_1}{c} - \frac{\pi \nu_{13}}{L}\right\} \sinh p_1 + A_3 \left\{\frac{F_2 p_2}{c} - \frac{\nu_{13} \pi}{L}\right\} \sinh p_2 = 0 \tag{A.21}$$

$$A_1 \left\{\frac{p_1}{c} + \frac{F_1 \pi}{L}\right\} \cosh p_1 + A_3 \left\{\frac{p_2}{c} + \frac{\pi}{L}\right\} F_2 \cosh p_2 = 0 \tag{A.22}$$

The frequency determinant is

$$\begin{vmatrix} \left\{\frac{F_1 p_1}{c} - \frac{\pi \nu_{13}}{c}\right\} \sinh p_1 & \left\{\frac{F_2 p_2}{c} - \frac{\nu_{13} \pi}{L}\right\} \sinh p_2 \\ \left\{\frac{p_1}{c} + \frac{F_1 \pi}{L}\right\} \cosh p_1 & \left\{\frac{p_2}{c} + \frac{\pi F_2}{L}\right\} \cosh p_2 \end{vmatrix} = 0 \tag{A.23}$$

Consequently

$$\frac{\tanh p_1}{\tanh p_2} = \frac{(p_2 r_2 - \nu_{13}\xi)}{(p_1 r_1 - \nu_{13}\xi)} \frac{(p_1 + r_1\xi)}{(p_2 + r_2\xi)} \tag{A.24}$$

Equation (A.24) is solved numerically to obtain the smallest value of c_p. The phase velocity parameter $\bar{c}/c_s$, which was used in the dispersion curves, is obtained from Equations (139A) and (A.9). The result is

$$\bar{c}/c_s = c_p \xi \sqrt{\frac{E_{11}}{\rho_{13}(1 - \nu_{13}\nu_{31})}} \tag{A.25}$$

Axial Stress Distribution

An expression for σ_{xx} is obtained below with the aid of Equations (A.1), (A.13) and (A.14).

$$\frac{\sigma_{xx}^c}{\bar{E}_{11}} = \left\{ A_1 \sinh \frac{p_1 z}{c} (\nu_{13} r_1 p_1 - \xi) + A_3 \sinh \frac{p_2 z}{c} (\nu_{31} r_2 p_2 - \xi) \right\}$$

$$\sin \frac{\pi x}{L} \sin \omega t \tag{A.26}$$

The above is used in the validation study of dynamic theory.

Transverse Displacement

With the aid of Equations (A.14) and (A.19) w is expressed as

$$w = \left\{ r_1 A_1 \cosh \frac{p_1 z}{c} + r_2 A_3 \cosh \frac{p_2 z}{c} \right\} \sin \frac{\pi x}{L} \sin \omega t \tag{A.27}$$

Consequently, W is given by

$$w = (F_1 A_1 + F_2 A_3) \sin \frac{\pi x}{L} \sin \omega t \qquad (A.28)$$

A comparison of Equations (A.28) and (134) indicates that the following needs to be satisfied so that present theory stress may be compared with the exact

$$w_o = F_1 A_1 + F_2 A_3 \qquad (A.29)$$

REFERENCES

1. Love, A.E. H., A Treatise on the Mathematical Theory of Elasticity, Fourth Edition, Cambridge University Press, 1952.
2. Todhunter, I. and Pearson, K., A History of the Theory of Elasticity, Vol. 1 and 2, Dover Publications, New York, 1960.
3. Scholaikoff, I.S., Mathematical Theory of Elasticity, Second Edition, McGraw Hill, 1956, p. 1.
4. Germain, S., Recherches Sur la Théorie des Surfaces Elastiques, Paris, 1821.
5. Navier, M., "Extrait des Recherches Sur la Flexion des Plans Elastiques," Bulletin de la Société Philomatique, 1823, pp. 95-102.
6. Poisson, S.D., "Mémoire Sur l'Equilibre et le Mouvement des Corps Elastiques," Annales de Chimie, Vol. 37, 1828, pp. 337-355.
7. Cauchy, A.L., "Sur l'Equilibre et le Mouvement d'une Plaque Solide," Exercices de Mathématiques, Vol. 3, 1828.
9. Kirchhoff, G., "Über die Schwingungen Einer Kreisförmigen Elastischen Scheibe," Poggendorffs Annalen, Vol. 81, 1850, pp. 258-264.
9. Lamb, H., "On the Waves in an Elastic Plate," Proceedings of the Royal Society of London, England, Series A, Vol. 93, 1917, pp. 114-128.
10. Rayleigh, L., Theory of Sound, Second Edition, The Macmillan Co., New York, NY, Vol. 1, pp. 256.
11. Pochhammer, L., "Über die Fortpflanzungsgeschwindigkeiten Schwingungen in Einem Isotropen Kreiscylinder," Crelle's Journal, Vol. 81, 1876, pp. 324-336.
12. Chree, C., Trans. Cambridge Phil. Soc., Vol. 14, 1889, p. 250.
13. Von Karman, Th., "Über die Grundlagen der Balkentheorie," Abhandl. Aerodynam., Inst. Tech. Hochschule, Aachen, Vol. 7, 1927, pp. 3-10.

14. Seewald, Von Friedrich, "Die Spannungen and Formänderungen von Balken mit rechteckigem Querschnitt," Abhandl, Aerodynam., Inst., Tech. Hochschule, Aachen, Vol. 7, 1927, pp. 11-33.

15. Goodier, J.N., On the Problems of the Beam and Plate in the Theory of Elasticity, Transactions of Royal Society of Canada, Third Series, Vol. 32, Section 3, 1938, pp. 65-68.

16. Donnell, L.H., "Bending of Rectangular Beams," Journal of Applied Mechanics, Vol. 19, 1952, p. 123.

17. Donnell, L.H., "A Theory for Thick Plates," Proc.2nd U.S. Natl. Congr. of Applied Mechanics, ASME, 1955, p. 369.

18. Eashin, Z., "On the Determination of Airy Polynomial Stress Functions," Bull. of the Research Council of Israel, Vol. 8, Series C, 1960, pp. 93-102.

19. Eashin, Z., "Plane Anisotropic Beams," Journal of Applied Mechanics, Vol. No. 34, June 1967, pp. 257-262.

20. Heou, C.Y., "Direct Method for Determining Airy Polynomial Stress Functions," Journal of Applied Mechanics, Transactions of ASME, Vol. 24, 1957, pp. 387-390.

21. Cheng Shun, "Elasticity Theory of Plates and Refined Theory," Journal of Applied Mechanics, Vol. 46, 1979, pp. 644-650.

22. Timoshenko, S.P., Goodier, J.N., Theory of Elasticity, McGraw Hill Book Co., 3rd Edition, New York, 1970.

23. Timoshenko, S.P., "On the Correction for Shear of the Differential Equation for Transverse Vibrations of Prismatic Bars," Philosophical Magazine, Series 6, Vol. 41, 1921, pp. 744-746.

24. Timoshenko, S.P., "On the Transverse Vibrations of Bars of Uniform Cross Section," Philosophical Magazine, Series 6, Vol. 43, 1922, pp. 125-131.

25. Uflyand, Y.S., "The Propagation of Waves in the Transverse Vibrations of Bars and Plates," Prikl. Matem. I. Mekh., Vol. 12, 1949, pp. 287-300 (In Russian).

26. Mindlin, R.D., "Influence of Rotatory Inertia and Shear on Flexural Motions of Isotropic, Elastic Plates," Journal of Applied Mechanics, Vol. 18, 1951, pp. 31-38.

27. Mindlin, R.D., and Deresiewicz, H., "Timoshenko's Shear Coefficient for Flexural Vibrations of Beams," Proceedings of the Second National Congress of Applied Mechanics, 1955, pp. 175-178.

28. Mindlin, R.D., "Thickness-Shear and Flexural Vibrations of Crystal Plates," Journal of Applied Mechanics, Vol. 22, No. 3, March, 1951, pp. 316-323.

29. Mindlin, R.D., "Forced Thickness-Shear and Flexural Vibrations of Piezoelectric Crystal Plates," Journal of Applied Physics, Vol. 23, No. 1, Jan. 1952, pp. 83-88.

30. Traill-Nash, R.W., and Collar, A.R., "The Effects of Shear Flexibility and Rotary Inertia on the Bending Vibrations of Beams," Quarterly Journal of Mechanics and Applied Mathematics, Vol. 6, 1953, pp. 186-222.

31. Goodman, L.E., and Sutherland, J.G., Discussion of Paper, "Natural Frequencies of Continuous Beams of Uniform Span Length," by R.S. Ayre and L.S. Jacobsen, Journal of Applied Mechanics, Vol. 18, Trans. ASME, Vol. 73, 1951, pp. 217-218.

32. Kaneko, T., "On Timoshenko's Correction for Shear in Vibrating Beams," Journal of Physics D: Applied Physics, Vol. 8, 1975, pp. 1927-1936.

33. Cowper, G.R., "The Shear Coefficient in Timoshenko's Beam Theory," Journal of Applied Mechanics, Vol. 33, 1966, pp. 335-340.

34. Kennard, E., and Leibowitz, R., "Theory of Freely Vibrating Non-uniform Beams, Including Methods of Solutions and Applications to Ships," David Taylor Model Basin, Report 1317, 1961.

35. Aalami, B., and Atzori, B., "Flexural Vibrations and Timoshenko's Theory," AIAA Journal, Vol. 12, 1974, pp. 679-685.

36. Stephen, N.G., and Levinson, M., "A Second Order Beam Theory," Journal of Sound and Vibration, Vol. 67, 1979, pp. 293-305.

37. Reissner, E., "The Effect of Transverse Shear Deformation on the Bending of Elastic Plates," Journal of Applied Mechanics, Vol. 12, 1945, pp. A69-A77.

38. Reissner, E., "On Bending of Elastic Plates," Quarterly of Applied Mathematics, Vol. 5, 1947, pp. 55-68.

39. Reissner, E., "On Transverse Bending of Plates, Including the Effect of Transverse Shear Deformation," International Journal of Solids and Structures, Vol. 11, No. 5, May, 1975, pp. 569-573.

40. Panc, V., Theories of Elastic Plates, Noordhoff, Leyden, 1975.

41. Naghdi, P.M., "On the Theory of Thin Elastic Shells," Quarterly of Applied Mathematics, Vol. 14, 1957, pp. 369-380.

42. Hildebrand, F.B., Reissner, E., and Thomas, G.G., "Notes on the Foundations of the Theory of Small Displacements of Orthotropic Shells," NACA TN No. 1833, 1949.

43. Whitney, J.M., and Sun, C.T., "A Refined Theory for Laminated Anisotropic, Cylindrical Shells," Journal of Applied Mechanics, Vol. 41, No. 2, Trans. ASME, Vol. 96, Ser. E., June, 1974, pp. 471-476.

44. Nelson, R.B., and Lorch D.R., "A Refined Theory of Laminated Orthotropic Plates," Journal of Applied Mechanics, Vol. 41, 1974, pp. 171-183.

45. Essenburg, F., "On the Significance of the Inclusion of the Effect of Transverse Normal Strain in Problems Involving Beams with Surface Constraints," Journal of Applied Mechanics, Vol. 47, No. 1, Trans. ASME, Vol. 97, Series E, Mar. 1975, pp. 127-132.

46. Lo, K.H., Christensen, R.M., and Wu, E.M., "A Higher Order Theory of Plate Deformation - I. Homogeneous Plates," Journal of Applied Mechanics, Vol. 44, No. 4, December 1977, pp. 663-668.

47. Lo, K.H., Christensen, R.M., and Wu, E.M., "A High Order Theory of Plate Deformation - II Laminated Plates," Journal of Applied Mechanics, Vol. 44, No. 4, December 1977, pp. 669-676.

48. Wang, J.T.S., Dickson, J.N., "Elastic Beams of Various Orders," AIAA Journal, May 1979, pp. 535-537.

49. Lo, K.H., Christensen, R.M., and Wu, E.M., "Stress Solution Determination For High Order Plate Theory," Int. Journal of Solids and Structures, Vol. 14, 1978, pp. 655-662.

50. Sokolnikoff, I.S., Mathematical Theory of Elasticity, Second Edition, McGraw Hill, 1956, p.421.

51. Timoshenko, S.P., Goodier, J.N., Theory of Elasticity, McGraw Hill Book Co., 3rd Edition, New York, 1970, pp. 61-62.

52. Little, R.W., "Elasticity," Prentice-Hall, Inc., Englewood Cliffs, New Jersey, 1973, pp. 109-110.

53. Pagano, N.J., "Exact Solutions for Composite Laminates in Cylindrical Bending," Journal of Composite Materials, Vol. 3, July 1969, pp. 398-411.

54. Koiter, W.T., "A Consistent First Approximation in the General Theory of Thin Elastic Shells," Proceedings of I.U.T.A.M. Symposium on the Theory of Thin Elastic Shells (Delft, August 1959), North-Holland Publishing Company, Amsterdam (1960), 12-33.

55. Koiter, W.T., "A Systematic Simplification of the General Equations in the Linear Theory of Thin Shells," Koninklijke Nederlandse Akademie Van Wetenschappen, Proceedings Series B, Physical Sciences, Vol. 64, Amsterdam 1961, pp. 612-619.

56 Zazac, E.E., "Propagation of Elastic Waves," in Handbook of Engineering Mechanics, edited by W. Flugge, McGraw Hill 1962, Chapter 64.

57. Huang, T.C., "The Effect of Rotatory Inertia and of Shear Deformation on the Frequency and Normal Mode Equations of Uniform Beams with Simple End Conditions," Journal of Applied Mechanics, Vol. 28, 1961, pp. 579-584.

58. Timoshenko, S.P., Young, D.H. Weaver, Jr., W., Vibration Problems in Engineering, John Wiley & Sons, Inc., Fourth Edition, New York, 1974.

59. Browning, C.E., Husman, G.E., and Whitney, J.M., "Moisture Effects in Epoxy Matrix Composites," Composite Materials; Testing and Design (Fourth Conference), ASTM STP 617, American Society for Testing and Materials. Philadelphia, Pennsylvania, 1977, pp. 481-496.

60. Chamis, C.C., Lark, R.F., and Sinclair, J.H., "An Integrated Theory for Predicting the Hygrothermomechanical Response of Advanced Composite Structural Components," NASA TM-73812, 1977.